TECHNISCHE UNIVERSITÄT MÜNCHEN

Fakultät für Medizin

I. Medizinische Klinik des Klinikums rechts der Isar, Molekulare Kardiologie

Patient-Specific Induced Pluripotent Stem-Cell Models of Cardiac Disease

Christian B. Jung

Vollständiger Abdruck der von der Fakultät für Medizin der Technischen Universität München zur Erlangung des akademischen Grades eines

Doctor of Philosophy (Ph.D.)

genehmigten Dissertation.

Vorsitzende/r: Univ.- Prof. Dr. Steffen Massberg

Prüfer der Dissertation:

1. Univ.- Prof. Dr. Karl-Ludwig Laugwitz
2. Univ.- Prof. Dr. Franz Hofmann (i.R.)

Die Dissertation wurde am 07.02.2012 bei der Fakultät für Medizin der Technischen Universität München eingereicht und durch die Fakultät für Medizin am 28.02.2012 angenommen.

DECLARATION

I hereby declare, that the here presented Ph.D. thesis was prepared by myself without the illegitimate help of a third party or resources other than the ones I quoted in the references. The thesis was completed within the time of three months from the start.

This thesis was not presented to any other board of examiners.

Munich, January 2012

Christian B. Jung

TABLE OF CONTENTS

GLOSSSARY

AP	Action potential
APD	Action potential duration
bFGF	basic fibroblast growth factor
BMP4	Bone morphogenetic protein 4
Ca^{2+}	Calcium
CaMKII	Ca2+/Calmodulin dependent kinase II
CHD	Congenital heart disease
CICR	Calcium induced calcium release
CPVT	Catecholaminergic polymorphic ventricular tachycardia
cTnC	Cardiac troponin I
CTnI	Cardiac troponin C
DAD	Delayed afterdepolarization
DNA	Deoxyribonucleic acid
EAD	Early afterdepolarization
EB	Embryoid body
ECC	Electric-Contraction coupling
FHF	First heart field
hESC	Human embryonic stem cell
iPSC	Induced pluripotent stem cell
LIF	Leukemia inhibitory factor
LQT	Long QT syndrome
LTCC	L-type Ca2+ channel
mESC	Mouse embryonic stem cell
NCX	Na+/Ca2+ exchanger
OFT	Outflow tract
PKA	Protein kinase A
RYR	Ryanodine receptor
SCD	Sudden cardiac death
SCNT	Somatic cell nuclear transfer
SHF	Second heart field
SOICR	Store overload induced Ca^{2+} release
SR	Sarcoplasmatic reticulum
TALEN	Transcription activator-like effector nucleases
TdP	Torsade de Pointes

Part 1. SUMMARY

Stem cells, despite being the subject of ethical and political debates, provide fascinating prospects for biomedical applications by both their ability to renew themselves and to differentiate into specialized cell types *in vitro*. Since the first isolation of murine embryonic stem cells in 1981, remarkable advances and groundbreaking findings were observed. During the past five years, the field gained further momentum by the discovery of a new platform technology (induced pluripotent stem cell (iPSC) technology) allowing the artificial creation of cells identical to embryonic stem cells from a donor's adult somatic cells. The ability to readily obtain patient-specific stem cells and to differentiate them into a variety of embryonic tissue-specific progenitors and adult somatic cells has opened the door to the development of stem cell based models of human diseases. This cumulative thesis relies on the iPSC technology to investigate how patient-specific induced pluripotent stem cells can be used as an *in vitro* model system to study congenital and adult forms of genetic cardiac diseases, such as long-QT syndrome and catecholaminergic polymorphic ventricular tachycardia, and to investigate the potential of these cells for screening drug compounds and for developing patient-specific therapies.

ZUSAMMENFASSUNG

Durch ihre Fähigkeiten sich selbst zu erneuern und *in vitro* in verschiedenste spezialisierte Zellen auszureifen, bieten Stammzellen faszinierende Aussichten für biomedizinische Anwendungen wenngleich sie immer noch Grund ethischer und politischer Diskussionen sind. Seit der ersten Isolierung von murinen embryonischen Stammzellen im Jahr 1981 wurden beachtliche Fortschritte erzielt und bahnbrechende Entdeckungen gemacht. Während der letzten fünf Jahre hat dieses Forschungsfeld weiteres Momentum aufgebaut durch die Entdeckung einer neuen Plattformtechnologie (induzierte pluripotente Stammzell (iPSC) -Technologie) die es erlaubt künstlich aus adulten somatischen Spenderzellen Zellen zu erzeugen, die identisch sind zu embryonalen Stammzellen. Die Möglichkeit nun auf einfachem Wege patienten-spezifische Stammzellen zu erhalten und diese in eine Vielzahl von embryonalen, gewebsspezifischen Vorläuferzellen zu differenzieren hat die Tür geöffnet hin zur Entwicklung von Stammzell-basierten Zellmodellen humaner Erkrankungen. Diese kumulative Promotionsarbeit nutzt die iPSC Technologie um zu untersuchen, inwieweit patienten-spezifische induzierte Stammzellen als ein *in vitro* Modellsystem dienen können um kongenitale und Erwachsenen-Formen genetischer Herzkrankheiten, wie z.B. das Long-QT Syndrom und die katecholaminerge polymorphe ventrikuläre Tachykardie zu studieren und herauszufinden, ob sich diese Zellen nutzen lassen um neuartige Pharmaka zu screenen und patienten-spezifische Therapien zu entwickeln.

Part 2. INTRODUCTION

2.1 STEM CELLS

The human body consists out of 10^{14} cells attributable to different tissues, some of which constantly need to be replaced due to normal cell turnover, apoptosis or injury. Formation of the body in the embryonical state and maintenance of the integrity and the function of its organs in post-natal life are all processes involving stem cells.

2.1.1 THE CONCEPT OF STEM CELL PLASTICITY AND DIFFERENTIATION

A stem cell is a cell that has both the capacity to make more stem cells by cell division (self-renewal) and to differentiate into mature, specialized cells (potency). The more different cells a stem cell can give rise to, the higher its potency. The cell with the highest potency is the cell that directly results from the union of sperm and egg during fertilization. These cells are called totipotent as they can give rise to all cells of the embryo including the extraembryonical components of the trophoblast and the placenta which are required to support development and birth. Totipotent cells are the only cells that can drive the development of an entire organism.

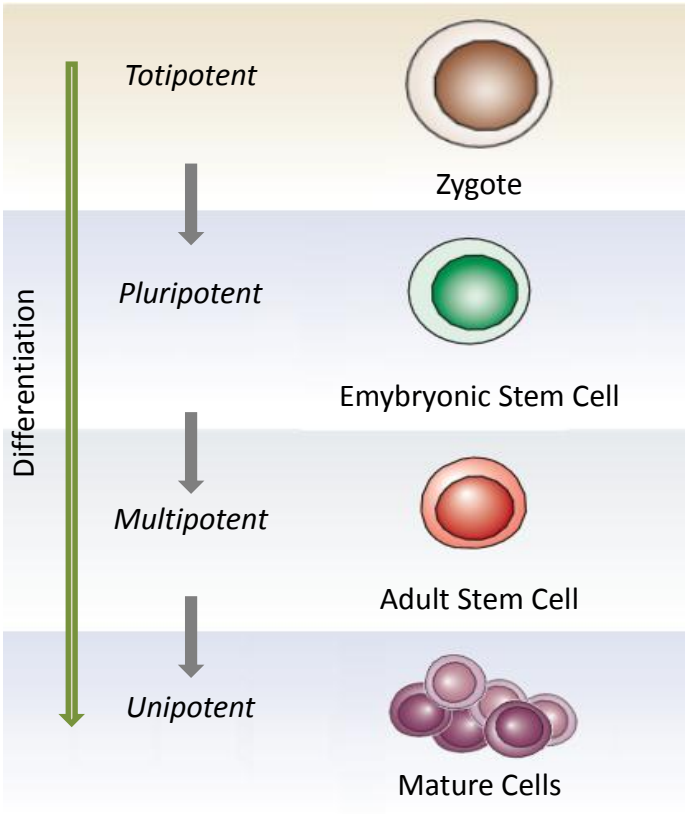

Multicellular organisms such as the human body develop from the stem cells that form the inner cell mass of the embryo. These cells are pluripotent. They are able to generate the more than 300 different somatic cell types of the body through a process called differentiation.

When isolated from the blastocyst *in vitro*, the pluripotent stem cells can be maintained in culture as embryonic stem cell (ESC) lines. Murine (m)ESCs were first isolated in 1981 [1] and human (h)ESCs were isolated and characterized in late 1998 [2].

Figure 1. Decrease in potency by differentiation.

As the embryo develops, its cells become progressively more specialized and pluripotency is lost (Figure 1), although some tissues retain what are called multipotent cells (or adult stem cells) that can only give rise to cells of that specific tissue and that are considered reminiscent of the embryonic tissue-restricted progenitors. Adult stem cells maintain the integrity and function of organ systems during adult life by replacing the cells that are lost owing to normal cell turnover, apoptosis or injury. Adult stem cells have been identified in several postnatal organs, e.g. the blood (hematopoietic stem cells), the brain (neural stem cells) or the bone-marrow (mesenchymal stem cells) [3].

Cells that can no longer give rise to cells other than of their own type are referred to as unipotent.

2.2 INDUCED PLURIPOTENCY

All nucleated cells of the human body, although functionally very different, maintain complete genomes. Yet, a neuronal cell does not naturally turn into a cell of the gut. What determines the cellular identity of a neuron and ultimately makes it different from an intestinal cell is hence not the fact that it carries different genes but the fact that a different set of genes is being expressed in the respective cells. Thus, the state of a cell is determined by its transcriptome, which is regulated by epigenetic modifications.

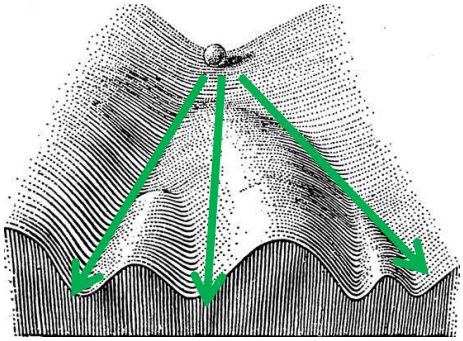

Figure 2. Waddington's classical epigentical landscape (modified).

As early as in 1957, Conrad Waddington described his conceptual image of development termed “epigenetic landscape” [4] (Figure 2). Waddington used a sloping landscape in which a ball can move across “hills” and “valleys” as a metaphor for cellular decision-making during development in which cells take different paths of differentiation. In this model, differentiation follows permitted trajectories but is not terminal, as different cell states are only separated by “hills” (read epigenetic barriers) that can be overcome upon addition of sufficient energy to the system. Enough energy (epigenetic modifications) could even lead the ball back to the highest point (pluripotency).

According to this model and provided, that terminally differentiated cells are in principle able to activate genes required for the stem cell state, it could be expected that a somatic cell can be converted back into an embryonic stem cell by changing its expression profile.

As opposed to the process of differentiation in which the potency decreases, the attempt to change a - unipotent - somatic cell into a pluripotent embryonic stem cell would result in an increase of potency which is why this process is called dedifferentiation (or reprogramming) (Figure 3).

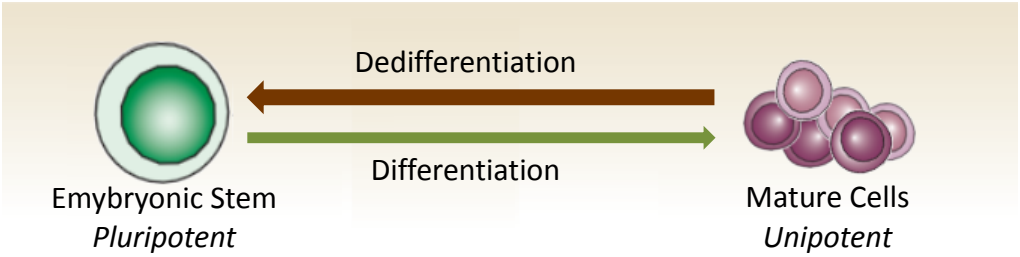

Figure 3. Model of differentiation and dedifferentiation.

2.2.1 THE REGULATORY NETWORKS OF PLURIPOTENCY

The immense scientific interest in embryonic stem cells is largely owned to their potential to differentiate into all cell types, hence their pluripotent properties. In order for embryonic stem cells to be used as a research tool one has to be able to keep them in culture for prolonged periods of time without loss of their differentiation potential. This requires well-defined culture conditions and a deep understanding of how embryonic stem cells sustain their undifferentiated state on a molecular basis through transcription factors and signaling pathways.

Early studies have shown that there are significant differences between mESCs and hESCs. While mESCs require leukemia inhibitory factor (LIF) and bone morphogenetic protein 4 (BMP4) as essential growth factors in culture, hESCs rely on Activin A and basic fibroblast growth factor (bFGF)[2, 5, 6].

However, there is a set of key pluripotency factors, namely Oct4, Sox2 and Nanog, which are central to the regulation of pluripotency in both mESC and hESC and constitute a core transcriptional network. These transcription factors regulate themselves and each other, showing features of feed-forward loops, and co-act in activating other pluripotency factors as well as in repressing differentiation genes [7, 8]. Recent studies suggest PRDM14 to also be part of the core transcriptional network in hESCs [9].

2.2.2 HISTORY OF REPROGRAMMING

Nuclear reprogramming describes the process of changing the gene expression pattern of a specific cell to that of another, unrelated cell of a different type.

Historically, two experimental approaches have been used to make these changes in gene expression possible, aiming to confer the state of pluripotency on a somatic cell, namely somatic cell nuclear transfer (SCNT) and cell fusion (Figure 4).

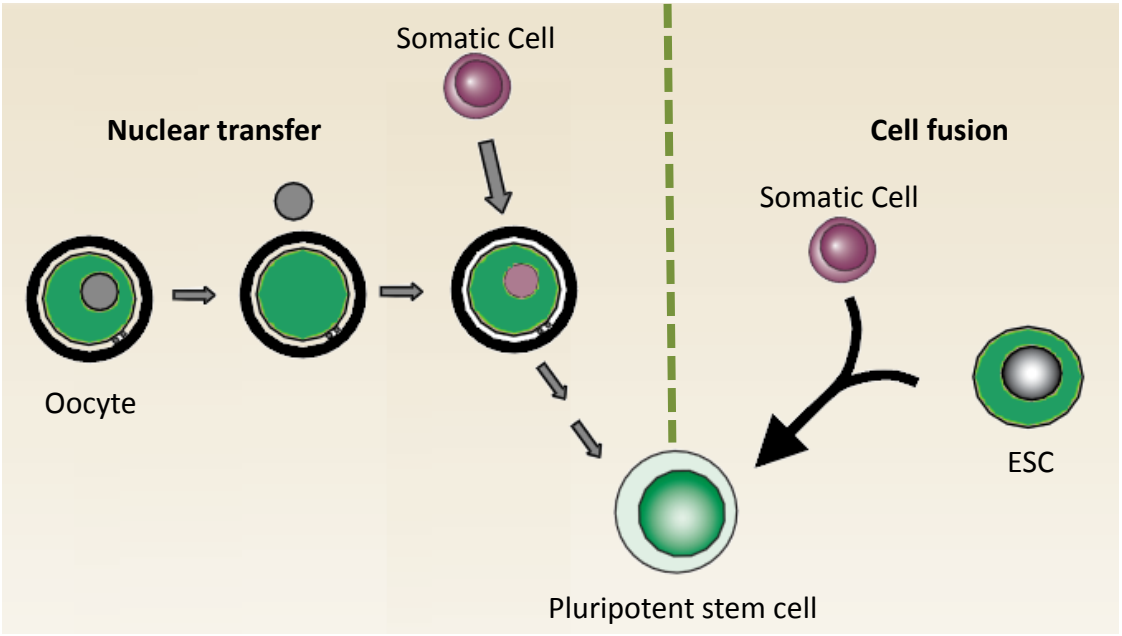

Figure 4. Historical methods to reprogramm somatic cells into pluripotent cells.

In SCNT, also known as “cloning”, the nucleus of a somatic cell is being introduced into the cytoplasm of an enucleated egg. The first to successfully use this technique were Briggs and King, who, in 1952 produced viable tadpoles of *Rana pipiens* by transplanting the nuclei from cells of the blastula [10]. 10 years later, this same technique was used with eggs from the frog *Xenopus laevis* [11] and ultimately led to the creation of the sheep Dolly in 1996 [12]. These experiments demonstrated that the cytoplasm of enucleated eggs contain the components necessary to fully reverse the differentiation of adult somatic cells.

Yet, the low frequency of success (1-2%), combined with the ethical concerns regarding harvesting human unfertilized eggs and the fact that most embryos created by SCNT exhibit phenotypic and gene expression abnormalities, make this technique unsuitable for human use as of now.

Another historic strategy for reprogramming a somatic cell nucleus to pluripotency is by fusing it with an ESC and was first reported for hESCs in 2005 [13]. After the fusion, the dominant cell, which is normally the larger and more rapidly dividing cell, in this case the ESC, will impose its pattern of gene

expression on the partner cell. It appears therefore, that ESCs possess factors in either their nucleus [14] or their cytoplasm [15] that are able to induce pluripotency in somatic cells. As these pluripotent cells generated by fusion maintain the chromosomes from both cells (tetraploid), rejection upon implantation is likely.

2.2.3 DIRECT REPROGRAMMING

The fact that somatic cell nuclei can be reprogrammed by transfer into oocytes or fusion with ESCs indicates that oocytes and ESCs contain reprogramming factors.

In 2006, the identification of these reprogramming factors by the group behind Shinya Yamanaka brought significant advance to this field. For the first time, mouse somatic cells were reprogrammed into an ESC state without the contribution of a second pluripotent cell but only by forced expression of four specific pluripotency-associated genes that were singled out by screening a pool of 24 candidate genes. These cells were named induced pluripotent stem cells (iPSCs) and shared many properties with ESCs [16], e.g. morphology, growth characteristics and gene expression.

iPSCs were then defined as a type of pluripotent stem cells that can be generated from various adult somatic cell types by forced expression of certain combinations of key ESC- associated transcription factors and that are similar to ESCs in their morphology, expression of important ESC marker genes, and their ability to form teratomas and yield live chimaeras when injected into mouse blastocysts.

2.2.3.1 GENERATION OF INDUCED PLURIPOTENT STEM CELLS

The first human iPSCs were generated in 2007, using the same method that was successfully used one year earlier in the mouse, namely by retroviral transduction of a set of four transcription factors (OCT4, SOX2, KLF4, C-MYC) into fibroblasts derived from skin biopsies of a healthy individual [17] (Figure 5) and also by using a new combination of factors (OCT4, SOX2, NANOG/Lin28), which were delivered *via* lentiviruses [18]. Later, it was shown that omission of the oncogenic C-MYC is possible [19]. Hunagfu and colleagues reprogrammed human fibroblasts using only OCT4 and SOX2 [20] and in 2009 human adult neural stem cells were reprogrammed with OCT4 as only factor [21].

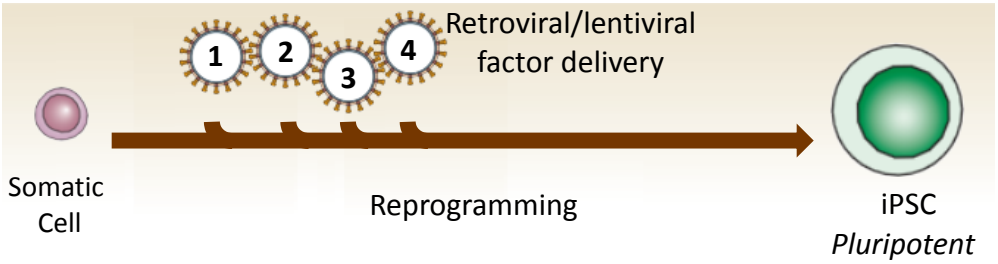

Figure 5. iPSC induction by direct reprogramming

2.2.3.2 MOLECULAR DYNAMICS OF REPROGRAMMING

Reprogramming of cells into iPSCs is not an instant event but a dynamic process over a period of 3-4 weeks. During this time, the epigenomic pattern of the somatic cell is being reset to the one of an embryonic stem cell. The rate at which this successfully happens is extremely low (0,01-0,1%) and two models have been proposed to explain this low efficiency, the “elite” and the “stochastic” model.

The “elite model”, in brief, proposes that the low efficiency of iPSC generation goes back to the fact that not all, but only a few cells in a culture of somatic cells are amenable to reprogramming in the first place and that these are somatic stem or progenitor cells, that can be found in most adult tissue cultures and that are closer to the state of pluripotent cells than terminally differentiated cells [22].

In contrast, the “stochastic model” postulates that all cells are equally suited for reprogramming, but for a cell to become pluripotent, a series of stochastic epigenetic events (“roadblocks”) needs to happen and only a strict minority of cells will successfully pass all these “roadblocks”. According to a working model proposed by Nagy [23], mainly three phases in the molecular changes of a somatic cell can be distinguished during reprograming (Figure 6).

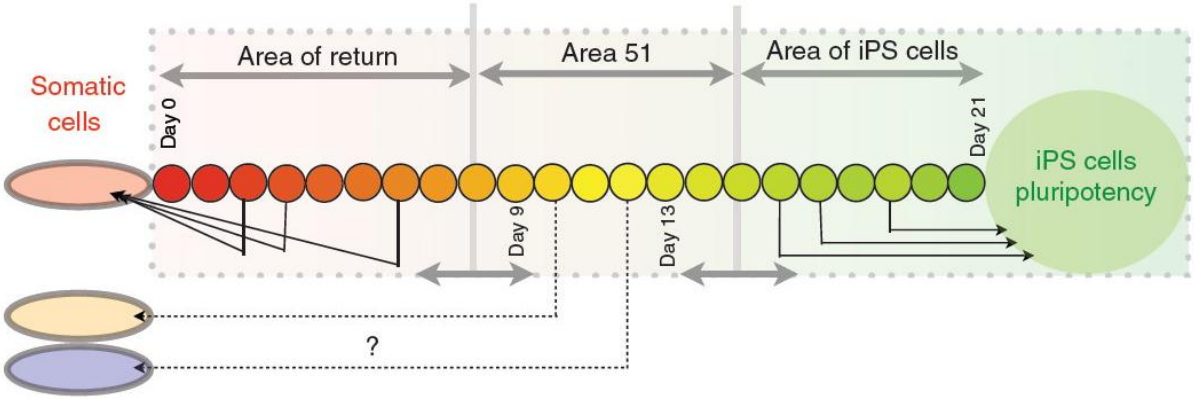

Figure 6. iPSC generation is a multistep process. Adopted from [23].

In the early phase, termed “Area of return”, the somatic cell starts to change its morphology and to down-regulate the expression of its somatic markers. The reprogramming process is purely driven by the presence of pluripotency transcription factors originating from the forced expression of the transgenes. The “roadblock” during this phase could be the extinction of the somatic program.

At the beginning of the middle phase, referred to as “Area 51”, the cell has not yet switched on its own endogenous copies of the pluripotency genes. Provided that the expression from the exogenous sequences is sufficiently strong, the transcription factors will start to activate the endogenous gene

loci and make the cells increasingly independent from the exogenes over time. This is likely to be the criteria to exit “Area 51” and the main important regulator of successful reprogramming.

Although the exact temporal sequence of changes during the late phase, “Area of iPS cells”, remains elusive, it marks the point at which the expression of pluripotency proteins from the endogenes becomes sufficiently strong to, in part, support the further transition of a cell towards a pluripotent state as the silencing of the viral sequences starts as a consequence of the reprogramming. In this stage, ESC-like colonies (“pre-iPSCs”) become obvious, genome-wide remodeling of chromatin modifications, such as DNA and histone tail methylation, takes place and the cell starts to express early pluripotency markers such as SSEA-1 and alkaline phosphatase. Yet, the acquisition of pluripotency remains incomplete and awaits the full independence of exogenous factor expression and complete activation of endogenous pluripotency genes, finalized X chromosome reactivation and loss of repressive chromatin character at many pluripotency genes marked by expression of Nanog and Oct4.

The vast majority of all cells will not continue along this timeline but rather become defective during reprogramming and will be either selected out by culture conditions or ultimately revert to its state of origin.

2.3 ESCS/IPSCS IN CARDIOVASCULAR MEDICINE

The ability to generate functional cell types from ESCs and iPSCs offers unprecedented opportunities to develop novel cell-based therapies for degenerative diseases, to establish predictive drug toxicity test or to model human disease in culture.

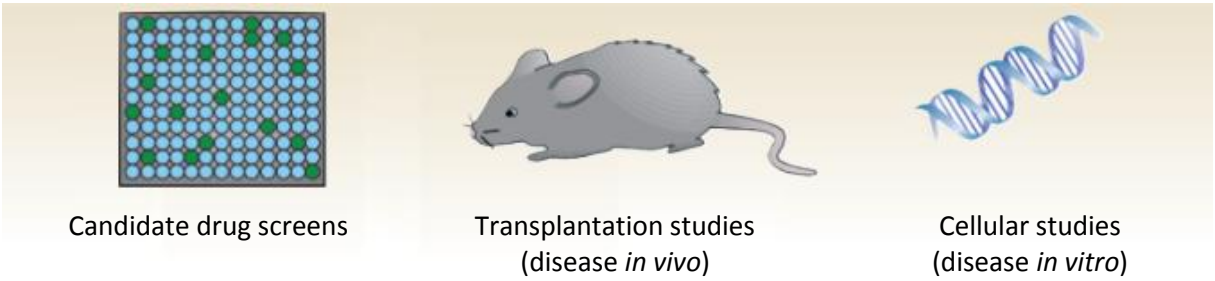

Figure 7. Possible fields of application for the iPS technology.

Yet, all these applications critically depend on the availability of highly efficient protocols for the differentiation of iPSCs into the lineage of interest. Development of such protocols requires an in-depth understanding of, and mostly seeks to recapitulate, the *in vivo* modulation of the regulatory pathways that control the establishment of the corresponding lineage during embryonic development.

2.3.1 HEART DEVELOPMENT AND CONGENITAL HEART DISEASE

The mammalian heart is a highly specialized organ and is the first to develop during embryogenesis. Its proper function relies on the controlled development of atrial and ventricular myocardium, endocardium, the outflow tract, the coronary tree, the heart valves and the conduction system. Despite decades of tracing cell lineages and descriptive embryology of the heart's origins, a more complete and accurate picture of cardiogenesis has only recently emerged [24-26].

2.3.1.1 HEART PROGENITOR CELLS

During cardiogenesis three populations of progenitors have been identified to contribute to the different compartments of the heart (Figure 8) and each of these populations gives rise to distinct cardiac cell types: the cardiogenic mesoderm forms the major proportion of myocytes of the ventricles, the atria and the outflow tract (OFT) and additionally contributes to cells of the conduction system and to the cushion cells of the aortic and pulmonary valves; the cardiac neural crest progenitors give rise to the distal smooth muscle cells of the OFT and to the autonomic nervous system of the heart; and finally, the proepicardial organ produces the vascular support cells of the coronary vessels, the interstitial fibroblasts embedded in the myocardium and some myocytes, mainly in the atrioventricular septum [27, 28].

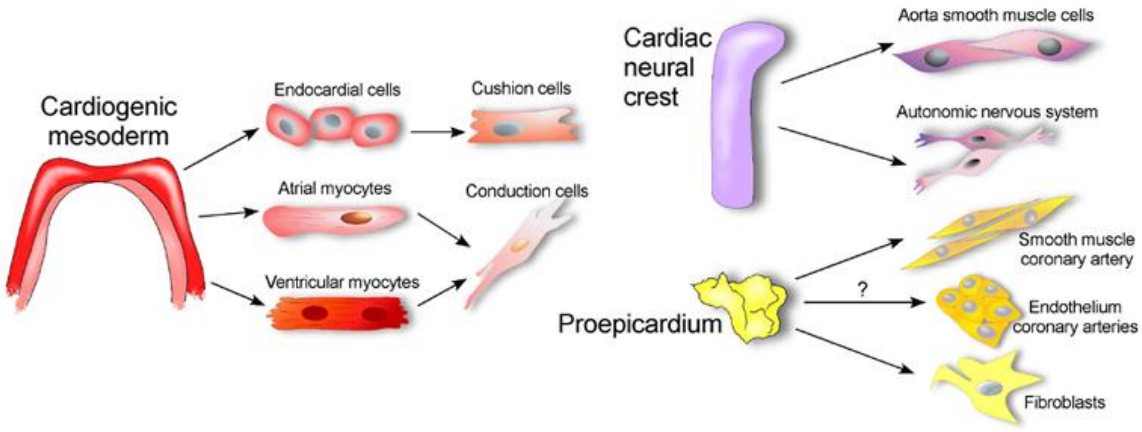

Figure 8. Origin and lineage relationship of cardiac cell types. Adopted from [24].

An important principle in heart development is that the regulation of different cardiac precursors must be tightly controlled so that the correct progenitor population proliferates, migrates and differentiates at the correct time and in the correct location.

Due to this complexity, many errors may happen during heart development, which commonly leads to the appearance of congenital heart diseases (CHDs). CHDs constitute a major percentage of clinically significant birth defects with an estimated incidence of 4-14 per 1000 live infants [29].

Although in the past decades human genetic studies have identified numerous genes that are associated with inherited and sporadic forms of CHDs, the mechanisms of how deficiencies in these genes translate to structural defects still remain unknown [30].

2.3.1.2 PRECURSOR CELLS OF THE CARDIOGENIC MESODERM

The identification of two distinct populations of cardiac precursors within the cardiogenic mesoderm, one that exclusively forms the left ventricle (first heart field (FHF)) and the other that mainly forms the OFT, the right ventricle and most of the atria (second heart field (SHF)), hints at a novel approach of understanding CHDs not so much as a defect in a specific gene, but rather as a defect in the lineage decision in a defined subset of cardiac precursors.

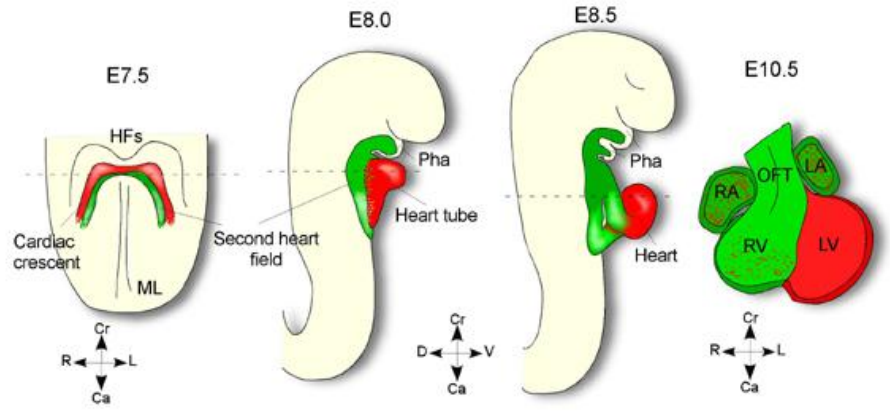

Figure 9. FHF and SHF contribution to the developing heart. Adopted from [24].

Figure 9 shows the relative position, movement and contribution of the SHF progenitors (green) relative to the FHF cells (red) from the cardiac-crescent through to the looping stages of mouse heart development.

2.3.1.2.1 ISL1 PROGENITORS

The SHF is marked by the LIM-homeodomain transcription factor Isl1 and comprises cells of the pharyngeal mesoderm situated dorsally and medially to the FHF, which gives rise to the linear heart tube [31]. The pivotal role of Isl1 within the SHF is demonstrated by the fact that this transcription factor is required for survival, proliferation and migration of the SHF progenitors into the primitive heart tube, resulting in its elongation and further morphogenesis [31-34]. However, how Isl1 controls the molecular mechanisms regulating these biological processes is largely unknown and the downstream targets involved in these signalling events and the transcriptional and epigenetic programs regulating the development of $Isl1^{+}$ precursors are still far from being understood.

In 2005, it has been demonstrated, using tamoxifen-inducible Cre/lox technology, that Isl1 is a developmental lineage marker for undifferentiated cardiac progenitors and enables their isolation from embryonic and postnatal mouse and human hearts [32]. Cardiac fibroblasts allow the cells to self-renew, maintaining their ability to subsequently differentiate into functional myocytes with action potential characteristics of atrial, ventricular, or conduction cells and intact excitation-contraction coupling (ECC) [32, 35].

Cardiac precursors expressing Isl1 can also be isolated from differentiating mESCs during cardiogenesis *in vitro* and comprise distinct Isl1$^+$ progenitor pools with defined differentiation potential, including a multipotent precursor which can give rise to all three major cell lineages of the heart, cardiac, smooth muscle, and endothelial cells [33]. These multipotent cardiovascular progenitors can be identified by the co-expression of the transcription factor Nkx2-5, another key regulator of the cardiogenic program, and the surface receptor Flk1, one of the earliest mesodermal differentiation marker for the endothelial and blood lineages [33, 36, 37].

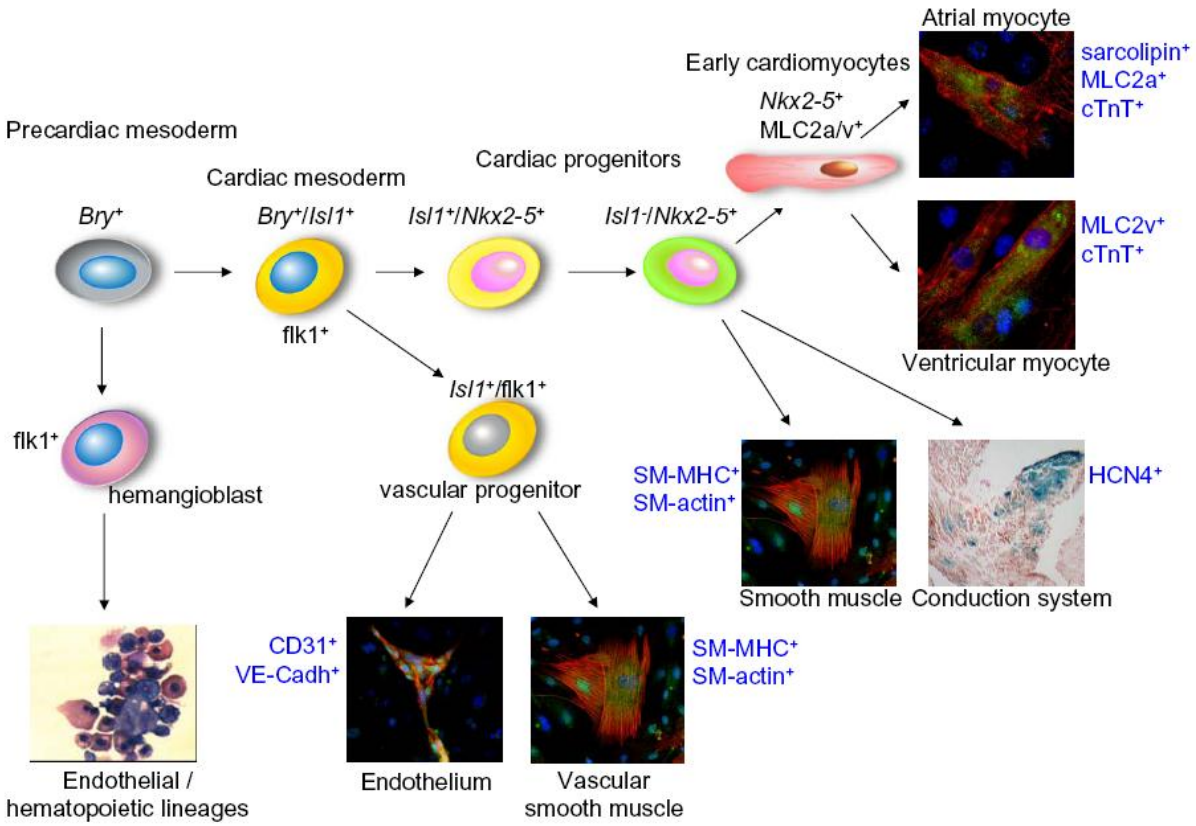

Figure 10. Cellular hierarchy of cardiac progenitors and their lineage specification. Adopted from [24].

Although it is clear that Isl1$^+$ cardiovascular progenitor cells play a pivotal role during heart development, important questions still remain reagarding the molecular mechanisms of Isl1$^+$ cardiac

progenitor maintenance, lineage specification and differentiation and how causative genes of CHDs affect cell-fate decisions in the ISL1 lineage during human cardiogenesis.

The ability to isolate and selectively expand $ISL1^{+}$ cardiovascular progenitors offers a powerful cell-based *in vitro* system to answer these questions and generate human models of CHDs.

2.4 GENETIC ADULT CARDIAC DISEASE

Cardiovascular disease remains the leading cause of death worldwide accounting for 12.8% of all deaths in 2008 (WHO website).

This is in part attributable to the lifestyle and unhealthy diet in the industrialized world but also owed to the lack of suitable models that fully reflect the genetically diverse nature of these diseases and adequately address their long-term development.

Genetic cardiac disease can be subdivided into two classes, cardiomyopathies and channelopathies. Cardiomyopathies go back to structural and functional abnormalities of the heart. In contrast, channelopathies occur in the absence of structural defects and are caused by dysfunctional cardiac ion channels causing electrical instability of the cells. Since the normal heart pumping function relies on proper electrical propagation through the ventricles, channelopathies can trigger life-threatening arrhythmias that may result in sudden cardiac death (SCD). Approximately 10-20% of all sudden deaths happen in absence of structural cardiac abnormalities.

At present, the class of cardiac channelopathies comprises four distinct conditions namely, congenital long-QT syndrome (LQT), catecholaminergic polymorphic ventricular tachycardia (CPVT), Brugada syndrome, and short-QT syndrome.

2.4.1 LQT SYNDROME

The LQT syndrome is a disease characterized by delayed cardiac repolarization, which causes prolongation of the QT interval on the surface electrocardiogram. The clinical manifestations of the disorder involve polymorphic ventricular tachycardia (often termed torsades de pointes (TdP)) and syncopal episodes, which often result in cardiac arrest and sudden death in otherwise healthy young individuals [38]. Besides the symptomatic treatment with β-blockers and the implantation of automated defibrillators to terminate fatal arrhythmia, no causal therapy is currently available [39].

The most frequent forms of LQTS are acquired as an adverse effect of treatment with medications that block cardiac potassium channels, such as class III antiarrhythmic drugs and antihistamines, or by electrolyte disturbances that alter the electrochemical conditions needed for normal cardiac

excitability. Less commonly, LQTS is inherited as an autosomal dominant (Romano-Ward syndrome) or recessive (Jervell and Lange-Nielsen syndrome) disorder.

Congenital LQTS has been subdivided into types based on the gene in which causative mutations occur. At least 12 different LQTS-associated genes have been identified so far, most of which encode ion channels specifically involved in the generation of the cardiac action potential (AP) [40, 41]. However, in ~80-90% of genotyped patients, the underlying causes are mutations in two main genes: the KCNQ1 (also known as KVLQT1 or Kv7.1) gene, which encodes the pore-forming α-subunits of the channels generating the IKs current (LQT1 syndrome), and the KCNH2 (also known as HERG or Kv11.1) gene, which produces the α-subunits of the channels responsible for the IKr conductance (LQT2 syndrome) [41-43].

2.4.1.1 MOLECULAR MECHANISM OF MUTATIONS UNDERLYING LQT1

The delayed rectifier potassium current, IK, is responsible for the late repolarization phase of the AP and regulates AP duration (APD) in many species. IK has two components, one with a slow activation speed (IKs) and one that activates more rapidly (IKr) (Figure 11).

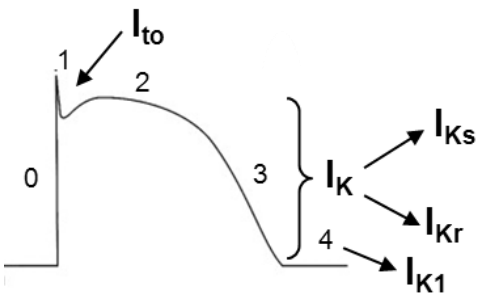

Figure 11. Activity of voltage-dependent potassium channels during different phases of the AP.

APD is very tightly tuned *via* the regulation of IKs and IKr. Among other modulations, the APD is shortened by a β-adrenoceptor-mediated increase in the magnitude of IKs by the action of catecholamines [44, 45]. Additionally, under high frequencies, IKs' contribution is enhanced due to the incomplete slow deactivation of the current [46].

Functional cardiomyocytes shorten their AP at higher frequencies to guarantee that the cell will have completed the repolarization process upon arrival of the next AP. In LQT1 patients however, due to mutations in KCNQ1 and the associated defects in IKs, the cardiomyocytes fail to sufficiently shorten their AP under stress. This, in turn, results in the development of arrhythmias.

2.4.2 CATECHOLAMINERGIC POLYMORPHIC VENTRICULAR TACHYCARDIA

CPVT is an inherited arrhythmogenic disorder caused by dysfunctional calcium (Ca^{2+}) cycling. Clinically CPVT is characterized by adrenergically mediated occurrence of life-threatening arrhythmia followed by syncopes and sudden cardiac death at a young age in patients with structurally normal hearts. It is a rare disease with a prevalence of approximately 1 in 10.000. Two genetic forms of the

disease have been described: CPVT1 accounting for at least 50% of all cases and associated with autosomal dominant mutations in the cardiac ryanodine receptor (RYR2*)*, and the very rare form CPVT2, linked to recessive mutations in calsequestrin (CSQ2) [47]. Both proteins belong to the multimolecular Ca^{2+} release channel complex of the sarcoplasmic reticulum (SR) that supports myocyte Ca^{2+} cycling and contractile activity. Despite the high mortality of 30-50% by the age of 35 years, to date, no causative treatment exists and patients are treated purely symptomatically with β-blockers and implantable defibrillators or, as a last resort, by sympathetic denervation.

2.4.2.1 RYR CHANNELS

Ryanodine receptors were originally identified during the testing of ryanodine, a plant alkaloid , as a potential insecticide due to its paralyzing effect on insects [48]. Ryanodine was subsequently found to induce widespread paralysis in cardiac and skeletal muscles and to bind to a specific component of the SR [49]. So far, three mammalian isoforms of RYR have been described. RYR1, predominantly expressed in skeletal muscle, RYR2, the cardiac isoform, and RYR3 mainly found in neuronal tissue.

RYR2 is a homotetramer built out of four 565kDa (4965 amino acids) monomers. Mutations in RYR2 are mainly associated with CPVT1 and were first described in 1999 [50] and 2001 [51]. By now, more than 150 RYR2 mutations have been reported and they are not randomly spread over the full length of the protein but rather confined to three mutation "hotspots" (Figure 12), inferring that these regions are of particular importance for the well-functioning of the receptor.

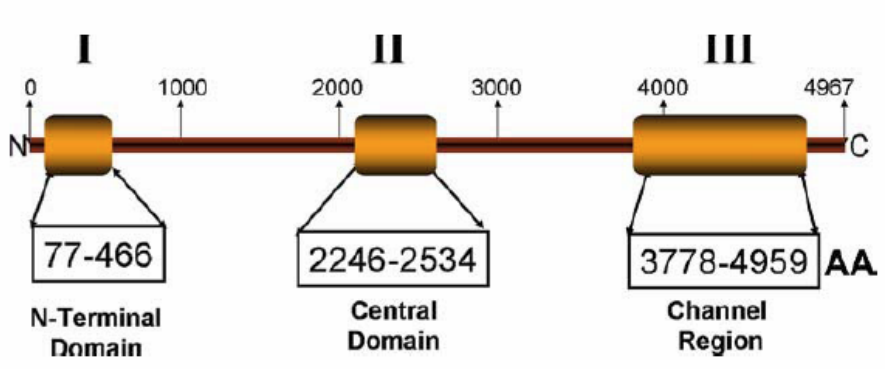

Figure 12. Mutation hotspots within RYR2 channel.

2.4.2.2 ABERRANT FUNCTION OF MUTATED RYR2 IN CA^{2+} HANDLING

A functional cardiomyocyte must be able to mechanically respond (contraction) to an electrical stimulus (action potential), a process termed excitation-contraction coupling. During normal ECC coupling, action potential evoked Ca^{2+} influx into the cytosol *via* cardiac L-type Ca^{2+} channels (LTCC) leads to a local rise in Ca^{2+}. This Ca^{2+} binds to and activates the RYR2 channels, hereby triggering massive Ca^{2+} release from the SR into the cytosol and rapidly increasing the cytosolic Ca^{2+} concentration ($[Ca^{2+}]_i$) from 100nM to 1uM. This process is termed calcium induced calcium release (CICR) [52] (Figure 13). This increase in calcium marks the beginning of systole and activates the contraction by binding to cardiac troponin C (cTnC) of the myofilaments. This leads in turn to the detachment of cardiac troponin I (cTnI) which induces conformational changes in the troponin/myosin complex and allows shortening of the myofilaments through myosin-actin interaction. During the diastolic phase, SR Ca^{2+} release is terminated, 70% of the Ca^{2+} released in systole is pumped back through the Ca^{2+} pump SERCA2a and the remaining 30% leave the cell through the Na^{+}/Ca^{2+} exchanger (NCX), effectively lowering the cytosolic $[Ca^{2+}]_i$ and allowing the dissociation of Ca^{2+} from the myofilaments and muscle relaxation

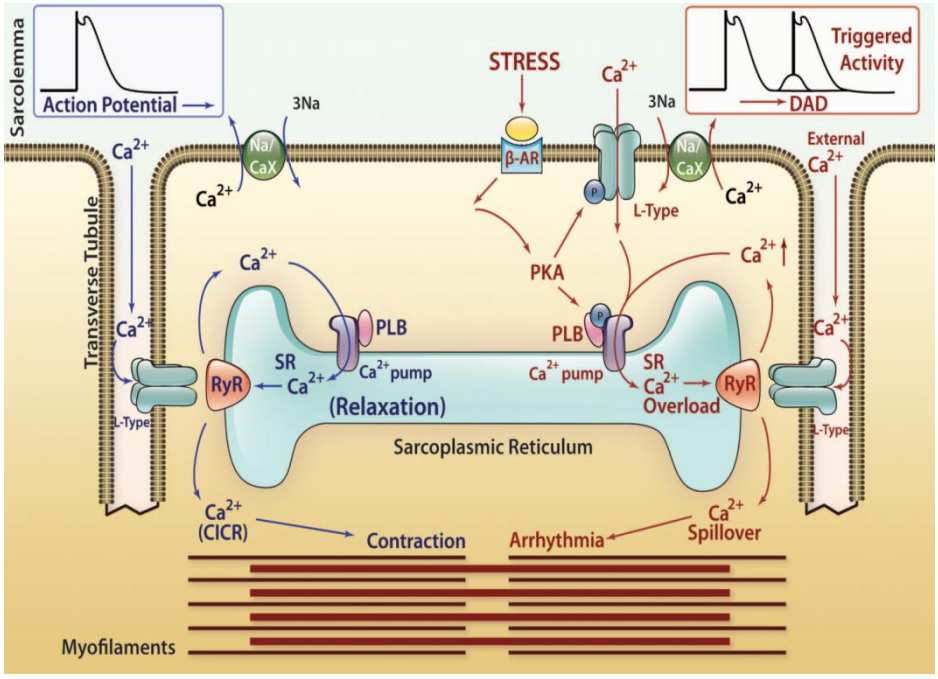

Figure 13. Ca^{2+} cycling in functional cardiomyocytes.

Under basal conditions, Ca^{2+} handling in CPVT is not impaired. However, under the influence of β-adrenergic stimulation, the activation of key proteins of the Ca^{2+} cycling machinery (LTCC, RYR2, Phospholamban) by phosphorylation through protein kinase A (PKA) and Ca^{2+}/Calmodulin dependent

kinase II (CaMKII) is evoking the disease phenotype. Under this condition of augmented Ca^{2+} influx and SR Ca^{2+} uptake, resulting in SR Ca^{2+} overload, the mutant RYR2 channel is no longer able to remain tightly closed in diastole. This leads to aberrant Ca^{2+} release during diastole and hence to augmented diastolic $[Ca^{2+}]_i$, which has the potential to reverse the mode of action of NCX. Instead of pumping Na^+ out of the cell at this stage, NCX is pumping Na^+ into the cell, resulting in arrythmogenic membrane depolarization, visible as delayed afterdepolarization (DADs). If this depolarization reaches a certain threshold, the voltage-activated Na^+ channels open, which can lead to a full spontaneous AP (triggered activity).

2.4.2.3 DISEASE MECHANISM OF ACTION

Data gained from knock-in/out mice and channel overexpression in HEK cells have led to the formulation of three hypotheses on how mutations in RYR2 may lead to diastolic SR Ca^{2+} leak and arrhythmias.

The first hypothesis is developed around the disruption of the critical interaction between the RYR2 channel and one of its modulating proteins, FKBP12.6. In 2004, Wehrens and colleagues conducted experiments in FKBP12.6 null and heterozygous mice and found that they exhibited ventricular arrhythmias and SCD after β-adrenergic stimulation, while being normal at rest. Occurrence of arrhythmias could be abolished by administration of JTV519, a drug with RYR2/FKBP12.6 stabilizing properties, in FKBP12.6$^{+/-}$ but not in FKBP12.6$^{-/-}$ mice [53]. They concluded that RYR2 leakiness results from a decreased receptor affinity to FKBP12.6 due to the mutation. Although it may be possible that selected mutations alter FKBP12.6 binding to RYR2, this hypothesis has been recently challenged and an increasing body of evidence clearly demonstrates that alterations in FKBP12.6-RYR2 interaction are unlikely to be the common cause of CPVT1 [54-58].

The second hypothesis is called store-overload induced Ca^{2+}-release (SOICR). Evidences suggest that RYR2 channels also sense the SR Ca^{2+} by a luminal Ca^{2+} activation site distinct from the cytosolic Ca^{2+} activation site. Jiang and colleagues [59] proposed that the mutations in RYR2 lead to an altered luminal SR Ca^{2+} sensing which in turn lowers the SR Ca^{2+} threshold at which RYR2-mediated Ca^{2+} release happens. While this is benign under baseline conditions when SR Ca^{2+} load is normal and far under the threshold level, it becomes pathological under the influence of β-adrenergic stimulation, when the SR store is filled to a higher level due to the action of PKA on phospholamban. In this condition of store-overload, luminal Ca^{2+} levels shoot above the Ca^{2+} release threshold of mutated RYR2 channels, leading to repetitive, premature RYR2 activation.

The last and youngest of the three hypotheses was first formulated by the group of Mazsuzaki and is based on the idea of “domain unzipping” between the N-terminal domain and the central domain of RYR2. The N-terminal and central regions, although separated by ~2000 residues in the linear sequence, interact with each other to form a “domain switch” that stabilizes the closed state of RYR channels [60, 61]. Due to the mutation and the resulting conformational changes in RYR2, the two domains are no longer able to interact (“domain unzipping”), leading to destabilization of the closed state and ultimately leakage through the RYR2 (Figure 14).

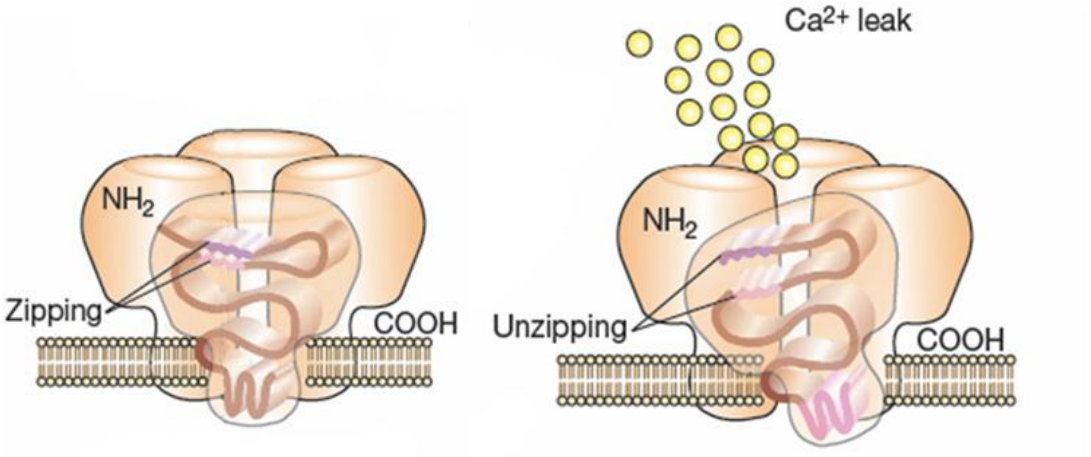

Figure 14. Mutation-induced domain unzipping in RYR2 channels.

Dantrolene is a drug used in emergency medication for the treatment of malignant hyperthermia caused by mutations in the RYR1, the skeletal isoform of RYR that has a very high level of homology to RYR2. The therapeutic action of dantrolene seems to be due to its binding to a N-terminal sequence of RYR1, which restores inter-domain interactions critical for the closed state of the channel [62]. Recently, dantrolene has been shown to target a corresponding sequence in RYR2 [63] and to improve intracellular Ca^{2+} handling in failing cardiomyocytes from a canine model of heart failure [64] and arrhythmias in a mouse model of CPVT1 [65, 66]. Taken together, there is strong evidence that dantrolene has stabilizing effects on mutated RYR2 channels without affecting the gating properties of normal RYR2 channels.

2.5 AIM OF THE PROJECT

To date, many of the most critical and puzzling human cardiovascular disorders cannot be adequately studied because specific human cardiovascular cell types, such as cardiomyocytes, coronary endothelial and smooth muscle cells, cannot be easily obtained. Two crucial steps towards reaching the goal of studying specific cardiovascular cell types from patients with various forms of congenital or acquired heart diseases have recently been made: **1**) the identification of multipotent cardiovascular progenitor cells not only in mammalian embryos and postnatal (adult) heart but also as an intermediate stage during differentiation of embryonic stem cells; **2**) the breakthrough discovery that adult somatic cells can be reprogrammed back to a pluripotent state by ectopic expression of few defined transcription factors - iPSC technology. Therefore, iPSCs could be an ideal source to obtain patient-specific cardiac progenitors and in turn large number of cardiovascular cells with the disease-causing mutation. This will represent a powerful *in vitro* system to study pathogenesis of cardiovascular diseases at the cellular level and perform molecular and genetic screens to enable patient-specific drug design.

In a series of connected projects, this work first focused on validating the mouse and human iPSC system as a source of functional cardiovascular progenitors and their differentiated derivatives (cardiomyocytes, smooth muscle cells and endothelial cells). Successive studies aimed to generate patient-specific iPSC-based models of inherited arrythmogenic cardiac disorders affecting the functionality of cardiac myocytes and use these models to study disease mechanisms and test potential disease aggravators and possible novel customized treatment options. The specific aims of the different projects are detailed below:

Project 1. *Mouse and human iPSCs as a source for multipotent Isl1$^+$ cardiovascular progenitors.*

- Generation of iPSCs from Isl1-Cre / R26R indicator mouse lines enabling irreversible marking and isolation of Isl1$^+$ cardiovascular progenitors and their differentiated progeny.
- Molecular and functional characterization of mouse iPSC-derived Isl1$^+$ cardiovascular precursors *in vitro* and *in vivo*.
- Generation of human iPSCs from healthy individuals and establishment of a differentiation protocol to obtain human ISL1$^+$ cardiovascular progenitors

Project 2. *Patient-specific iPSC models for LQT syndrome*

- Generation of human iPSC lines from patients affected by the long QT1 syndrome and healthy controls.

- Disease phenotype analysis: characterization of the electrophysiological properties (AP and ion currents, particularly IKs) of patient-specific LQT1-iPSC-derived cardiomyocytes compared to control-iPSC-generated cells under normal and stress conditions.
- Examination of the pathophysiological mechanisms of the KCNQ1 R190Q mutation.
- Demonstration of the protective effect of β-blockade in LQT1 patient-specific cells and validation of the model system as a platform for drug testing.

Project 3. *Dantrolene rescues arrythmogenic RYR2 defect in a patient-specific stem cell model of catecholaminergic polymorphic ventricular tachycardia*

- Generation of human iPSC lines from a patient affected by CPVT1 and carrying a novel RYR2 S406L mutation.
- Disease phenotype analysis: characterization of Ca^{2+} handling properties in CPVT1-derived cardiomyocytes and susceptibility to DADs and triggered activity under normal and stress conditions.
- Demonstration of the disease phenotype rescue by dantrolene as a novel causal therapy for CPVT1.

Part 3. DISCUSSION

3.1 PATIENT-SPECIFIC IPSCS AS IN VITRO SYSTEMS FOR MODELLING CARDIOVASCULAR DISEASES AND DRUG DEVELOPMENT

The derivation of the first mESC line in 1981 and the subsequent genetic manipulation initiated a new era towards a better understanding of molecular mechanisms of disease. Numerous mouse strains carrying defined mutations in their genome have been generated ever since and used for the analysis of gene function *in vivo,* generating a tremendous amount of new data helping to increase our understanding of disease mechanisms. For cardiovascular diseases, however, mouse models and heterologous systems are not always able to fully recapitulate the disease phenotype seen in patients, due to species differences at both physiological and genetic levels. This is the case, for example, for the mouse models of LQT1 syndrome, since little or no IKs has been observed in adult mouse myocytes [67]. As human heart donor cells are not readily available, it has been difficult to study cardiac disorders directly in patient cells and the research has been awaiting for alternative human models of cardiovascular diseases.

Human pluripotent stem cells represent good candidates for generating such models, as they can generate an unlimited number of cardiomyocytes of all three subtypes: ventricular, atrial and nodal. Until four years ago, human disease-specific pluripotent cells could only be made by genetically modifying existing human ESC lines or by establishing new human ESCs from embryos carrying those monogenic disorders detectable via pre-implantation genetic diagnosis. For different reasons each of this methods is very restrictive, and few diseases have been captured in this way. In addition, many genetic disorders display variable penetrance and severity of clinical symptoms from patient to patient. This lack of consistency is due to the complex interactions between genetic background and environment and may extend to the properties of derived pluripotent stem cells. However, disease-specific hESCs can never have such clinical history owing to their origins. The ability to reprogram human somatic cells to a pluripotent state using the iPSC technology offers now the possibility to produce large quantities and a variety of cells with a person's own genetic background.

Since the initial publication on human iPSCs, this technology has captured scientists with promise and hope based on the potential that these cells hold for disease modeling, drug development, and regenerative medicine without the drawbacks of hESCs, which remain ethically and legally disputed because of their origin that requires the destruction of embryos during isolation.

Over the course of this series of projects, we could first demonstrate that m/hiPSCs can serve as a source of $Isl1^{+}$ cardiac progenitors and that they display multipotency into all three cardiovascular

lineages (cardiac myocytes, smooth muscle, and endothelial cells) *in vitro* and *in vivo* [68]. A genetic marking technique in the mouse has enabled us to purify iPSC-derived Isl1^{+} progenitors by FACS and to perform a genome-wide transcriptional profile of the cells at different stages of cardiac development *in vitro*. Moreover, we have optimized a protocol to direct human iPSCs, reprogrammed from healthy individuals, to the cardiac lineage and efficiently generated individual-specific ISL1^{+} cardiovascular progenitors and functional cardiac myocytes [46]. This work offers a foundation for *in vitro* model systems using ISL1^{+} cardiovascular precursors to identify signaling pathways controlling SHF renewal, lineage specification and differentiation and to study pathogenesis of human CHDs resulting from the alterations in transcriptional and epigenetic programs of SHF ISL1^{+} cardiovascular progenitors. Moreover, it demonstrates the feasibility of large-scale production of multipotent, non-tumorigenic cardiac cells for clinical and translational applications in the future.

Later, we were able to prove for the first time, that human iPSCs can be used to model the specific pathology seen in two different genetically inherited cardiac diseases, LQT1 syndrome and CPVT1, and to investigate the therapeutic action of medications, illustrating the promise of iPSC technology for gaining new insights into human cardiac disease pathogenesis and patient-specific treatment [69, 70].

Several issues should be considered when using iPSCs to model adult forms of cardiac diseases. First, differentiation of ESCs/iPSCs into the cardiac lineage leads to the generation of all three major subtypes of myocytes of the heart, namely ventricular, atrial, and nodal cells, which can be distinguished based on their electrophysiological properties and specific molecular marker expression. This is a double edge sword: while obtaining different types of myocytes allows to model cardiac disorders affecting different heart lineages, for some diseases it could be necessary to analyze specifically one myocyte subtype, and, if the AP is not the read-out of the disease assay, it is challenging to identify the subtype of interest. Tracking approaches using cell-type-specific lineage reporters or identification of cell-type-specific surface markers could greatly advance iPSC modeling in the cardiac field. Secondly, hESC-/hiPSC-derived cardiomyocytes resemble immature embryonic or fetal cardiomyocytes more closely than adult ones, as demonstrated by the expression profile analysis of key genes involved in ECC and Ca^{2+} handling performed in this work and by the AP characteristics. While this aspect did not impair the ability of LQT1- and CPVT1-iPSC-derived myocytes to fully recapitulate the pathophysiological features of the disorders, it may become a limitation for modeling other cardiac diseases, for instance late on-set acquired disorders. Hence, tools improving *in vitro* maturation of iPSC-derived cardiomyocytes need to be developed in order to attain the full potential of the iPSC technology for cardiac disease modeling.

All the iPSC models of cardiac diseases reported so far, including the two described in this work, are monogenetic disorders [71-73]. However, most of the diseases affecting the cardiovascular system, such as coronary heart disease, hypertension, diabetes, cardiomyopathy, are complex and multi-factorial. It will be decisive to see, whether iPSCs will be able to reliably model such diseases as well in the future. Additionally, even monogenetic diseases do not always present full penetrance in a given family, as in the case of LQT syndrome. Future research will have to show whether or not this can be adequately reproduced *in vitro*, or whether the epigenetic changes occurring during reprogramming and continued cell culture erase these differences.

Pharmaceutical drug development requires test systems that are capable of fully recapitulating the molecular and physiological hallmarks of a disease phenotype while generating reproducible data when used for high-throughput screening of large compound libraries. Due to the large interspecies variability in heart electrophysiology this holds especially true for disorders associated with mutations in cardiac ion channels ("channelopathies").

Up to now, however, drug discovery was hampered by the lack of disease-specific *in vitro* models and mostly relied on transgenic animal cells or heterologous systems which often did not accurately reproduce all aspects of the human disease phenotype or generated ambiguous results owned to limitations due to interspecies variability. Having unlimited access to cells harboring disease-specific mutations has the potential to radically increase the possibilities in the process of target identification and target validation by being able to uncover the molecular mechanism and cellular basis of the disease in question.

With respect to drug testing, multiple potential blockbuster drugs have been pulled out of the market in recent years due to cardiotoxicity. In fact, occurrence of drug-induced arrhythmic events was the single most common cause of drug-withdrawal in the recent decade. The iPSC technology has the potential to help to overcome these problems in the future by providing patient-specific cardiomyocytes on which promising compounds can be tested before entering the cost-intensive clinical stage.

Many human diseases don't only arise from mutations in one specific gene but can go back to mutations in a variety of genes. Although all patients may present with similar clinical phenotypes, the affected molecular pathways can be very different and efficient therapy only possible if the functional heterogeneity of the disease is properly addressed by the development of mutation-specific drugs. The iPSC technology holds the potential to provide genetically matched cells from any patient, rendering patient-specific drug design possible and providing the option to safely assess the therapeutic benefit of a drug for a patient *in vitro* prior to administration.

3.2 POTENTIAL OF HUMAN IPSCS FOR CARDIAC REGENERATIVE MEDICINE

One of the most exciting aspects of the iPSC technology is the possibility to generate autologous cells for transplantation therapy without the risk of immune rejection, since the cells are genetically identical to the prospective recipient (Figure 15).

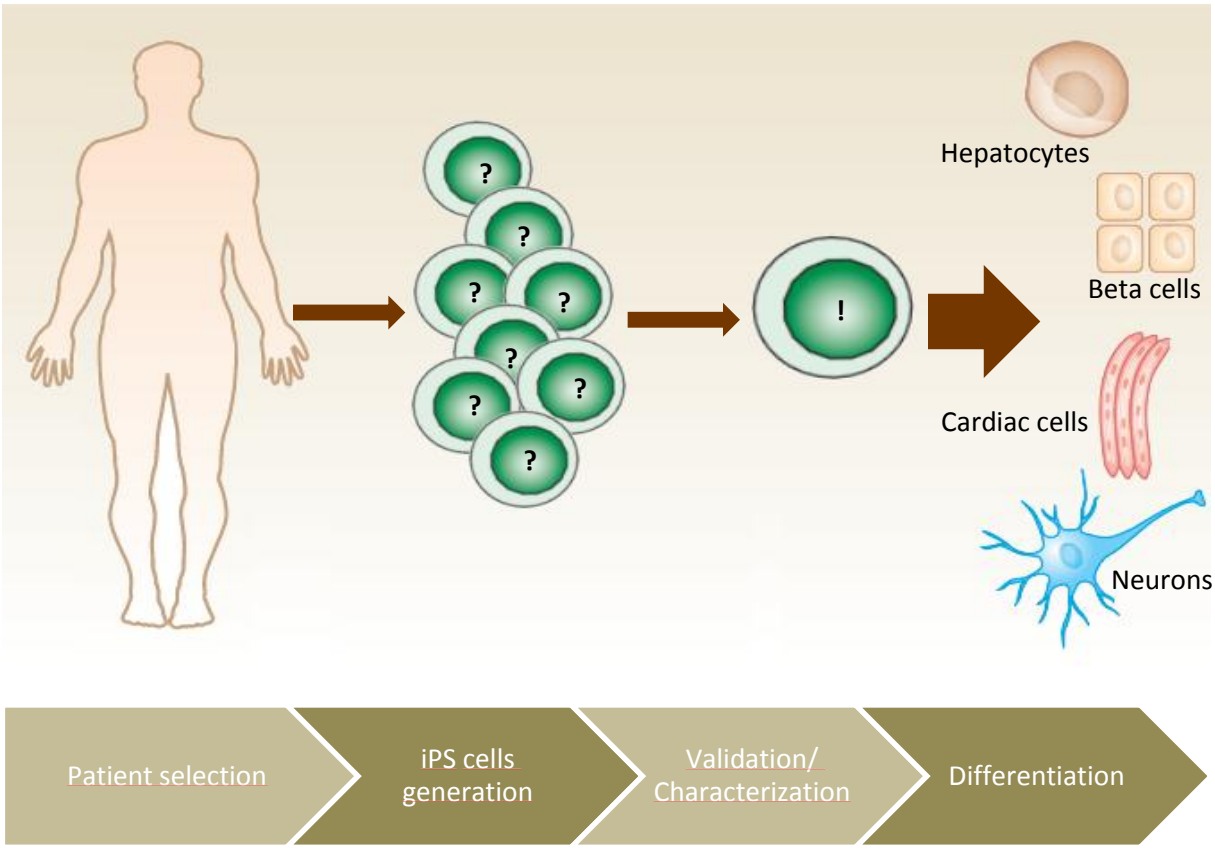

Figure 15: The different steps of generating patient-specific cells for transplantation.

Especially in the field of cardiac cell therapy, the prospect of being able to use patient-specific cardiomyocytes/cardiac progenitors for transplantation is very appealing. Results of the current work regarding the transplantation of mouse iPSC-derived $Isl1^{+}$ cardiovascular progenitors into normal heart suggest, that lineage specific multipotent progenitors could ideally have an advantage over more developed cardiovascular cells, as they should be able to proliferate and differentiate into diverse mature lineages, thus contributing to both remuscularization and revascularization. Moreover, since they are restricted in their potency and can differentiate only into distinct cells of the mature heart, they cannot produce teratomas and represent a safe cell type for future clinical and translational applications. The capability to identify and isolate these multipotent progenitor cells from human iPSCs, without the need of genetic marking, will be an indispensable step towards their clinical application.

Besides using iPSC-derived cells directly for transplantation *in vivo*, they can also be potentially valuable in tissue engineering approaches. As opposed to direct cell transplantation, cardiac tissue engineering strives to take into account the three-dimensionality of the heart and the fact, that the highly complex function of the myocardium relies on a variety of cells embedded in a mesh of extracellular matrix for its well-functioning rather than just purely on cardiomyocytes. Being able to isolate cells at the cardiac progenitor state from iPSCs could prove extremely helpful in the generation of functional cardiac patches for future regenerative therapeutic approaches.

3.3 FUTURE PERSPECTIVES OF HUMAN IPSC TECHNOLOGY

Although iPSC derivation is legally and ethically less problematic than work on embryonic stem cells and the field is rapidly advancing, the technology still needs to overcome several issues in order to serve as an efficient research tool and ultimately be of use in clinical applications.

3.3.1 REPROGRAMMING STRATEGIES

Two major hurdles stand in the way of reliable, consistent derivation of patient-specific iPSCs: the accessibility of patient material and the reliance on integrating viral vectors as the most efficient method to deliver reprogramming factors.

Human iPSCs have been obtained from distinct somatic cell populations, including neural cells [74], keratinocytes [75, 76], stomach and liver cells [77], adipocytes[78], and recently T-lymphocytes [79-81] isolated from whole blood samples. Sampling of peripheral blood is one of the most commonly performed and least invasive clinical procedures and blood can be easily stored. Thus, the recent reports describing the generation of iPSCs from peripheral blood obtained from healthy donors encourage the hope that the same could be achieved with blood from patients. This would progress the field and bring it closer to clinical use by allowing for the bio-banking of patient material and providing a simple source to obtain patient specific iPSCs.

For delivery of the reprogramming factors, the most widely practiced method, transduction via retrovirus or lentivirus, results in random integration of foreign genetic elements into the genome, which may cause insertional mutagenesis and inadvertently affect the differentiation of iPSCs into relevant cell types. Random integrations render each iPSC line genetically distinct. Although the integrated viruses are transcriptionally silenced following reprogramming, re-expression of any of the reprogramming factors may interfere with differentiation and subsequent cell behavior [82]. Alternative approaches, such as the use of single [83] or multiple transient transfections [84], non-integrating vectors [85], excisable vectors [86-88], direct protein transduction [89-91], RNA-based Sendai viruses [92-94], mRNA-based transcription factor delivery [95, 96] and microRNA transfections

[97], have been reported to solve some of the concerns related to viral integration (Figure 16). However, many of these approaches either suffer from poor efficiency or they are costly and time-consuming.

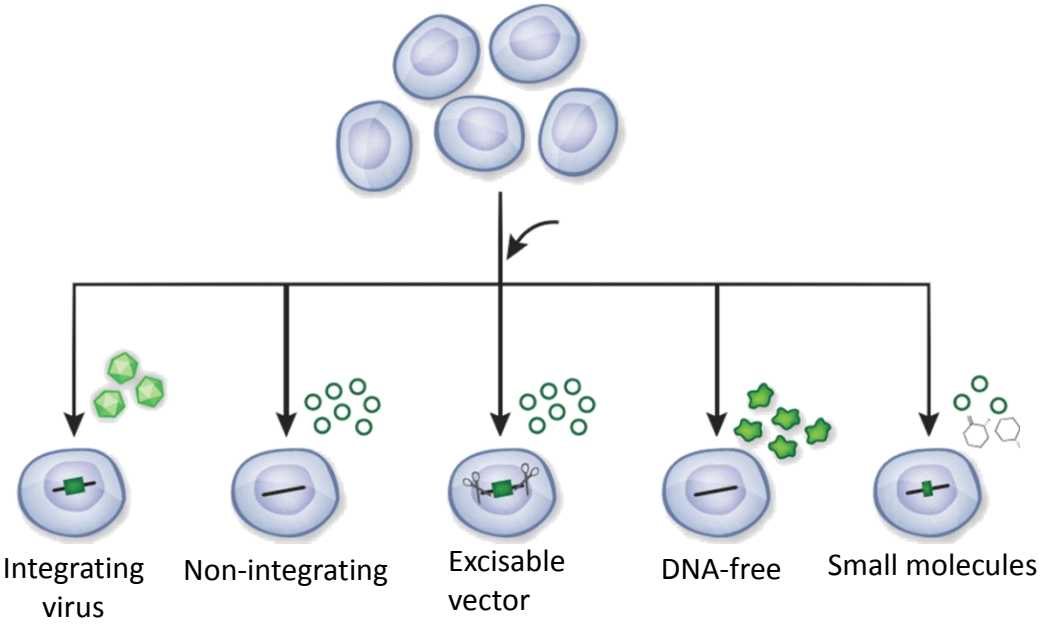

Figure 16. Different approaches for reprogramming factor delivery. Modified and Adopted from [23].

Recently, attempts to reprogram cells by delivering the reprogramming factors as purified recombinant proteins have been made to circumvent the use of nucleic acids. Although this method probably marks the future of iPS cell generation, so far the process is extremely inefficient and relies on addition of the small molecule valproic acid, a histone deacetylase inhibitor.

Similar to valproic acid, other compounds have been identified in chemical screens, which can improve the overall low efficiency of iPSC generation and in some cases even replace individual reprogramming factors [98].

3.3.2 MOLECULAR MECHANISMS OF REPROGRAMMING AND SELECTION OF APPROPRIATE CONTROLS

The process of reprogramming a cell from a somatic state to a pluripotent state is a highly complex and intangible process that is not yet fully understood. The exact conditions under which the reprogramming factors establish the settings in which the epigenetic state of the cell is reorganized remain elusive. A better understanding of what rearrangements happen in a cell during this process and exactly which pathways (related or non-related to pluripotency) are being modified is crucial to any application in humans, as this might have repercussions on how the cells will behave *in vivo*.

More general questions that still require a more thorough answer are how equal iPSCs actually are to hESCs on genomic and epigenomic levels and to what extent iPSC lines exhibit biological variability among themselves. As for the genetic level, several publications proved chromosomal aberrations [99], subchromosomal copy number variation [100] and point mutations in coding sequences [101]. In terms of epigenetic marking, it was shown that hiPSCs retain an epigenetic memory of their donor cells and that this influences their differentiation potential [102]. In-depth profiling and documentation of new iPSC lines is hence going to be crucial to assure comparability between results coming from cell lines generated in different laboratories.

In order for results generated with iPS-derived cells to be meaningful, the selection of proper controls is of the highest importance. Ideally, an age-matched, unaffected individual from the same pedigree is chosen, and even then, the controls may differ in their genetic background as every person carries disease-relevant polymorphisms. It is quite possible, that only mutation-corrected iPSC lines of the same individual are a satisfying control. However, genetic modification of hiPSC lines has remained challenging and cost-intensive due to the difficulty of targeting specific endogenous genes in hiPSC. Zinc-finger nucleases and transcription activator–like effector nucleases (TALENs) represent a new promising technology to significantly enhance the ability to genetically modify human iPSCs, due to the enzyme-mediated introduction of double-stranded breaks in genomic DNA at the site of a desired alteration [103, 104].

3.4 FINAL REMARKS

While at present human iPSCs serve mainly as *in vitro* models to study disease mechanisms and for drug screening, their future in cell transplantation studies is yet unclear and will depend on future research and how well issues concerning safety and efficacy of reprogramming as well as costliness of patient-specific generation, testing and monitoring of iPSCs under good manufacturing practice (GMP) will be addressed. Recently, it could be shown that fibroblasts can also be trans-differentiated (direct cell conversion), without the bypass of the potentially tumorigenic iPSC state, into neurons [105], cardiomyocytes [106] or blood progenitors[107]. This constitutes an interesting way to increase the safety of the technology, especially with eyes on potential future methods of *in vivo* reprogramming.

Yet, in all likelihood, iPSC technology will not be able to offer treatment for degenerative disease nor model all diseases for decades more than years. Despite this, one can be optimistic given the pace of big advances that the field of stem cell technology has experience ever since the discovery of induced pluripotent stem cells.

Part 4. ACKNOWLEGEMENTS

A lot of people were involved directly or indirectly in the successful completion of this work and it would not have been possible for me to write this thesis without the help and continuous support of the wonderful people around me. I could not possibly leave the institute without expressing my sincere gratitude.

First of all, I would like to thank my principal supervisor Prof. Karl-Ludwig Laugwitz for offering me the possibility to perform my Ph.D. studies in his Laboratory for Molecular Cardiology at the Klinikum rechts der Isar. I cannot put in words how much I appreciated the active support at all stages of the project. I am grateful for assistance in selecting collaborators, valuable advice and the outstanding freedom I was able to enjoy in the laboratory.

Everything I know about stem cell culture and how good experimental science is done, I learned through my direct supervisor Dr. Alessandra Moretti. I most highly appreciate all the significant contributions in time, ideas, and in reviewing data, that were necessary to make my Ph.D. experience productive and successful. Her joy and enthusiasm for research was contagious and motivational for me, even during tough times in the Ph.D. pursuit. I am also thankful for the excellent example of a successful scientist she set for me.

During the experimental work of this Ph.D. study a number of excellent scientists were involved in different aspects of the projects. I would like to especially thank Dr. Milena Bellin, Dr. Jason Lam and Dr. Tatjana Dorn who quickly became friends rather than colleagues.

Other past and present group members that I had the pleasure to work with or alongside are Dr. Harold Ayetey, Dr. Laura Iop, Dr. Thomas Brade, Jessica Haas and Elvira Parotta. I would like to thank Diana Grewe , Christina Scherb and Sabine Teuber for technical support.

A big thank you is owed to the people involved in our collaborations for their invaluable help with performing experiments relative to the CPVT and the LQT1 project. These were mainly PD Dr. Michael Mederos and Dr. Ursula Storch from the Pharmacology Department at the LMU Munich and Prof. Peter Lipp at the Universität des Saarlandes and PD Dr.Andrea Welling at the Department of Pharmacology of the TU Munich.

I would like to thank Prof. Steffen Massberg and Prof. Franz Hofmann for reading and evaluating this thesis and for agreeing to be part of my thesis defense committee.

Also and importantly, I would like to thank the Luxembourgish Fonds National de la Recherche for providing me with funding for this project in general and its publication.

Part 5. REFERENCES

1. Evans, M.J. and M.H. Kaufman, *Establishment in culture of pluripotential cells from mouse embryos.* Nature, 1981. **292**(5819): p. 154-6.

2. Thomson, J.A., et al., *Embryonic stem cell lines derived from human blastocysts.* Science, 1998. **282**(5391): p. 1145-7.

3. Eckfeldt, C.E., E.M. Mendenhall, and C.M. Verfaillie, *The molecular repertoire of the 'almighty' stem cell.* Nat Rev Mol Cell Biol, 2005. **6**(9): p. 726-37.

4. Waddington, C.H., *The Strategy of the Genes; a Discussion of Some Aspects of Theoretical Biology* ed. A. Unwin. 1957, London.

5. Ying, Q.L., et al., *BMP induction of Id proteins suppresses differentiation and sustains embryonic stem cell self-renewal in collaboration with STAT3.* Cell, 2003. **115**(3): p. 281-92.

6. James, D., et al., *TGFbeta/activin/nodal signaling is necessary for the maintenance of pluripotency in human embryonic stem cells.* Development, 2005. **132**(6): p. 1273-82.

7. Boyer, L.A., et al., *Core transcriptional regulatory circuitry in human embryonic stem cells.* Cell, 2005. **122**(6): p. 947-56.

8. Silva, J., et al., *Nanog is the gateway to the pluripotent ground state.* Cell, 2009. **138**(4): p. 722-37.

9. van den Berg, D.L., et al., *An Oct4-centered protein interaction network in embryonic stem cells.* Cell Stem Cell, 2010. **6**(4): p. 369-81.

10. Briggs, R. and T.J. King, *Transplantation of Living Nuclei From Blastula Cells into Enucleated Frogs' Eggs.* Proceedings of the National Academy of Sciences of the United States of America, 1952. **38**(5): p. 455-63.

11. Gurdon, J.B., *The developmental capacity of nuclei taken from intestinal epithelium cells of feeding tadpoles.* Journal of Embryology and Experimental Morphology, 1962. **10**: p. 622-40.

12. Wilmut, I., et al., *Viable offspring derived from fetal and adult mammalian cells.* Nature, 1997. **385**(6619): p. 810-3.

13. Cowan, C.A., et al., *Nuclear reprogramming of somatic cells after fusion with human embryonic stem cells.* Science, 2005. **309**(5739): p. 1369-73.

14. Do, J.T. and H.R. Scholer, *Nuclei of embryonic stem cells reprogram somatic cells.* Stem Cells, 2004. **22**(6): p. 941-9.

15. Strelchenko, N., et al., *Reprogramming of human somatic cells by embryonic stem cell cytoplast.* Reproductive Biomedicine Online, 2006. **12**(1): p. 107-11.

16. Takahashi, K. and S. Yamanaka, *Induction of pluripotent stem cells from mouse embryonic and adult fibroblast cultures by defined factors.* Cell, 2006. **126**(4): p. 663-76.

17. Takahashi, K., et al., *Induction of pluripotent stem cells from adult human fibroblasts by defined factors.* Cell, 2007. **131**(5): p. 861-72.

18. Yu, J., et al., *Induced pluripotent stem cell lines derived from human somatic cells.* Science, 2007. **318**(5858): p. 1917-20.

19. Nakagawa, M., et al., *Generation of induced pluripotent stem cells without Myc from mouse and human fibroblasts.* Nat Biotechnol, 2008. **26**(1): p. 101-6.

20. Huangfu, D., et al., *Induction of pluripotent stem cells from primary human fibroblasts with only Oct4 and Sox2.* Nat Biotechnol, 2008. **26**(11): p. 1269-75.

21. Kim, J.B., et al., *Oct4-induced pluripotency in adult neural stem cells.* Cell, 2009. **136**(3): p. 411-9.

22. Yamanaka, S., *Elite and stochastic models for induced pluripotent stem cell generation.* Nature, 2009. **460**(7251): p. 49-52.

23. Nagy, A. and K. Nagy, *The mysteries of induced pluripotency: where will they lead?* Nature Methods, 2010. **7**(1): p. 22-4.

24. Laugwitz, K.L., et al., *Islet1 cardiovascular progenitors: a single source for heart lineages?* Development, 2008. **135**(2): p. 193-205.

25. Buckingham, M., S. Meilhac, and S. Zaffran, *Building the mammalian heart from two sources of myocardial cells.* Nat Rev Genet, 2005. **6**(11): p. 826-35.

26. Srivastava, D., *Making or breaking the heart: from lineage determination to morphogenesis.* Cell, 2006. **126**(6): p. 1037-48.

27. Hutson, M.R. and M.L. Kirby, *Model systems for the study of heart development and disease. Cardiac neural crest and conotruncal malformations.* Semin Cell Dev Biol, 2007. **18**(1): p. 101-10.

28. Martin-Puig, S., Z. Wang, and K.R. Chien, *Lives of a heart cell: tracing the origins of cardiac progenitors.* Cell Stem Cell, 2008. **2**(4): p. 320-31.

29. Hoffman, J.I. and S. Kaplan, *The incidence of congenital heart disease.* J Am Coll Cardiol, 2002. **39**(12): p. 1890-900.

30. Bruneau, B.G., *The developmental genetics of congenital heart disease.* Nature, 2008. **451**(7181): p. 943-8.

31. Cai, C.L., et al., *Isl1 identifies a cardiac progenitor population that proliferates prior to differentiation and contributes a majority of cells to the heart.* Dev Cell, 2003. **5**(6): p. 877-89.

32. Laugwitz, K.L., et al., *Postnatal isl1+ cardioblasts enter fully differentiated cardiomyocyte lineages.* Nature, 2005. **433**(7026): p. 647-53.

33. Moretti, A., et al., *Multipotent embryonic isl1+ progenitor cells lead to cardiac, smooth muscle, and endothelial cell diversification.* Cell, 2006. **127**(6): p. 1151-65.

34. Sun, Y., et al., *Islet 1 is expressed in distinct cardiovascular lineages, including pacemaker and coronary vascular cells.* Dev Biol, 2007. **304**(1): p. 286-96.

35. Qyang, Y., et al., *The renewal and differentiation of Isl1+ cardiovascular progenitors are controlled by a Wnt/beta-catenin pathway.* Cell Stem Cell, 2007. **1**(2): p. 165-79.

36. Kattman, S.J., T.L. Huber, and G.M. Keller, *Multipotent flk-1+ cardiovascular progenitor cells give rise to the cardiomyocyte, endothelial, and vascular smooth muscle lineages.* Dev Cell, 2006. **11**(5): p. 723-32.

37. Wu, S.M., et al., *Developmental origin of a bipotential myocardial and smooth muscle cell precursor in the mammalian heart.* Cell, 2006. **127**(6): p. 1137-50.

38. Roden, D.M., *Clinical practice. Long-QT syndrome.* N Engl J Med, 2008. **358**(2): p. 169-76.

39. Sauer, A.J., et al., *Long QT syndrome in adults.* J Am Coll Cardiol, 2007. **49**(3): p. 329-37.

40. Saenen, J.B. and C.J. Vrints, *Molecular aspects of the congenital and acquired Long QT Syndrome: clinical implications.* J Mol Cell Cardiol, 2008. **44**(4): p. 633-46.

41. Crotti, L., et al., *Congenital long QT syndrome.* Orphanet J Rare Dis, 2008. **3**: p. 18.

42. Curran, M.E., et al., *A molecular basis for cardiac arrhythmia: HERG mutations cause long QT syndrome.* Cell, 1995. **80**(5): p. 795-803.

43. Sanguinetti, M.C., et al., *Coassembly of K(V)LQT1 and minK (IsK) proteins to form cardiac I(Ks) potassium channel.* Nature, 1996. **384**(6604): p. 80-3.

44. Sanguinetti, M.C., et al., *Isoproterenol antagonizes prolongation of refractory period by the class III antiarrhythmic agent E-4031 in guinea pig myocytes. Mechanism of action.* Circulation Research, 1991. **68**(1): p. 77-84.

45. Walsh, K.B. and R.S. Kass, *Regulation of a heart potassium channel by protein kinase A and C.* Science, 1988. **242**(4875): p. 67-9.

46. Jurkiewicz, N.K. and M.C. Sanguinetti, *Rate-dependent prolongation of cardiac action potentials by a methanesulfonanilide class III antiarrhythmic agent. Specific block of rapidly activating delayed rectifier K+ current by dofetilide.* Circulation Research, 1993. **72**(1): p. 75-83.

47. Priori, S.G. and S.R. Chen, *Inherited dysfunction of sarcoplasmic reticulum Ca2+ handling and arrhythmogenesis.* Circ Res, 2011. **108**(7): p. 871-83.

48. Rogers, E.F., F.R. Koniuszy, and et al., *Plant insecticides; ryanodine, a new alkaloid from Ryania speciosa Vahl.* Journal of the American Chemical Society, 1948. **70**(9): p. 3086-8.

49. Jenden, D.J. and A.S. Fairhurst, *The pharmacology of ryanodine.* Pharmacological Reviews, 1969. **21**(1): p. 1-25.

50. Swan, H., et al., *Arrhythmic disorder mapped to chromosome 1q42-q43 causes malignant polymorphic ventricular tachycardia in structurally normal hearts.* Journal of the American College of Cardiology, 1999. **34**(7): p. 2035-42.

51. Priori, S.G., et al., *Mutations in the cardiac ryanodine receptor gene (hRyR2) underlie catecholaminergic polymorphic ventricular tachycardia.* Circulation, 2001. **103**(2): p. 196-200.

52. Greenstein, J.L. and R.L. Winslow, *Integrative systems models of cardiac excitation-contraction coupling.* Circulation Research, 2011. **108**(1): p. 70-84.

53. Wehrens, X.H., et al., *FKBP12.6 deficiency and defective calcium release channel (ryanodine receptor) function linked to exercise-induced sudden cardiac death.* Cell, 2003. **113**(7): p. 829-40.

54. George, C.H., G.V. Higgs, and F.A. Lai, *Ryanodine receptor mutations associated with stress-induced ventricular tachycardia mediate increased calcium release in stimulated cardiomyocytes.* Circulation Research, 2003. **93**(6): p. 531-40.

55. Jiang, D., et al., *Enhanced store overload-induced Ca2+ release and channel sensitivity to luminal Ca2+ activation are common defects of RyR2 mutations linked to ventricular tachycardia and sudden death.* Circulation Research, 2005. **97**(11): p. 1173-81.

56. Liu, N., et al., *Arrhythmogenesis in catecholaminergic polymorphic ventricular tachycardia: insights from a RyR2 R4496C knock-in mouse model.* Circulation Research, 2006. **99**(3): p. 292-8.

57. Xiao, J., et al., *Removal of FKBP12.6 does not alter the conductance and activation of the cardiac ryanodine receptor or the susceptibility to stress-induced ventricular arrhythmias.* J Biol Chem, 2007. **282**(48): p. 34828-38.

58. Guo, T., et al., *Kinetics of FKBP12.6 binding to ryanodine receptors in permeabilized cardiac myocytes and effects on Ca sparks.* Circulation Research, 2010. **106**(11): p. 1743-52.

59. Jiang, D., et al., *RyR2 mutations linked to ventricular tachycardia and sudden death reduce the threshold for store-overload-induced Ca2+ release (SOICR).* Proceedings of the National Academy of Sciences of the United States of America, 2004. **101**(35): p. 13062-7.

60. Yamamoto, T., R. El-Hayek, and N. Ikemoto, *Postulated role of interdomain interaction within the ryanodine receptor in Ca(2+) channel regulation.* J Biol Chem, 2000. **275**(16): p. 11618-25.

61. Liu, Z., et al., *Dynamic, inter-subunit interactions between the N-terminal and central mutation regions of cardiac ryanodine receptor.* J Cell Sci, 2010. **123**(Pt 10): p. 1775-84.

62. Paul-Pletzer, K., et al., *Identification of a dantrolene-binding sequence on the skeletal muscle ryanodine receptor.* J Biol Chem, 2002. **277**(38): p. 34918-23.

63. Paul-Pletzer, K., et al., *Probing a putative dantrolene-binding site on the cardiac ryanodine receptor.* Biochem J, 2005. **387**(Pt 3): p. 905-9.

64. Kobayashi, S., et al., *Dantrolene, a therapeutic agent for malignant hyperthermia, markedly improves the function of failing cardiomyocytes by stabilizing interdomain interactions within the ryanodine receptor.* J Am Coll Cardiol, 2009. **53**(21): p. 1993-2005.

65. Uchinoumi, H., et al., *Catecholaminergic polymorphic ventricular tachycardia is caused by mutation-linked defective conformational regulation of the ryanodine receptor.* Circ Res, 2010. **106**(8): p. 1413-24.

66. Kobayashi, S., et al., *Dantrolene, a therapeutic agent for malignant hyperthermia, inhibits catecholaminergic polymorphic ventricular tachycardia in a RyR2(R2474S/+) knock-in mouse model.* Circ J, 2010. **74**(12): p. 2579-84.

67. Marx, S.O., et al., *Requirement of a macromolecular signaling complex for beta adrenergic receptor modulation of the KCNQ1-KCNE1 potassium channel.* Science, 2002. **295**(5554): p. 496-9.

68. Moretti, A., et al., *Mouse and human induced pluripotent stem cells as a source for multipotent Isl1+ cardiovascular progenitors.* Faseb J, 2010. **24**(3): p. 700-11.

69. Jung, C.B., et al., *Dantrolene rescues arrhythmogenic RYR2 defect in a patient-specific stem cell model of catecholaminergic polymorphic ventricular tachycardia.* EMBO Molecular Medicine, 2011.

70. Moretti, A., et al., *Patient-specific induced pluripotent stem-cell models for long-QT syndrome.* New England Journal of Medicine, 2010. **363**(15): p. 1397-409.

71. Yazawa, M., et al., *Using induced pluripotent stem cells to investigate cardiac phenotypes in Timothy syndrome.* Nature, 2011. **471**(7337): p. 230-4.

72. Carvajal-Vergara, X., et al., *Patient-specific induced pluripotent stem-cell-derived models of LEOPARD syndrome.* Nature, 2010. **465**(7299): p. 808-12.

73. Itzhaki, I., et al., *Modelling the long QT syndrome with induced pluripotent stem cells.* Nature, 2011. **471**(7337): p. 225-9.

74. Eminli, S., et al., *Reprogramming of neural progenitor cells into induced pluripotent stem cells in the absence of exogenous Sox2 expression.* Stem Cells, 2008. **26**(10): p. 2467-74.

75. Maherali, N., et al., *Directly reprogrammed fibroblasts show global epigenetic remodeling and widespread tissue contribution.* Cell Stem Cell, 2007. **1**(1): p. 55-70.

76. Aasen, T., et al., *Efficient and rapid generation of induced pluripotent stem cells from human keratinocytes.* Nat Biotechnol, 2008. **26**(11): p. 1276-84.

77. Aoi, T., et al., *Generation of pluripotent stem cells from adult mouse liver and stomach cells.* Science, 2008. **321**(5889): p. 699-702.

78. Sun, N., et al., *Feeder-free derivation of induced pluripotent stem cells from adult human adipose stem cells.* Proceedings of the National Academy of Sciences of the United States of America, 2009. **106**(37): p. 15720-5.

79. Loh, Y.H., et al., *Reprogramming of T cells from human peripheral blood.* Cell Stem Cell, 2010. **7**(1): p. 15-9.

80. Staerk, J., et al., *Reprogramming of human peripheral blood cells to induced pluripotent stem cells.* Cell Stem Cell, 2010. **7**(1): p. 20-4.

81. Seki, T., et al., *Generation of induced pluripotent stem cells from human terminally differentiated circulating T cells.* Cell Stem Cell, 2010. **7**(1): p. 11-4.

82. Haile, R.W., et al., *A molecular/epidemiologic analysis of expression of cyclooxygenases 1 and 2, use of nonsteroidal antiinflammatory drugs, and risk of colorectal adenoma.* Clinical Colorectal Cancer, 2005. **4**(6): p. 390-5.

83. Ma, B., et al., *Comparison of the protein-protein interfaces in the p53-DNA crystal structures: towards elucidation of the biological interface.* Proceedings of the National Academy of Sciences of the United States of America, 2005. **102**(11): p. 3988-93.

84. Okita, K., et al., *Generation of mouse induced pluripotent stem cells without viral vectors.* Science, 2008. **322**(5903): p. 949-53.

85. Stadtfeld, M., et al., *Induced pluripotent stem cells generated without viral integration.* Science, 2008. **322**(5903): p. 945-9.

86. wapek, V.V. and P. Chvosta, *Consistent approximations in generalized-master-equation theories: Application to the asymptotic-time symmetry-breaking problem.* Phys Rev A, 1991. **43**(6): p. 2819-2826.

87. C, W.B., *Cancer Research.* Science, 1912. **35**(913): p. 979-80.

88. C, W.S., *Pictures in cell biology Microtubule dynamics in migrating cells.* Trends in Cell Biology, 1997. **7**(10): p. 407.

89. Robins, H., et al., *A relative-entropy algorithm for genomic fingerprinting captures host-phage similarities.* Journal of Bacteriology, 2005. **187**(24): p. 8370-4.

90. C, W.W., *The Total Eclipse of September 9, 1904.* Science, 1904. **20**(519): p. 812.

91. Waddington, C., et al., *Open-label, randomised, parallel-group, multicentre study to evaluate the safety, tolerability and immunogenicity of an AS03(B)/oil-in-water emulsion-adjuvanted (AS03(B)) split-virion versus non-adjuvanted whole-virion H1N1 influenza vaccine in UK children 6 months to 12 years of age.* Health Technology Assessment, 2010. **14**(46): p. 1-130.

92. Klemm, P., et al., *Unleashing animal-assisted therapy.* Nursing, 2010. **40**(10): p. 12-3.

93. Nilsen, B.S., et al., *Fragmentation cross sections of relativistic 8436Kr and 10947Ag nuclei in targets from hydrogen to lead.* Phys Rev C Nucl Phys, 1995. **52**(6): p. 3277-3290.

94. Geer, L.Y., et al., *Charge-changing fragmentation of 10.6 GeV/nucleon 197Au nuclei.* Phys Rev C Nucl Phys, 1995. **52**(1): p. 334-345.

95. McKennis, A.T. and C. Waddington, *Thyroplasty type I for unilateral vocal cord paralysis.* AORN Journal, 1994. **60**(1): p. 38-42.

96. Chen, C., et al., *Interactions in hydrogen of relativistic neon to nickel projectiles: Total charge-changing cross sections.* Phys Rev C Nucl Phys, 1994. **49**(6): p. 3200-3210.

97. McKennis, A.T. and C. Waddington, *Unilateral vocal cord paralysis.* ORL-Head and Neck Nursing, 1994. **12**(1): p. 9.

98. Desponts, C. and S. Ding, *Using small molecules to improve generation of induced pluripotent stem cells from somatic cells.* Methods in Molecular Biology, 2010. **636**: p. 207-18.

99. Mayshar, Y., et al., *Identification and classification of chromosomal aberrations in human induced pluripotent stem cells.* Cell Stem Cell, 2010. **7**(4): p. 521-31.

100. Hussein, S.M., et al., *Copy number variation and selection during reprogramming to pluripotency.* Nature, 2011. **471**(7336): p. 58-62.

101. Gore, A., et al., *Somatic coding mutations in human induced pluripotent stem cells.* Nature, 2011. **471**(7336): p. 63-7.

102. Bar-Nur, O., et al., *Epigenetic memory and preferential lineage-specific differentiation in induced pluripotent stem cells derived from human pancreatic islet Beta cells.* Cell Stem Cell, 2011. **9**(1): p. 17-23.

103. Binns, W.R., et al., *Charge, mass, and energy changes during fragmentation of relativistic nuclei.* Phys Rev C Nucl Phys, 1989. **39**(5): p. 1785-1798.

104. Waddington, C.J., et al., *Stopping of relativistic heavy ions in various media.* Phys Rev A, 1986. **34**(5): p. 3700-3706.

105. Vierbuchen, T., et al., *Direct conversion of fibroblasts to functional neurons by defined factors.* Nature, 2010. **463**(7284): p. 1035-41.

106. Ieda, M., et al., *Direct reprogramming of fibroblasts into functional cardiomyocytes by defined factors.* Cell, 2010. **142**(3): p. 375-86.

107. Szabo, E., et al., *Direct conversion of human fibroblasts to multilineage blood progenitors.* Nature, 2010. **468**(7323): p. 521-6.

Part 6. ARTICLES

MOUSE AND HUMAN INDUCED PLURIPOTENT STEM CELLS AS A SOURCE FOR MULTIPOTENT ISL1+ CARDIOVASCULAR PROGENITORS FASEB J. 2010 MAR;24(3):700-11.

PATIENT-SPECIFIC INDUCED PLURIPOTENT STEM-CELL MODELS FOR LONG-QT SYNDROME. N ENGL J MED. 2010 OCT 7;363(15):1397-409.

DANTROLENE RESCUES ARRHYTHMOGENIC RYR2 DEFECT IN A PATIENT-SPECIFIC STEM CELL MODEL OF CATECHOLAMINERGIC POLYMORPHIC VENTRICULAR TACHYCARDIA. EMBO MOL MED. 2012 MAR;4(3):180-91.

Mouse and human induced pluripotent stem cells as a source for multipotent Isl1$^+$ cardiovascular progenitors

Alessandra Moretti,*[,1] Milena Bellin,*[,1] Christian B. Jung,*[,1] Tu-Mai Thies,* Yasuhiro Takashima,[§] Alexandra Bernshausen,* Matthias Schiemann,[†] Stefanie Fischer,[‡] Sven Moosmang,[‡] Austin G. Smith,[§] Jason T. Lam,*[,2] and Karl-Ludwig Laugwitz*[,2]

*Klinikum rechts der Isar and Deutsches Herzzentrum, Medical Department, Molecular Cardiology, [†]Institute of Medical Microbiology, Immunology, and Hygiene, and [‡]Institute of Pharmacology, Technical University of Munich, Munich, Germany; and [§]Wellcome Trust Centre for Stem Cell Research, University of Cambridge, Cambridge, UK

ABSTRACT **Ectopic expression of defined sets of genetic factors can reprogram somatic cells to create induced pluripotent stem (iPS) cells. The capacity to direct human iPS cells to specific differentiated lineages and to their progenitor populations can be used for disease modeling, drug discovery, and eventually autologous cell replacement therapies. During mouse cardiogenesis, the major lineages of the mature heart, cardiomyocytes, smooth muscle cells, and endothelial cells arise from a common, multipotent cardiovascular progenitor expressing the transcription factors Isl1 and Nkx2.5. Here we show, using genetic fate-mapping, that Isl1$^+$ multipotent cardiovascular progenitors can be generated from mouse iPS cells and spontaneously differentiate in all 3 cardiovascular lineages *in vivo* without teratoma. Moreover, we report the identification of human iPS-derived ISL1$^+$ progenitors with similar developmental potential. These results support the possibility to use patient-specific iPS-generated cardiovascular progenitors as a model to elucidate the pathogenesis of congenital and acquired forms of heart diseases.—Moretti, A., Bellin, M., Jung, C. B., Thies, T.-M., Takashima, Y., Bernshausen, A., Schiemann, M., Fischer, S., Moosmang, S., Smith, A. G., Lam, J. T., Laugwitz, K.-L. Mouse and human induced pluripotent stem cells as a source for multipotent Isl1$^+$ cardiovascular progenitors. *FASEB J.* 24, 700–711 (2010). www.fasebj.org**

Key Words: iPS cells · reprogramming · cardiac development · regenerative medicine

FORMATION OF THE MATURE multichambered heart requires the contribution of diverse cell types with specialized functions, including cardiomyocytes, endothelial cells, and vascular smooth muscle cells. Studies of mouse embryos and the embryonic stem (ES) cell system have provided evidence indicating that these 3 lineages develop from a common multipotent cardiovascular progenitor that represents one of the earliest stages in cardiac mesoderm specification (1–3). This multipotent cardiac precursor can be identified by expression of the transcription factors Isl1 and Nkx2.5, key regulators of the cardiogenic program, and the surface receptor Flk1, one of the earliest mesodermal differentiation markers for the endothelial and blood lineages (1, 2, 4). The ability to isolate and selectively expand multipotent Isl1$^+$ progenitors offers a powerful cell-based *in vitro* system that allows rapid and direct characterization of signaling pathways controlling renewal, lineage specification, and differentiation during cardiogenesis (5–7). Generation of cardiovascular progenitors and differentiated cardiac cell types from human cell sources would form the basis for establishing heart disease models to develop technologies, such as drug screening, tissue engineering, and eventually new therapeutic strategies, for restoring cardiac functions in a variety of degenerative heart diseases (8, 9).

The recent landmark discovery that mouse and human somatic cells can be reprogrammed to a ground state of pluripotency by ectopic expression of only a few defined transcription factors (10–16) offers a novel fascinating route to patient-specific pluripotent cells, without the technical and ethical limitations of somatic cell nuclear transfer. In the past months, generation of induced pluripotent stem (iPS) cells from individual patients harboring a variety of both simple and complex genetic disorders has been reported (17–20). It has been found that iPS cells closely resemble ES cells in gene expression, pluripotency, and epigenetic state (21). However, for iPS cells to fulfill their potential for *in vitro* disease modeling and regenerative medicine, efficient differentiation protocols to derive specific cell lineages need to be established. Recent studies have shown that mouse iPS cells can be efficiently directed into hematopoietic and neuronal precursors able to give rise to a variety of differentiated cell types of the blood and nervous system *in vitro* and *in vivo* (22, 23).

[1] These authors contributed equally to this work.

[2] Correspondence: Klinikum rechts der Isar and Deutsches Herzzentrum, Technical University of Munich, I. Medical Department, Molecular Cardiology, Ismaninger Strasse 22, 81675 Munich, Germany. E-mail: K.-L.L., klaugwitz@med1.med.tum.de; J.T.L., jtlam@med1.med.tum.de

doi: 10.1096/fj.09-139477

0892-6638/10/0024-0700 © FASEB

The aim of the current study was to test whether iPS cells could be a source of Isl1$^+$ cardiovascular progenitors that display multipotency into all 3 cardiovascular lineages *in vitro* and *in vivo*. As proof of principle, we first generated iPS cells from Isl1-Cre/R26R-YFP or -LacZ double-heterozygous mice, which are genetically marked to allow identification and purification of Isl1-expressing cells and their differentiated progeny. Through transcriptional profiling of purified mouse YFP$^+$ cells at different developmental stages we identified the Isl1$^+$ cardiovascular precursor state and proved its multipotency by spontaneous differentiation *in vivo*. Using skin fibroblasts from 2 healthy individuals we produced human iPS (hiPS) cell lines possessing a gene expression signature similar to that of human ES cells and able to differentiate into cell types of all 3 germ layers. We have used these iPS cells to efficiently generate individual-specific ISL1$^+$ cardiovascular progenitors and functional cardiac myocytes.

These results represent a first step toward the generation of patient-specific iPS-cell-based ISL1$^+$ cardiovascular precursors, which would be extremely valuable in designing disease-specific assays for screening of drug cardiotoxicity, in identifying and validating therapeutic targets, and in studying mechanisms of cardiovascular disorders. Furthermore, the accessibility of patient-specific iPS-cell-derived cardiac progenitors may represent a significant advantage over differentiated cells or pluripotent stem cells to achieve large-scale production of multipotent, tumor-free cardiac cells for clinical and translational applications in the future.

MATERIALS AND METHODS

Mice

Isl1-Cre mice were generously provided by Sylvia Evans (University of California–San Diego, La Jolla, CA, USA) (24). The conditional Cre reporter mouse lines R26R-LacZ and R26R-YFP were generated by Philippe Soriano (Mt. Sinai School of Medicine, New York, NY, USA) (25) and Frank Costantini (Columbia University Medical Center, New York, NY, USA) (26), respectively. Isl1-Cre/R26R double-heterozygous mice were generated by crossing single-heterozygous mice. Mice are in a mixed 129 × C57Bl/6 background.

Cell culture

For isolation of dermal fibroblasts, skin from newborn Isl1-Cre/R26R mice and human dermal biopsies were minced into 2-mm pieces, placed on culture dishes, and incubated in Quantum 333 medium (PAA, Pasching, Austria). Cells migrating out of the explants were passaged in DMEM containing 10% FBS and used at passage 4 for iPS cell induction. Mouse iPS cells were grown on mitomycin-C-treated murine embryonic fibroblasts (MEF feeders) in standard ES medium [DMEM supplemented with 2 mM L-glutamine, 0.1 mM nonessential amino acids, 1 mM sodium pyruvate, 0.1 mM β-mercaptoethanol, 50 U/ml penicillin, 50 μg/ml streptomycin, and 0.1 μg/ml leukemia inhibitory factor (LIF)] containing 15% knockout serum replacement (KSR; Invitrogen, Karlsruhe, Germany) for 5 passages and then maintained in ES medium containing 15% FBS. Human iPS cells were grown on MEF feeders in human ES medium consisting of DMEM/F12 supplemented with 20% KSR, 2 mM L-glutamine, 0.1 mM nonessential amino acids, 0.1 mM β-mercaptoethanol, 50 U/ml penicillin, 50 μg/ml streptomycin, and 10 ng/ml human b-FGF (R&D System, Minneapolis, MN, USA). Human research subject protocol was approved by the institutional review boards and the ethics committee of both the Klinikum rechts der Isar and the Technical University of Munich.

Retroviral production and iPS cell induction

Isl1-Cre/R26R skin fibroblasts were infected overnight with pooled equal volumes of viral supernatants (supplemented with 8 μg/ml polybrene) generated by independent tranfections of HEK293T cells (Fugene HD; Roche, Basel, Switzerland) with pMXs-based retroviral vectors for the mouse *Oct4, Sox2, Klf4, and c-Myc* (Addgene plasmids 13366, 13367, 13370, and 13375; Addgene, Cambridge, MA, USA) and the packaging plasmid pCL-Eco (Addgene plasmid 12371) in DMEM containing 10% FBS, as previously reported (27). Four days after infection, skin fibroblasts were reseeded on MEF feeders (0.5×10^5 cells/10-cm dish for fibroblasts transduced with all 4 factors, and 3.5×10^5 cells/10-cm dish for fibroblasts transduced with 3 factors in absence of *c-Myc*) and maintained in ES medium supplemented with 15% KSR. Medium was changed every day, and colonies were picked for expansion at d 16 and 30 after 4-factor and 3-factor transduction, respectively. For human iPS cell induction, retroviruses for the 4 factors were independently produced by transfecting HEK293T cells (Fugene HD) with pMXs vectors encoding for the human *OCT4, SOX2, KLF4,* and *c-MYC* (Addgene plasmids 17217, 17218, 17219, and 17220) and the combination of moloney gag-pol plasmid pUMVC (Addgene plasmid 8449) and VSV envelope plasmid (Addgene plasmid 8454) in DMEM containing 10% FBS. Viral supernatants were harvested after 48 and 72 h, filtered through a 0.45-μm low-protein-binding cellulose acetate filter, concentrated by a spin column (Millipore, Billerica, MA, USA), and used directly to infect twice (24 h apart) 1.5×10^5 human fibroblasts in the presence of 8 μg/ml polybrene. After 6 d, cells were seeded on MEF feeders at the density of 5×10^4 cells/10-cm dish and cultured for 4 additional weeks in human ES medium before iPS colonies were manually picked.

Teratoma formation

We injected 0.5×10^6 mouse iPS cells in the left ventricular myocardium of SCID nude mice, and 4 wk later hearts were fixed in 4% formaldehyde and embedded in paraffin. Sections were stained with hematoxylin and eosin.

Chimera generation

After injection of 8–10 Isl1-Cre/R26R iPS cells in each blastocyst isolated from C57Bl/6 mice, blastocysts were transferred into E2.5 pseudo-pregnant CD1 females, and chimeras were analyzed at embryonic day 13–14 or after birth by YFP fluorescence or LacZ staining.

Immunohistochemistry, LacZ, and AP staining

Cells in culture and heart cryosections (10 μm) were fixed with 3.7% formaldehyde and subjected to specific immunostaining by using the following primary antibodies: mouse Nanog (1:500, rabbit polyclonal; Novus Biologicals, Littleton, CO, USA), human Nanog (1:500, rabbit polyclonal; Abcam, Cambridge, UK), TRA1–81-Alexa-Fluor-488-conjugated (1:20, mouse monoclonal; BD Pharmingen, San Diego, CA,

USA), Isl1 (1.5–2 μg/ml, mouse monoclonal antibody, clone 39.4D5; Developmental Hybridoma Bank, Iowa City, IA, USA), Nkx2.5 (1:100, rabbit polyclonal H114; Santa Cruz, Santa Cruz, CA, USA), human FLK1-FITC-conjugated (2.5 μg/ml, mouse monoclonal, clone 89106; R&D System), YFP (3 μg/ml, rabbit polyclonal; Acris, Herford, Germany), cardiac troponin T (0.4 μg/ml, mouse monoclonal clone 13-11; NeoMarkers, Fremont, CA, USA), α-actinin (1:300, mouse monoclonal, clone EA-53; Sigma, Munich, Germany), smooth muscle myosin heavy chain (1:100, rabbit polyclonal; Biomedical Technologies, Stoughton, MA, USA), smooth muscle actin (SMA; 1:400, mouse monoclonal, clone 1A4; Sigma), human CD31-PE conjugated (2.5 μg/ml, mouse monoclonal, clone 9G11; R&D System), mouse CD31 (5 μg/ml, rat monoclonal, clone MEC13.3; RDI, Concord, MA, USA), and mouse VE-cadherin (5 μg/ml, rat monoclonal, clone CW24; RDI). Alexa Fluor 488 (green), Alexa Fluor 594 (red), and Alexa Fluor 647 (cyan) -conjugated secondary antibodies specific to the appropriate species were used (1:500; Invitrogen). Nuclei were detected with 1 μg/ml Hoechst 33528. LacZ staining was performed on chimeras and cultured cells after fixation with 0.2% glutaraldehyde, by incubation in X-Gal solution containing 1.25 mM $K_3(Fe(CN)_6)$, 1.25 mM $K_4(Fe(CN)_6)$, 2 mM $MgCl_2$, 0.02% Nonidet P-40, and 0.25 mg/ml X-Gal in phosphate-buffered saline, pH 7.4. Direct AP activity was analyzed using the NBT/BCIP alkaline phosphatase blue substrate (Roche), according to the manufacturer's guidelines.

Microscopy was performed using a DMI6000-AF6000 Leica imaging system (Leica Microsystems, Wetzlar, Germany).

In vitro differentiation

Mouse iPS cells were differentiated as embryoid bodies (EBs) generated by aggregation of 6×10^4 cells/ml of ES cell

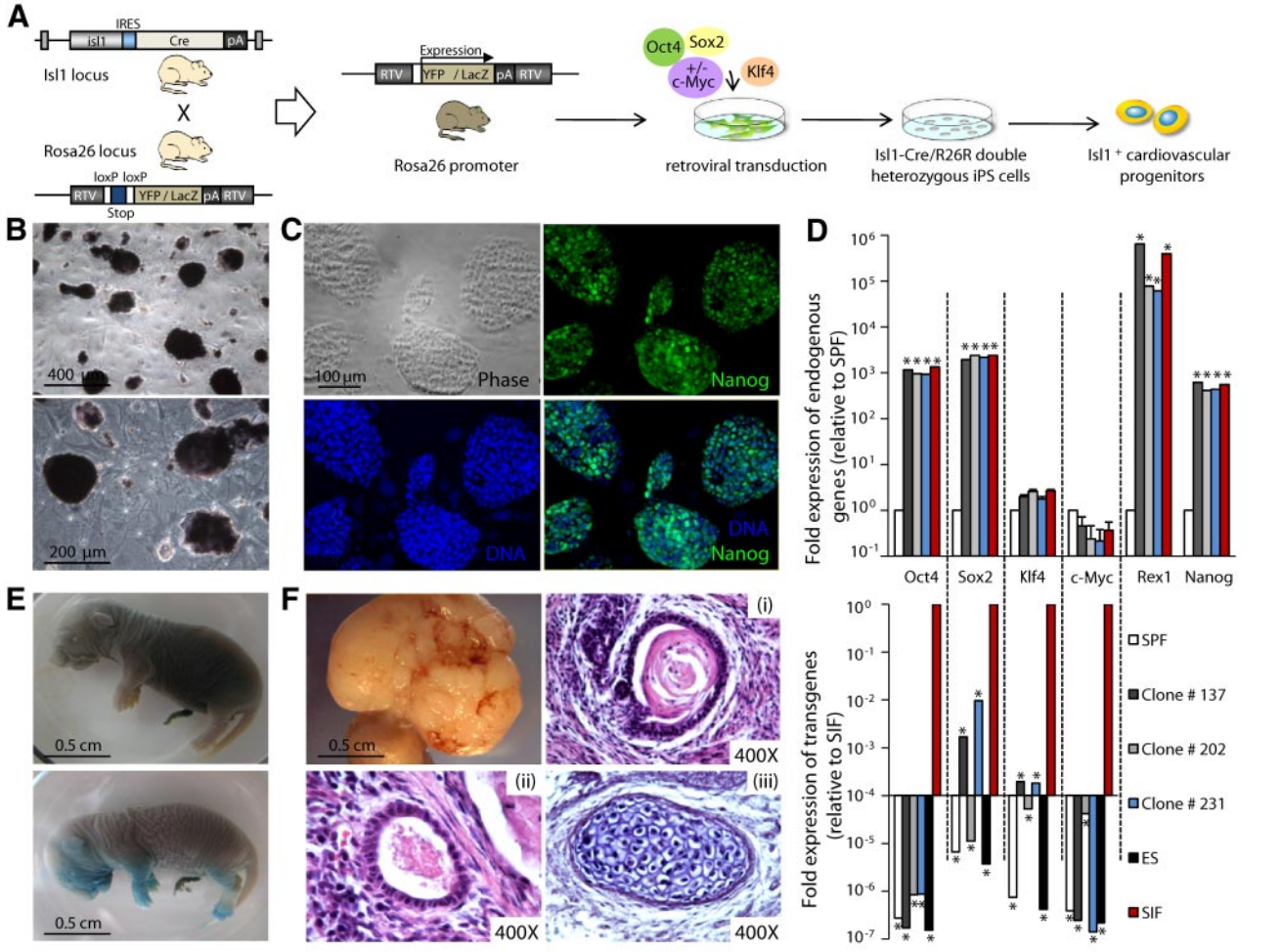

Figure 1. Generation of iPS cells from Isl1-Cre/R26R-indicator double-heterozygous mice. *A*) Scheme for *in vitro* reprogramming of skin fibroblasts with 3 or 4 defined transcription factors to generate genetically marked $Isl1^+$ cardiovascular progenitors. Isl1-Cre mice were crossed into the conditional Cre reporter strains R26R-YFP or R26R-LacZ, in which Cre-mediated removal of a stop sequence results in the ubiquitous expression of YFP or β-galactosidase under the control of the endogenous Rosa26 promoter. *B, C*) Representative Isl1-Cre/R26R-LacZ iPS clone (clone 137) stably expressing alkaline phosphatase (*B*) and Nanog (*C*). *D*) Quantitative RT-PCR for expression levels of endogenous genes of pluripotency (top panel) and retroviral transgenes (bottom panel) in 3 representative iPS clones, 137 (Isl1-Cre/R26R-LacZ, 4-factor reprogramming), 202 (Isl1-Cre/R26R-YFP, 4-factor reprogramming), and 231 (Isl1-Cre/R26R-YFP, 3-factor reprogramming), compared to ES cells. Relative gene expression to skin parental fibroblasts (SPF) or SPF after retroviral infection (SIF) are presented, $n = 3$. $^*P < 0.05$ *vs.* SPF (top panel) and SIF (bottom panel). *E*) Whole-mount X-Gal staining of neonatal pups from injection of iPS cells (clone 137) into blastocysts, showing chimera (bottom panel) and nonchimeric littermate (top panel). *F*) Teratoma derived from intramyocardial injection of 0.5×10^6 iPS cells (clone 202) containing derivatives of all 3 germ layers, such as skin (*i*) and intestinal epithelium (*ii*) and cartilage (*iii*).

medium containing 15% FBS (without LIF) in low attachment plates coated with 5% poly-HEMA (Sigma). For single cell analysis, EBs were dissociated at 37°C with 0.25% trypsin for 5 min (EBs at 3 to 7 d) or with 480 U/ml collagenase type II (Worthington, Lakewood, NJ, USA) for 20 min (EBs after d 7). Dissociated cells were plated on fibronectin-coated plastic cover slides for immunohistochemical analysis or subjected directly to fluorescence-activated cell sorting (FACS) analysis. For generation of human iPS cell EBs, iPS colonies were dissociated into clumps using PBS containing 2.5 mg/ml trypsin (USB, Staufen, Germany), 1 mg/ml collagenase IV (Invitrogen), 20% KSR, and 1 mM $CaCl_2$ (10 min at 37°C) and maintained for 3 d in MEF-conditioned human ES medium in low attachment plates. For spontaneous differentiation, medium was then replaced with DMEM/F12 supplemented with 20% FBS, 2 mM L-glutamine, 0.1 mM nonessential amino acids, 0.1 mM β-mercaptoethanol, 50 U/ml penicillin, and 50 μg/ml streptomycin, and EBs were analyzed at d 15 for expression of marker genes of the 3 different germ layers. To improve cardiac differentiation, ascorbic acid (50 μg/ml) was added to the medium, and EBs were plated at d 7 on gelatin-coated dishes for better detection of beating foci. Dissociation of human iPS-cell-derived EBs into single cells was performed as described above for the mouse. For induction of human cardiac progenitors, iPS cells were seeded on MEF feeders and, 1 d later, treated for 4 d with 10 ng/ml human BMP2 (R&D) and 1 μM SU5402 FGF receptor inhibitor (Calbiochem, Darmstadt, Germany) in RPMI 1640 medium supplemented with 2 mM L-glutamine and 2% B27 supplement without vitamin A (Invitrogen), as described previously (28). Conversion of human cardiac progenitors into myocytes and vascular cells (endothelial and smooth muscle cells) was induced by supplementing the culture medium with 50 μg/ml ascorbic acid and 10 ng/ml human VEGF (R&D System).

Flow cytometry analysis

On Isl1-Cre/R26R-YFP EB differentiation, cells were sorted into YFP^+ and YFP^- populations using a BD FACS ARIA (BD Biosciences, San Diego, CA, USA) and used for quantitative RT-PCR or plated on fibronectin-coated plastic cover slides for immunohistochemical analysis. FACS analysis was performed with FACS DIVA 6.1.1 (BD Biosciences).

Quantitative real-time PCR

Total mRNA was isolated using the Stratagene Absolutely RNA kit, and 1 μg was used to synthesize cDNA using the High-Capacity cDNA Reverse Transcrition kit (Applied Biosystems, Foster City, CA, USA). Gene expression was quantified by qPCR using 1 μl of the RT reaction and the Power SYBR Green PCR Master Mix or the TaqMan Universal PCR Master Mix from Applied Biosystems. A list of the primers and TaqMan assays is provided as Supplemental Table 1. Gene expression levels were normalized to *MrpS15* and to *GAPDH* for mouse and human, respectively.

In vivo differentiation and graft size assessment

YFP^+ cells (0.5 and 1×10^6) obtained by FACS sorting of dissociated Isl1-Cre/R26R-YFP EBs at d 4.5 of differentiation were resuspended in 30–50 μl of Hanks's balanced salt solution and injected into the left ventricular wall of SCID nude mice after left thoracotomy. Hearts were harvested at 5 and 12 wk after cell transplantation, equilibrated in PBS containing 0.3 M KCl, and embedded in optimal cutting temperature (OCT) compound for cryosectioning. Assessment of graft size was performed by counting YFP^+ cells present in a randomly chosen 0.15 mm^2 area every 100 μm in each transplanted heart and extrapolating the total number within the heart volume between the first and last sections containing YFP^+ cells.

Statistical analysis

All data were expressed as means ± SE from independent experiments. Differences between groups were examined for statistical analysis using a 2-tailed Student's *t* test. Values of $P < 0.05$ were considered significant.

RESULTS

Generation of iPS cells from Isl1-Cre/R26R-YFP and -LacZ double-heterozygous mice

To achieve an irreversible marking of $Isl1^+$ cardiovascular precursors and their progeny during iPS cell differentiation, we reprogrammed skin fibroblasts from both double-heterozygous Isl1-Cre/R26R-YFP- and Isl1-Cre/R26R-LacZ-indicator mice (**Fig. 1*A***). Isl1-Cre/R26R-YFP double-heterozygous embryos presented YFP expression throughout the developing heart, particularly in the outflow tract, right ventricle, and forming atria (Supplemental Fig. 1*A*), regions known to derive from $Isl1^+$ cardiac progenitors during cardiogenesis (4, 29). Similar expression pattern for β-galactosidase was observed in hearts of Isl1-Cre/R26R-LacZ adult animals (Supplemental Fig. 1*B*), demonstrating the specificity of the animal models to mark and trace Isl1 cardiovascular progenitors.

Dermal fibroblasts were isolated from 3-d-old Isl1-Cre/R26R-indicator double-heterozygous mice and retrovirally transduced with either 4 transcription factors, Oct4, Sox2, Klf4, and c-Myc, or with only 3 in the absence of c-Myc. As expected, ~3–4% of parental fibroblasts were already positive for the marker genes LacZ or YFP before transduction (Supplemental Fig. 1*C*), because Isl1 expression has been reported in melanocytes of the skin (30). Nevertheless, after retroviral infection, only 5 of 123 picked clones that generated cell lines with ES-like morphology were LacZ or YFP positive (Supplemental Fig. 1*D, E*), indicating that Isl1-derived skin cells are not more amenable to reprogramming. We excluded these clones from the present study and performed all further analysis on the marker negative ones. Thirty of 35 tested clones presented characteristics of iPS cells (31, 32), such as expression of ES cell markers (alkaline phosphatase and Nanog), reactivation of the endogenous pluripotency genes (*Oct4, Sox2, Klf4, c-Myc, Rex1,* and *Nanog*), and silencing of retroviral transgenes (Fig. 1*B–D*). Once transplanted into the heart of nude mice, 4 out of 4 iPS cell lines tested produced tumors that consisted of various tissues of all 3 germ layers, indicating their pluripotency (Fig. 1*F*). Furthermore, we determined the developmental potential of various iPS cell lines by chimera formation after injection into diploid blastocysts. We obtained high-percentage chimeras, in which iPS cell

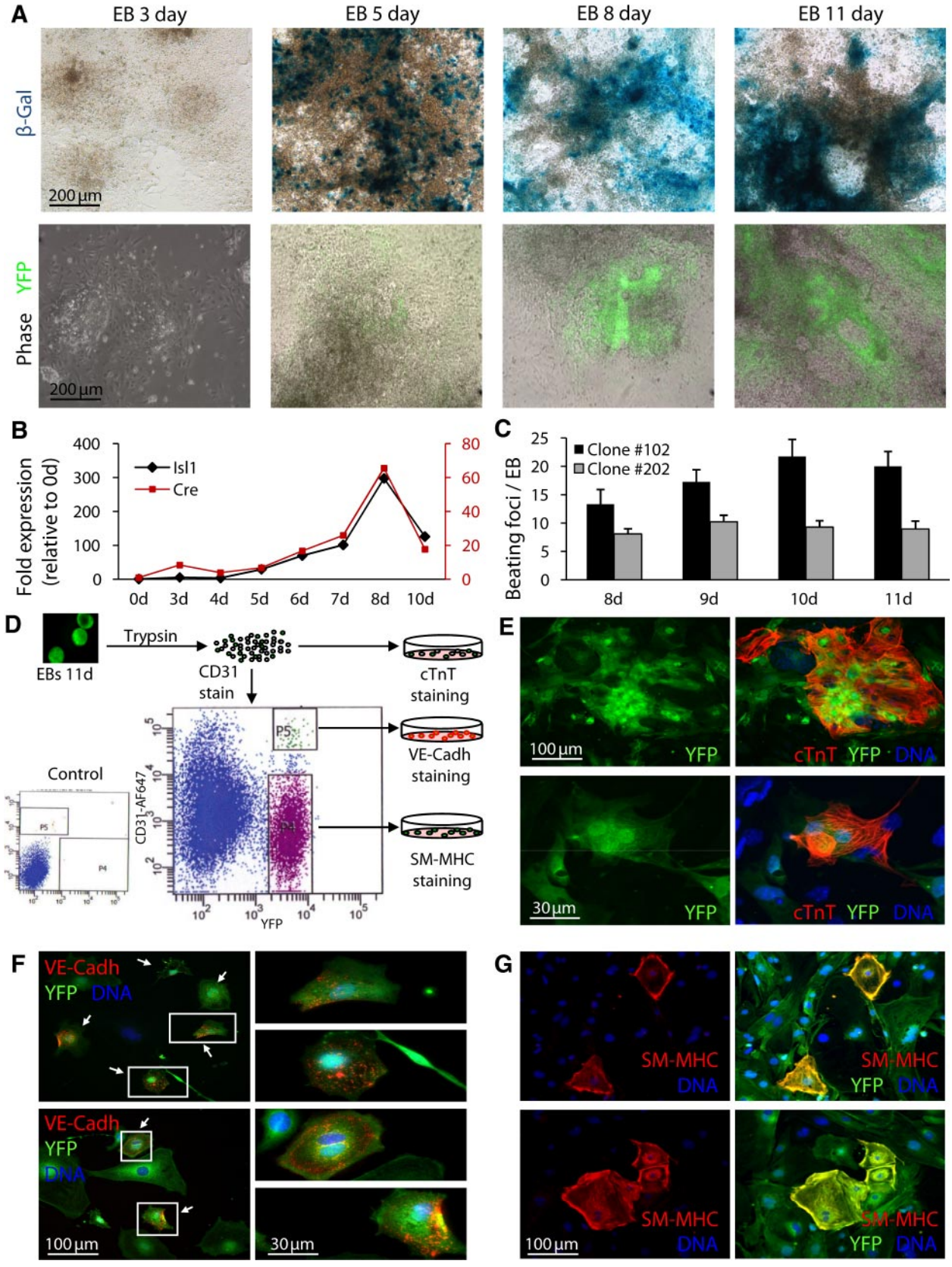

Figure 2. iPS cells from Isl1-Cre/R26R-indicator mice generate Isl1$^+$ cardiovascular progenitors and Isl1-derived cardiac lineages *in vitro*. *A*) Time course of LacZ (top panels) and YFP (bottom panels) reporter gene expression assessed by X-Gal staining and epifluorescence, respectively, during EB differentiation of Isl1-Cre/R26R-LacZ iPS clone 137 (top panels) and Isl1-Cre/R26R-YFP iPS clone 231 (bottom panels). *B*) Quantitative RT-PCR for expression of Isl1 (left axis) and Cre (right axis) during EB differentiation of Isl1-Cre/R26R-YFP iPS clone 202; $n = 3$. *C*) Quantification of beating foci in EBs at 8–11 d of differentiation

(*continued on next page*)

contribution to organs formed by cells known to derive from Isl1-expressing precursors during development (*e.g.,* motor neurons, myocardial cells, pancreatic and pulmonary cells, and skin melanocytes) could be visualized by expression of the marker genes YFP or LacZ (Fig. 1*E* for dermal melanocytes; data not shown for other organs) (3, 30, 33).

Reprogrammed fibroblasts from Isl1-Cre/R26R-indicator mice differentiate into Isl1$^+$ cardiovascular progenitors and Isl1-derived cardiac lineages *in vitro*

To determine the ability of Isl1-Cre/R26R-indicator iPS cells to generate Isl1$^+$ cardiovascular precursors and their derivatives *in vitro,* we induced differentiation in EBs. During EB development, the expression of Isl1 and Cre recombinase started at d 5 in concurrence with the appearance of the marker genes LacZ or YFP (**Fig. 2*A***) and correlated over time, as demonstrated by quantitative RT-PCR analysis (Fig. 2*B*). By d 8, several beating foci appeared in each EB (Fig. 2*C* and Supplemental Movie 1), and the majority were positive for the genetic markers (Supplemental Movie 2), which suggests that the myocytic lineage that derives from Isl1$^+$ progenitors can be generated from iPS cells *in vitro.* Immunohistochemical analysis on single cells dissociated from Isl1-Cre/R26R-YFP EBs at d 11 demonstrated that iPS cells can give rise to all 3 cardiac lineages (endothelial, cardiac, and smooth muscle), which originate from Isl1$^+$ precursors (Fig. 2*D–G*). A high number of cells costained positively for YFP and the cardiac muscle specific marker troponin T (cTnT; Fig. 2*E*), whereas only ~1% of YFP$^+$ cells expressed endothelial surface markers, such as CD31 and VE-cadherin (Fig. 2*D, F*), and the smooth-muscle-specific protein myosin heavy chain (SM-MHC; Fig. 2*G*), consistent with the relative contribution of Isl1$^+$ cardiovascular progenitors to the 3 heart lineages during development (1, 3).

To purify multipotent Isl1$^+$ cardiovascular progenitors arising during EB differentiation of Isl1-Cre/R26R-YFP iPS cells, we used FACS to isolate YFP$^+$ cells at different stages of cardiac specification within the time window of EB days (EBd) 3–6 (**Fig. 3*A***) and analyzed their transcriptional profile by quantitative RT-PCR (Fig. 3*B*). The *Isl1* message level was ≥3 times higher in the YFP$^+$ cells compared to the YFP$^-$ fraction throughout the whole time course. Expression of other markers identifying multipotent Isl1$^+$ cardiovascular progenitors, such as *Nkx2.5, Flk1, Gata4, Tbx20,* and *Fgf10* (1), was greatly enriched in the YFP$^+$ population at d 4.5, when these cells still expressed the first mesodermal gene *Brachyury T* and one of the earliest mesodermal markers of the cardiac lineage *Mesp2* (34) (Fig. 3*B*). The low levels of *Foxa2* and *Sox17* messages in the YFP$^+$ fraction during the different examined stages of differentiation indicate little, if any, presence of endodermal cells (35, 36), whereas the expression of *Gata1* suggests a small contamination of the YFP$^+$ population with cells undergoing hematopoietic commitment at EBd 5.5 and 6 (37). *Sox1* and *Pax6* genes were barely detectable in both YFP$^+$ and YFP$^-$ fractions at any time, indicating very little differentiation to the neuroectoderm lineage (38) (Fig. 3*B*). Taken together, these expression patterns suggest that the majority of cells within the YFP$^+$ population represents multipotent Isl1$^+$ cardiovascular progenitors at d 4.5 of EB development, and only later, starting from EB d 5.5, do the YFP$^+$ cells get more specified into subsets of cardiac progenitors and more restricted in their lineage differentiation potential, as demonstrated by the up-regulation of genes indicative of muscle progenitors (*Nkx2.5, Mef2c, cTnT,* and α*SMA*) and of vascular progenitors (α*SMA* and *CD31*) (1, 39). Moreover, by d 5.5 the YFP$^+$ population may also comprise cells entering the hematopoietic program.

Isl1$^+$ cardiovascular progenitors derived from iPS cells differentiate into cardiac, smooth muscle, and endothelial cells *in vivo*

To assess the lineage differentiation potential of the YFP$^+$ population obtained from EBs at d 4.5, we injected 0.5 and 1 × 10^6 cells (from clone 202, 4-factor reprogramming, or clone 231, 3-factor reprogramming) directly into the left ventricular wall of adult nude mice and analyzed the hearts at 5 wk (n=6) and 12 wk (n=6) following cell transplantation. As opposed to undifferentiated iPS cells, which generated teratoma in all animals (n=6), YFP$^+$ cells did not produce microscopic evidence for tumor formation in any of the injected hearts, even at 12 wk following cell transplantation (**Fig. 4*A***). These results suggest that the YFP$^+$ population is free from pluripotent undifferentiated cells and that reactivation of retroviral oncogenes in injected cells was absent within the 3-mo period, regardless the number of factors used for the reprogramming. Immunohistochemical analysis of heart sections revealed engraftment of YFP$^+$ cells in all transplanted animals (Fig. 4*E*) and their distribution throughout the myocardium. At the area of injection, most of the YFP$^+$ cells started to express the myocytic markers α-actinin and cTnT in an unorganized pattern (Fig. 4*B,* top panels). Several cells positive for both YFP and α-actinin were observed within the intact myocardium, which presented a more organized sarcomeric structure (Fig. 4*B,*

for iPS clone 102 (Isl1-Cre/R26R-LacZ; 3-factor reprogramming; black bar) and clone 202 (Isl1-Cre/R26R-YFP; 4-factor reprogramming; gray bar), n = 4. *D–G*) Scheme of the procedure and cell fractions used for characterization of Isl1-derived cardiovascular lineages during EB differentiation of Isl1-Cre/R26R-YFP iPS clone 202 (*D*). Cells dissociated from d 11 EBs were directly plated down for double-immunofluorescence staining for YFP (green) and the cardiac muscle-specific marker cTnT (red, *E*). To enrich for the endothelial lineage, dissociated cells were labeled with an anti-CD31-Alexa-Fluor-647 antibody. After FACS sorting, YFP$^+$/CD31$^+$ cells were stained for YFP (green) and VE-cadherin (red) for mature endothelial cells (*F*), and YFP$^+$/CD31$^-$ cells were costained for YFP (green) and the smooth-muscle-specific marker SM-MHC (red; *G*). *F*) Arrows indicate double-positive cells; right panels represent magnifications of cells framed in left panels.

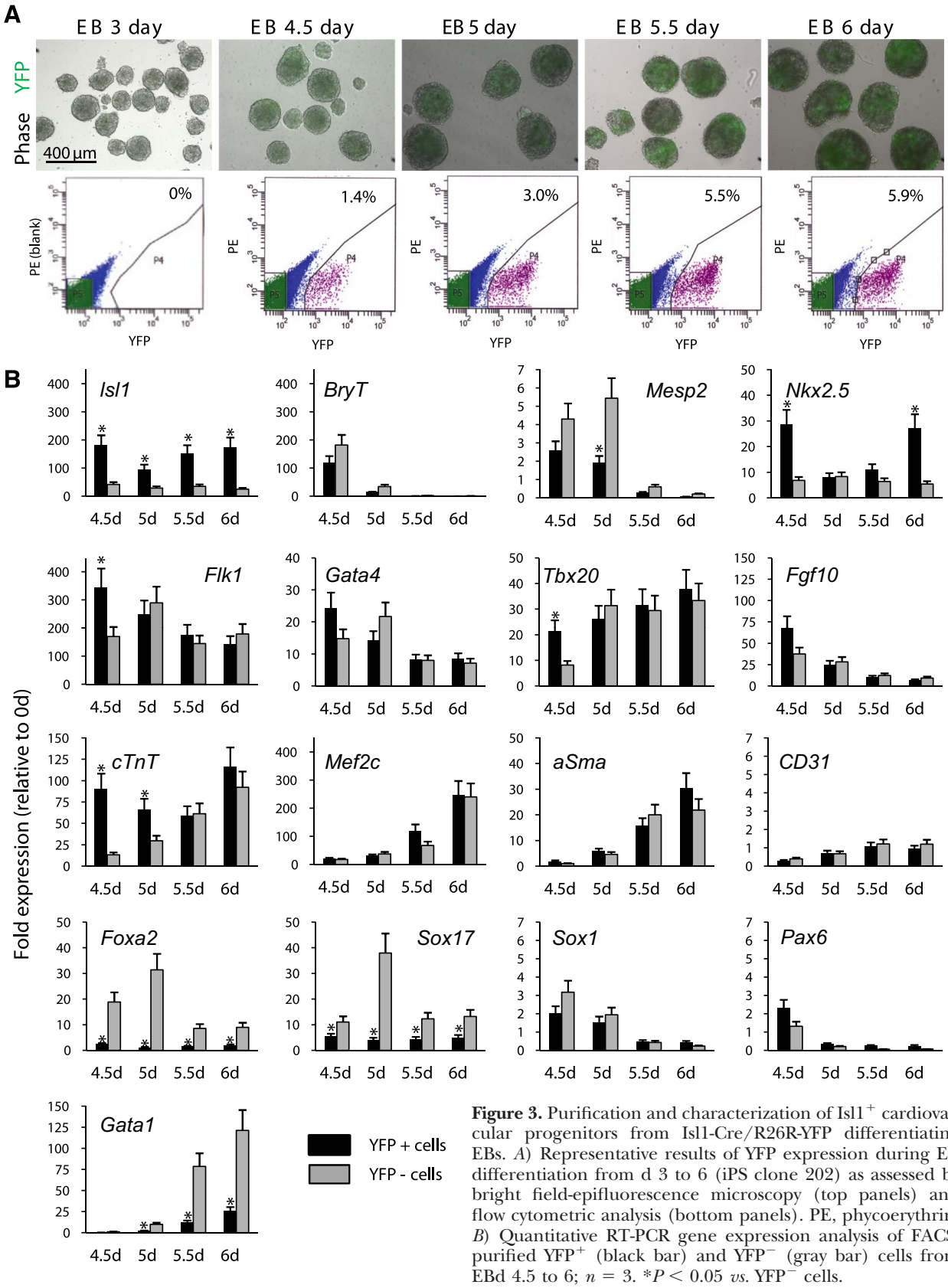

Figure 3. Purification and characterization of Isl1$^+$ cardiovascular progenitors from Isl1-Cre/R26R-YFP differentiating EBs. *A*) Representative results of YFP expression during EB differentiation from d 3 to 6 (iPS clone 202) as assessed by bright field-epifluorescence microscopy (top panels) and flow cytometric analysis (bottom panels). PE, phycoerythrin. *B*) Quantitative RT-PCR gene expression analysis of FACS-purified YFP$^+$ (black bar) and YFP$^-$ (gray bar) cells from EBd 4.5 to 6; $n = 3$. *$P < 0.05$ *vs.* YFP$^-$ cells.

bottom panels). Furthermore, YFP$^+$ cells costaining positively for SMA (Fig. 4*C*) and for endothelial specific markers, such as CD31 and VE-cadherin (Fig. 4*D*), could be found as part of mature vessels (bottom panels). A semiquantification of the percentage of YFP$^+$ cells expressing markers of differentiated cardiovascular lineages is presented in Fig. 4*F*. These results indicate that Isl1$^+$/YFP$^+$ cells arising at 4.5 d of iPS differentiation represent

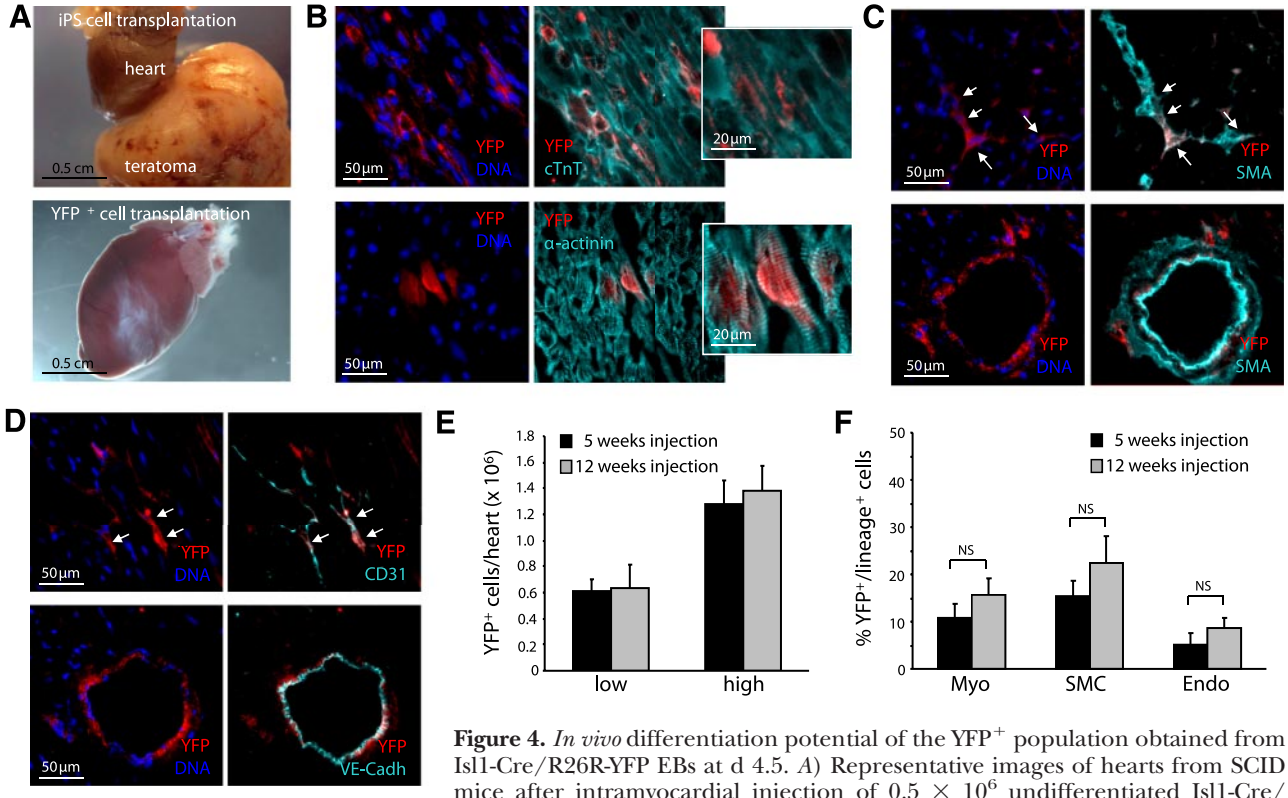

Figure 4. *In vivo* differentiation potential of the YFP$^+$ population obtained from Isl1-Cre/R26R-YFP EBs at d 4.5. *A*) Representative images of hearts from SCID mice after intramyocardial injection of 0.5×10^6 undifferentiated Isl1-Cre/R26R-YFP iPS cells (clone 202, top panel) or 0.5×10^6 YFP$^+$ cells purified after 4.5 d EB differentiation of the same iPS cell line (bottom panel). *B–D*) Double immunofluorescence staining for YFP (red) and lineage-specific markers (cyan) in sections of grafted hearts 5 wk after transplantation of 0.5×10^6 YFP$^+$ cells reveals that injected cells are capable of differentiating into myocytic (*B*), smooth muscle (*C*), and endothelial (*D*) lineages *in vivo*. Insets (*B*): magnification of areas of interest. *E*) Semiquantitative analysis of the number of YFP$^+$ cells throughout the myocardium 5 wk (black bar) and 12 wk (gray bar) post-transplantation of low (0.5×10^6) and high (1×10^6) number of YFP$^+$ cells; $n = 3$ animals/group. *F*) Semiquantitative analysis of the percentage of YFP$^+$ cells expressing markers of cardiac muscle (Myo), smooth muscle (SMC), and endothelial (Endo) cells, assessed in 20 sample sections from each heart at 5 wk (black bar) and 12 wk (gray bar) after cell transplantation; $n = 12$ hearts. NS, not significant.

cardiovascular progenitors able to generate all of the 3 cardiovascular cell types when exposed to the cardiac environment *in vivo*. In addition, these lineage-restricted precursors are incapable of teratoma formation, as opposed to those seen after transplantation of undifferentiated ES/iPS cells into the heart.

ISL1 is expressed in a population of cardiovascular progenitor cells arising during differentiation of human iPS

The isolation of cardiovascular progenitors from patient-specific iPS cells would await the identification of markers specific for this cell population and the availability of protocols to efficiently direct human iPS cells to the cardiac lineage. It has been shown that human iPS cells generated from healthy individuals are capable, as human ES (hES) cells, to differentiate into cardiac myocytes *in vitro* (11). Recent work has demonstrated that the cardiogenic program in humans implicates a multipotent progenitor population comparable to the one in mice and that these precursors can be similarly identified by the expression of the transcription factor ISL1 (40). However, it remains unclear whether ISL1$^+$ cardiovascular progenitors can be identified during human iPS cell differentiation. Therefore, we generated iPS cell lines from skin fibroblasts of 2 different healthy adults, H1 and H2, and analyzed the specification and differentiation of these cells toward the cardiac program *in vitro*. After retroviral transduction of the 4 factors *OCT4, SOX2, KLF4,* and c-*MYC,* we obtained 3 stable cell lines with a hES cell morphology from individual H1 and 2 from individual H2, and further characterized one line from each. Both cell lines exhibited strong alkaline phosphatase activity (data not shown) and expressed hES cell-specific antigens, such as TRA1-81 and NANOG (**Fig. 5*A***). Quantitative RT-PCR showed that the endogenous loci of genes associated with the pluripotent state (*OCT4, SOX2, NANOG, TDGF1/CRIPTO,* and *LEFTYA*) had become activated and that the retroviral transcripts had been silenced (Supplemental Fig. 2*A, B*). The capacity to form EBs and to up-regulate, during spontaneous differentiation, lineage markers representative of the 3 embryonic germ layers (Supplemental Fig. 2*C*) confirmed that both hiPS cell lines were pluripotent and completely reprogrammed.

To verify whether the transcription factor ISL1 is expressed during the onset of human cardiogenesis we used a defined protocol to induce differentiation of hiPS cells into the cardiac lineage (Fig. 5*B*). By d 12 of EB differen-

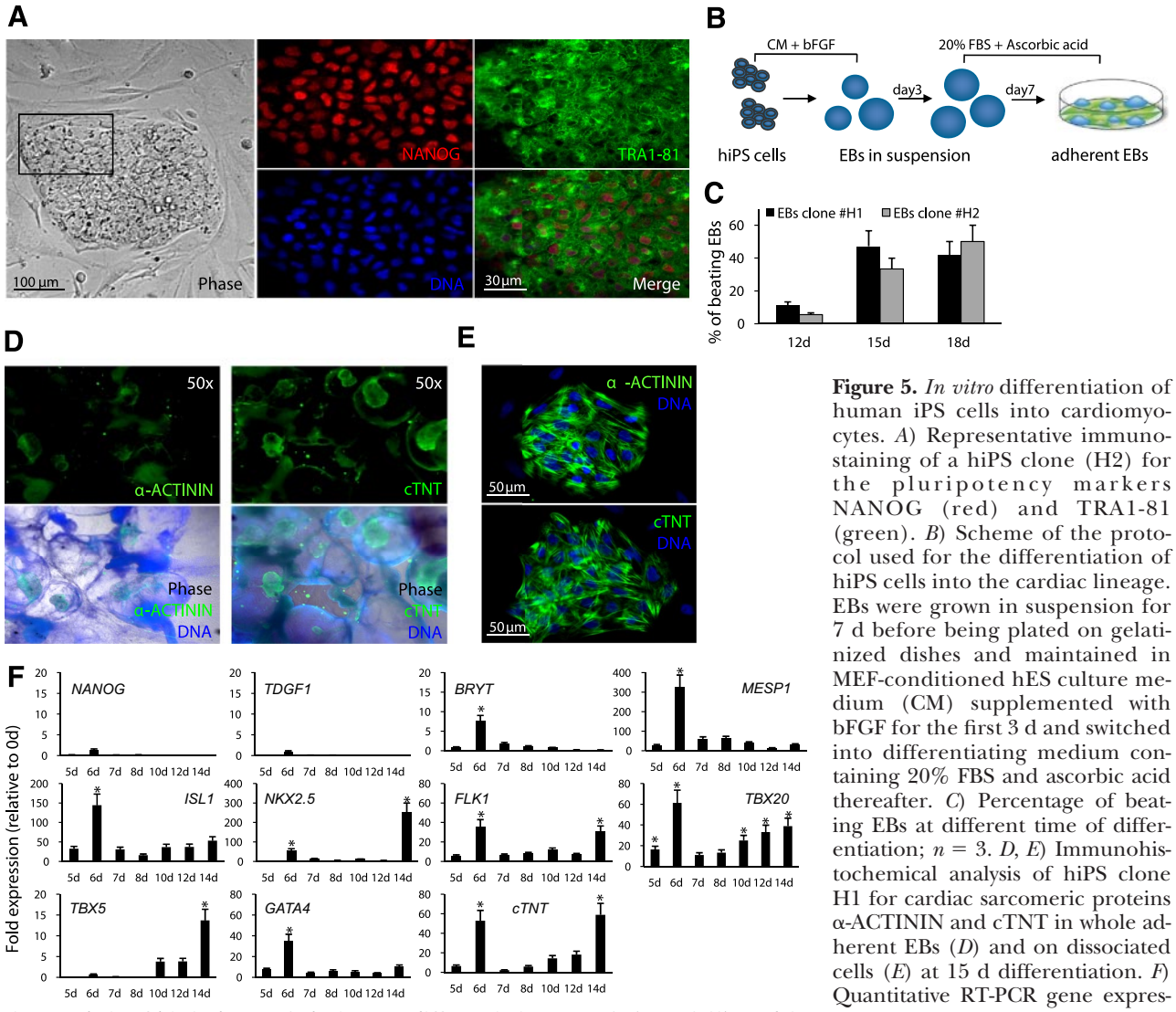

Figure 5. *In vitro* differentiation of human iPS cells into cardiomyocytes. *A*) Representative immunostaining of a hiPS clone (H2) for the pluripotency markers NANOG (red) and TRA1-81 (green). *B*) Scheme of the protocol used for the differentiation of hiPS cells into the cardiac lineage. EBs were grown in suspension for 7 d before being plated on gelatinized dishes and maintained in MEF-conditioned hES culture medium (CM) supplemented with bFGF for the first 3 d and switched into differentiating medium containing 20% FBS and ascorbic acid thereafter. *C*) Percentage of beating EBs at different time of differentiation; $n = 3$. *D*, *E*) Immunohistochemical analysis of hiPS clone H1 for cardiac sarcomeric proteins α-ACTININ and cTNT in whole adherent EBs (*D*) and on dissociated cells (*E*) at 15 d differentiation. *F*) Quantitative RT-PCR gene expression analysis of hiPS clone H2 during EB differentiation; $n = 3$. $^*P < 0.05$ *vs.* d 0.

tiation, the first beating foci appeared (Supplemental Movie 3), whose number increased in the following week (Fig. 5*C*), and clusters of cells expressing cardiomyocyte-specific sarcomeric proteins, as cTNT and α-ACTININ, could be detected (Fig. 5*D*, *E*). Molecular analysis of the developing EBs (Fig. 5*F*) revealed an early down-regulation of pluripotency genes (*NANOG* and *TDGF1/CRIPTO*), which coincided with the up-regulation of genes indicative of cardiac commitment (*BRYT* and *MESP1*). *ISL1* and *NKX2.5*, together with other genes expressed in mouse cardiac progenitors, as *FLK1*, *TBX20*, *GATA4*, and *cTNT* started to be expressed near the beginning of the differentiation, and the transcription factor *TBX5* was up-regulated later (Fig. 5*F*).

To determine whether an ISL1$^+$ population of cardiovascular progenitors could be obtained from differentiating hiPS cells, we plated colonies of 3–4 hiPS cells at very low density and induced the cardiac program by treating them with the cardiogenic factor BMP2 in combination with an FGF receptor-inhibitor (28) (**Fig. 6*A***). After 4 d treatment, most of the hiPS colonies appeared differentiated, and the majority of them contained a high proportion of cells expressing ISL1, some of which also resulted positive for NKX2.5 and FLK1 (Fig. 6*B*). Quantitative RT-PCR analysis confirmed that under this culture condition many genes associated with early cardiac development had been activated, and genes specific of pluripotent cells and genes indicative of hematopoietic, endoderm, and neuroectoderm commitment were nearly absent (Fig. 6*C*). Previous studies in mice had demonstrated that the transcriptional signature of *Isl1*$^+$/*Nkx2.5*$^+$/*Flk1*$^+$ defines a multipotent cardiovascular progenitor and that Flk1 and Nkx2.5 expression is important for the conversion of the progenitor into an endothelial and muscle cell, respectively (1). To assess whether the hiPS-derived ISL1$^+$ cells induced by the BMP2/FGFR-inhibitor treatment indeed represented cardiovascular precursors, we stimulated further differentiation in specific culture conditions promoting myocytic or vascular development (Fig. 6*A*). Immunofluorescence analysis revealed that after 8 d in the presence of ascorbic acid and VEGF most of the colonies contained differentiated cells of the main heart lineages (Fig. 6*D*). These results suggest that hiPS cells could represent a source of ISL1$^+$ cells displaying cardiovascular potential.

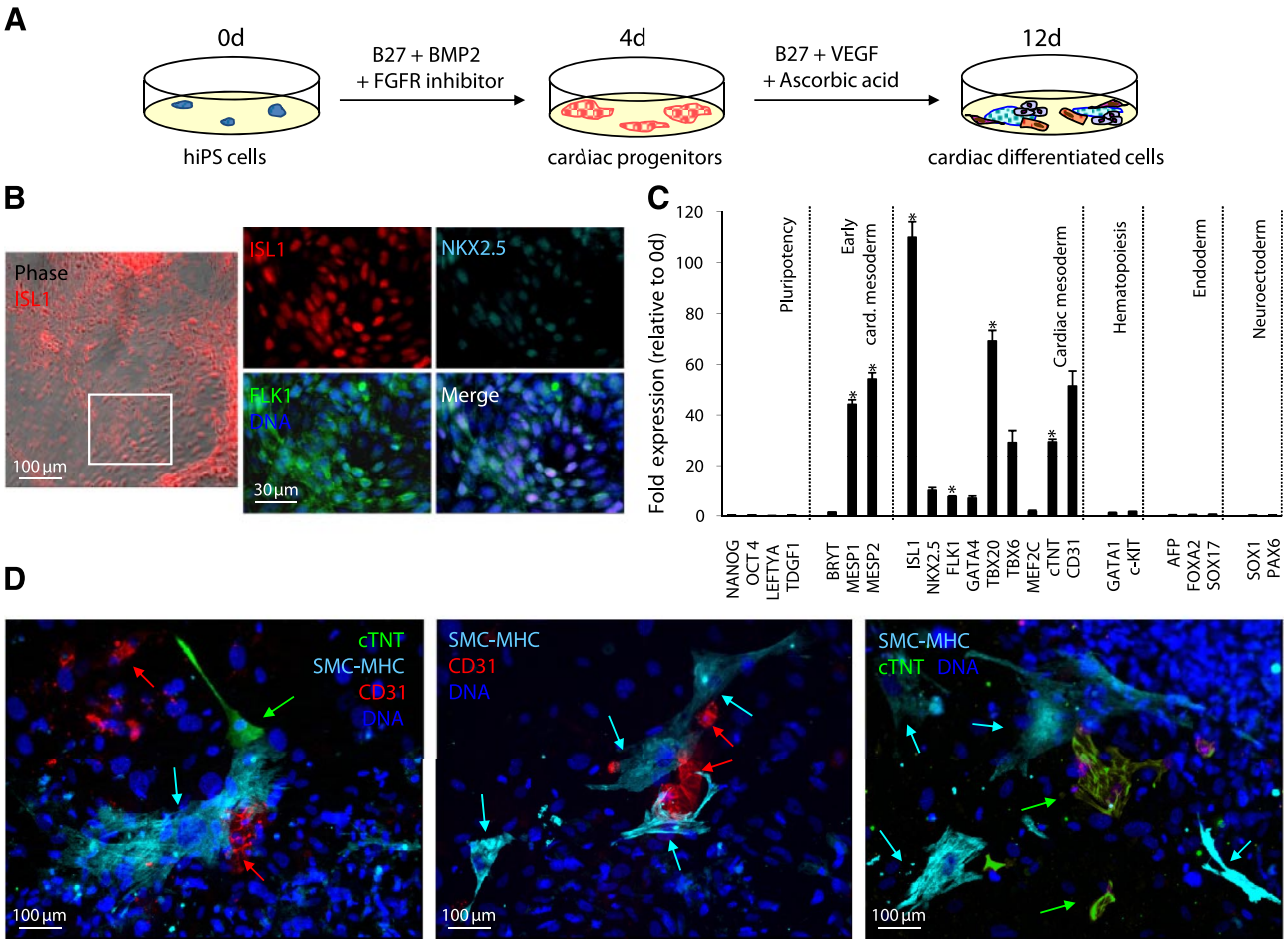

Figure 6. Generation and *in vitro* differentiation of ISL1$^+$ cardiovascular progenitors from human iPS cells. *A*) Scheme of the protocol used to induce specification of hiPS cells into ISL1$^+$ cardiovascular progenitors and to further differentiate them into cardiac and vascular cells. *B*) Left panel: representative image of an ISL1-immunostained hiPS cell colony (clone H1) after 4 d of treatment with BMP2/FGFR-inhibitor. Right panels: magnifications of boxed area in left panel after immunostaining for ISL1 (red), NKX2.5 (cyan), and FLK1 (green). *C*) Quantitative RT-PCR gene expression profile of hiPS cells after 4 d BMP2/FGFR-inhibitor treatment; $n = 3$. $^*P < 0.05$ *vs.* d 0. *D*) Representative triple immunofluorescence analysis for cTNT (green), SMC-MHC (cyan), and CD31 (red) on hiPS cells at d 12 of the differentiation protocol.

DISCUSSION

The ability to reprogram human somatic cells to a pluripotent state offers the possibility to produce large numbers of cell types with a patient's own genetic background, which raises exciting new prospects for biomedical research and autologous cell replacement therapies. The plasticity of ES and iPS cells renders them difficult to control and is considered a major obstacle on their route to clinical applications, because they possess the risk of teratoma formation. To this end, the accessibility of purified lineage-specific progenitors may represent a significant advantage for safer future clinical and translational applications. In addition, in organs such as the heart where multiple cell types have to be replaced, multipotent progenitors could ideally contribute to both remuscularization and revascularization, because they should be able to proliferate and differentiate into diverse mature cells in response to different microenvironmental cues (41).

In the current study, we generated mouse iPS cell lines that allow irreversible genetic marking of Isl1-expressing cells and demonstrated that iPS cells can serve as a source of multipotent Isl1$^+$ cardiovascular progenitors similar to the ones derived from ES cells. By using differentiation protocols established for mouse ES cells, recent work has demonstrated that functional myocytes and vascular cells can be generated from mouse iPS cells or iPS-derived Flk1$^+$ mesodermal precursors *in vitro* (42–44). The results of our study prove that, after myocardial injection, the Isl1$^+$ progenitor population could engraft into the host tissue and generate all of the 3 cardiovascular lineages *in vivo*. Even after 3 mo of cell transplantation, we did not observe any teratoma, indicating that the genetically marked precursors were free from any contamination of undifferentiated cells and stably directed toward the cardiac program.

The use of retroviruses to deliver the reprogramming factors may trigger cancer formation and disrupt endogenous gene expression. The absence of microscopic evidence of tumor in all injected hearts suggests that in both iPS cell lines used there was no reactivation of retroviral oncogenes or "undesired" viral genomic integration. Recent studies have demonstrated that *c-Myc* is dispensable (45) and that the problem of insertional mutagenesis can be surmounted through alternative methods of transgene

delivery and the use of small molecules, reducing one of the major drawbacks to the clinical application of iPS cells (16, 46–52). Although reprogramming of human fibroblasts was achieved by retroviral infection, both hiPS cell lines from different individuals could be terminally differentiated into functional beating cardiomyocytes. However, carefully conducted long-term studies will be needed to compare *in vitro* physiology of hiPS-derived cardiac muscle cells and those derived from human ES cell lines. The current study confirms the feasibility of using iPS cells for producing large numbers of cardiac myocytes with an individual exact genotype, which would be immune matched, an ultimate goal for regenerative medicine. Moreover, when generated from iPS cells obtained from patients with a genetic disease, *e.g.,* Long QT-Syndrome, cardiac muscle cells would bear the same genetic mutation and provide a useful *in vitro* system to study mechanisms of pathogenesis.

Our results on human reprogrammed cells also confirm recent findings in hES cells suggesting that cardiovascular development in humans is similar to that in the mouse (40, 53). Yang and colleagues have reported that during human EB differentiation a population of KDR(FLK1)^{low}/c-KIT^{neg} cells arises, which displays cardiac, endothelial, and vascular smooth muscle potential *in vitro* and *in vivo*. Using a genetic marking of hES cells, Bu and colleagues have shown that purified human ISL1$^+$ progenitors are capable of self-renewal and expansion before differentiation into the 3 major cardiovascular lineages *in vitro*. In concordance with these results, a subset of human iPS-derived ISL1$^+$ cardiovascular precursors described in our study also expresses FLK1 and/or NKX2.5. Because the VEGF receptor subtype-2, FLK1, also marks progenitors of the hematopoietic lineages, the identification of other surface markers expressed in the human ISL1$^+$ cells would be extremely valuable for their isolation and molecular characterization. The possibility to purify mouse Isl1$^+$ cardiovascular precursors from Isl1-Cre/R26R-YFP iPS cells allows us to analyze their transcriptional profile, and ongoing work is concentrated in identifying a combination of cell-surface antigens that could permit the isolation of human and patient-specific cardiac progenitors at different stages of development.

In summary, our findings demonstrate the generation of Isl1$^+$ cardiovascular progenitors from mouse iPS cells and their multipotency *in vivo* to differentiate into endothelial, smooth, and cardiac muscle cells, without the formation of teratoma. In addition, we describe the identification of human iPS-derived ISL1$^+$ cardiac precursors and the efficient induction of ISL1$^+$/NKX2.5$^+$/FLK1$^+$ mesodermal progenitors with subsequent differentiation into cardiovascular cell types. This approach will provide ready access to ISL1$^+$ cardiovascular progenitors and more mature populations for functional cell replacement analysis as well as for developmental biology studies defining the earliest molecular program involved in the specification and differentiation of this lineage. FJ

The authors thank Toshio Kitamura (University of Tokyo, Tokyo, Japan), Shinya Yamanaka (Kyoto University, Kyoto, Japan), and George Daley (Harvard Medical School, Boston, MA, USA) for providing viral vectors through Addgene. Some of the monoclonal antibodies were obtained from the Developmental Studies Hybridoma Bank, which was developed under the auspices of the National Institute Human Development and is maintained by the University of Iowa. The authors especially acknowledge K. Goetsch for her expertise in the FACS sorting analysis and M. Rudelius and D. Grewe for assistance in histology. This work was supported by a Marie Curie Excellence Team Grant from the European Research Council (MEXT-23208), the German Research Foundation (La 1238 3-1/4-1), and the German Ministry for Education and Research (01 GN 0826).

REFERENCES

1. Moretti, A., Caron, L., Nakano, A., Lam, J. T., Bernshausen, A., Chen, Y., Qyang, Y., Bu, L., Sasaki, M., Martin-Puig, S., Sun, Y., Evans, S. M., Laugwitz, K. L., and Chien, K. R. (2006) Multipotent embryonic isl1+ progenitor cells lead to cardiac, smooth muscle, and endothelial cell diversification. *Cell* **127,** 1151–1165
2. Kattman, S. J., Huber, T. L., and Keller, G. M. (2006) Multipotent flk-1+ cardiovascular progenitor cells give rise to the cardiomyocyte, endothelial, and vascular smooth muscle lineages. *Dev. Cell* **11,** 723–732
3. Sun, Y., Liang, X., Najafi, N., Cass, M., Lin, L., Cai, C. L., Chen, J., and Evans, S. M. (2007) Islet 1 is expressed in distinct cardiovascular lineages, including pacemaker and coronary vascular cells. *Dev. Biol.* **304,** 286–296
4. Laugwitz, K. L., Moretti, A., Lam, J., Gruber, P., Chen, Y., Woodard, S., Lin, L. Z., Cai, C. L., Lu, M. M., Reth, M., Platoshyn, O., Yuan, J. X., Evans, S., and Chien, K. R. (2005) Postnatal isl1+ cardioblasts enter fully differentiated cardiomyocyte lineages. *Nature* **433,** 647–653
5. Laugwitz, K. L., Moretti, A., Caron, L., Nakano, A., and Chien, K. R. (2008) Islet1 cardiovascular progenitors: a single source for heart lineages? *Development* **135,** 193–205
6. Wu, S. M., Chien, K. R., and Mummery, C. (2008) Origins and fates of cardiovascular progenitor cells. *Cell* **132,** 537–543
7. Moretti, A., Lam, J., Evans, S. M., and Laugwitz, K. L. (2007) Biology of Isl1+ cardiac progenitor cells in development and disease. *Cell. Mol. Life Sci.* **64,** 674–682
8. Murry, C. E., and Keller, G. (2008) Differentiation of embryonic stem cells to clinically relevant populations: lessons from embryonic development. *Cell* **132,** 661–680
9. Rubart, M., and Field, L. J. (2006) Cardiac regeneration: repopulating the heart. *Annu. Rev. Physiol.* **68,** 29–49
10. Takahashi, K., and Yamanaka, S. (2006) Induction of pluripotent stem cells from mouse embryonic and adult fibroblast cultures by defined factors. *Cell* **126,** 663–676
11. Takahashi, K., Tanabe, K., Ohnuki, M., Narita, M., Ichisaka, T., Tomoda, K., and Yamanaka, S. (2007) Induction of pluripotent stem cells from adult human fibroblasts by defined factors. *Cell* **131,** 861–872
12. Yu, J., Vodyanik, M. A., Smuga-Otto, K., Antosiewicz-Bourget, J., Frane, J. L., Tian, S., Nie, J., Jonsdottir, G. A., Ruotti, V., Stewart, R., Slukvin, I. I., and Thomson, J. A. (2007) Induced pluripotent stem cell lines derived from human somatic cells. *Science* **318,** 1917–1920
13. Kim, J. B., Zaehres, H., Wu, G., Gentile, L., Ko, K., Sebastiano, V., Arauzo-Bravo, M. J., Ruau, D., Han, D. W., Zenke, M., and Scholer, H. R. (2008) Pluripotent stem cells induced from adult neural stem cells by reprogramming with two factors. *Nature* **454,** 646–650
14. Silva, J., Barrandon, O., Nichols, J., Kawaguchi, J., Theunissen, T. W., and Smith, A. (2008) Promotion of reprogramming to ground state pluripotency by signal inhibition. *PLoS Biol.* **6,** e253
15. Aasen, T., Raya, A., Barrero, M. J., Garreta, E., Consiglio, A., Gonzalez, F., Vassena, R., Bilic, J., Pekarik, V., Tiscornia, G., Edel, M., Boue, S., and Belmonte, J. C. (2008) Efficient and rapid generation of induced pluripotent stem cells from human keratinocytes. *Nat. Biotechnol.* **26,** 1276–1284
16. Kim, J. B., Sebastiano, V., Wu, G., Arauzo-Bravo, M. J., Sasse, P., Gentile, L., Ko, K., Ruau, D., Ehrich, M., van den Boom, D., Meyer, J., Hubner, K., Bernemann, C., Ortmeier, C., Zenke, M., Fleischmann, B. K., Zaehres, H., and Scholer, H. R. (2009) Oct4-induced pluripotency in adult neural stem cells. *Cell* **136,** 411–419
17. Park, I. H., Arora, N., Huo, H., Maherali, N., Ahfeldt, T., Shimamura, A., Lensch, M. W., Cowan, C., Hochedlinger, K.,

and Daley, G. Q. (2008) Disease-specific induced pluripotent stem cells. *Cell* **134,** 877–886
18. Dimos, J. T., Rodolfa, K. T., Niakan, K. K., Weisenthal, L. M., Mitsumoto, H., Chung, W., Croft, G. F., Saphier, G., Leibel, R., Goland, R., Wichterle, H., Henderson, C. E., and Eggan, K. (2008) Induced pluripotent stem cells generated from patients with ALS can be differentiated into motor neurons. *Science* **321,** 1218–1221
19. Ebert, A. D., Yu, J., Rose, F. F., Jr., Mattis, V. B., Lorson, C. L., Thomson, J. A., and Svendsen, C. N. (2009) Induced pluripotent stem cells from a spinal muscular atrophy patient. *Nature* **457,** 277–280
20. Soldner, F., Hockemeyer, D., Beard, C., Gao, Q., Bell, G. W., Cook, E. G., Hargus, G., Blak, A., Cooper, O., Mitalipova, M., Isacson, O., and Jaenisch, R. (2009) Parkinson's disease patient-derived induced pluripotent stem cells free of viral reprogramming factors. *Cell* **136,** 964–977
21. Maherali, N., Sridharan, R., Xie, W., Utikal, J., Eminli, S., Arnold, K., Stadtfeld, M., Yachechko, R., Tchieu, J., Jaenisch, R., Plath, K., and Hochedlinger, K. (2007) Directly reprogrammed fibroblasts show global epigenetic remodeling and widespread tissue contribution. *Cell Stem Cell* **1,** 55–70
22. Hanna, J., Wernig, M., Markoulaki, S., Sun, C. W., Meissner, A., Cassady, J. P., Beard, C., Brambrink, T., Wu, L. C., Townes, T. M., and Jaenisch, R. (2007) Treatment of sickle cell anemia mouse model with iPS cells generated from autologous skin. *Science* **318,** 1920–1923
23. Wernig, M., Zhao, J. P., Pruszak, J., Hedlund, E., Fu, D., Soldner, F., Broccoli, V., Constantine-Paton, M., Isacson, O., and Jaenisch, R. (2008) Neurons derived from reprogrammed fibroblasts functionally integrate into the fetal brain and improve symptoms of rats with Parkinson's disease. *Proc. Natl. Acad. Sci. U. S. A.* **105,** 5856–5861
24. Cai, C. L., Martin, J. C., Sun, Y., Cui, L., Wang, L., Ouyang, K., Yang, L., Bu, L., Liang, X., Zhang, X., Stallcup, W. B., Denton, C. P., McCulloch, A., Chen, J., and Evans, S. M. (2008) A myocardial lineage derives from Tbx18 epicardial cells. *Nature* **454,** 104–108
25. Soriano, P. (1999) Generalized lacZ expression with the ROSA26 Cre reporter strain. *Nat. Genet.* **21,** 70–71
26. Srinivas, S., Watanabe, T., Lin, C. S., William, C. M., Tanabe, Y., Jessell, T. M., and Constantini, F. (2001) Cre reporter strains produced by targeted insertion of EYFP and ECFP into the ROSA26 locus. *BMC Dev. Biol.* **1,**
27. Takahashi, K., Okita, K., Nakagawa, M., and Yamanaka, S. (2007) Induction of pluripotent stem cells from fibroblast cultures. *Nat. Protoc.* **2,** 3081–3089
28. Leschik, J., Stefanovic, S., Brinon, B., and Puceat, M. (2008) Cardiac commitment of primate embryonic stem cells. *Nat. Protoc.* **3,** 1381–1387
29. Cai, C. L., Liang, X., Shi, Y., Chu, P. H., Pfaff, S. L., Chen, J., and Evans, S. (2003) Isl1 identifies a cardiac progenitor population that proliferates prior to differentiation and contributes a majority of cells to the heart. *Dev. Cell* **5,** 877–889
30. Schwahn, D. J., Timchenko, N. A., Shibahara, S., and Medrano, E. E. (2005) Dynamic regulation of the human dopachrome tautomerase promoter by MITF, ER-alpha and chromatin remodelers during proliferation and senescence of human melanocytes. *Pigment Cell Res.* **18,** 203–213
31. Okita, K., Ichisaka, T., and Yamanaka, S. (2007) Generation of germline-competent induced pluripotent stem cells. *Nature* **448,** 313–317
32. Wernig, M., Meissner, A., Foreman, R., Brambrink, T., Ku, M., Hochedlinger, K., Bernstein, B. E., and Jaenisch, R. (2007) In vitro reprogramming of fibroblasts into a pluripotent ES-cell-like state. *Nature* **448,** 318–324
33. Tsuchida, T., Ensini, M., Morton, S. B., Baldassare, M., Edlund, T., Jessell, T. M., and Pfaff, S. L. (1994) Topographic organization of embryonic motor neurons defined by expression of LIM homeobox genes. *Cell* **79,** 957–970
34. Kitajima, S., Takagi, A., Inoue, T., and Saga, Y. (2000) MesP1 and MesP2 are essential for the development of cardiac mesoderm. *Development* **127,** 3215–3226
35. Sasaki, H., and Hogan, B. L. (1993) Differential expression of multiple fork head related genes during gastrulation and axial pattern formation in the mouse embryo. *Development* **118,** 47–59
36. Kanai-Azuma, M., Kanai, Y., Gad, J. M., Tajima, Y., Taya, C., Kurohmaru, M., Sanai, Y., Yonekawa, H., Yazaki, K., Tam, P. P., and Hayashi, Y. (2002) Depletion of definitive gut endoderm in Sox17-null mutant mice. *Development* **129,** 2367–2379
37. Orkin, S. H. (1992) GATA-binding transcription factors in hematopoietic cells. *Blood* **80,** 575–581
38. Li, X. J., Du, Z. W., Zarnowska, E. D., Pankratz, M., Hansen, L. O., Pearce, R. A., and Zhang, S. C. (2005) Specification of motoneurons from human embryonic stem cells. *Nat. Biotechnol.* **23,** 215–221
39. Wu, S. M., Fujiwara, Y., Cibulsky, S. M., Clapham, D. E., Lien, C. L., Schultheiss, T. M., and Orkin, S. H. (2006) Developmental origin of a bipotential myocardial and smooth muscle cell precursor in the mammalian heart. *Cell* **127,** 1137–1150
40. Lei, B., Jiang, X., Martin-Puig, S., Caron, L., Zhu, S., Shao, Y., Roberts, D. J., Huang, P. L., Domian, I. J., and Chien, K. R. (2009) Human ISL1 heart progenitors generate diverse multipotent cardiovascular cell lineages. *Nature* **460,** 113–117
41. Passier, R., van Laake, L. W., and Mummery, C. L. (2008) Stem-cell-based therapy and lessons from the heart. *Nature* **453,** 322–329
42. Mauritz, C., Schwanke, K., Reppel, M., Neef, S., Katsirntaki, K., Maier, L. S., Nguemo, F., Menke, S., Haustein, M., Hescheler, J., Hasenfuss, G., and Martin, U. (2008) Generation of functional murine cardiac myocytes from induced pluripotent stem cells. *Circulation* **118,** 507–517
43. Schenke-Layland, K., Rhodes, K. E., Angelis, E., Butylkova, Y., Heydarkhan-Hagvall, S., Gekas, C., Zhang, R., Goldhaber, J. I., Mikkola, H. K., Plath, K., and MacLellan, W. R. (2008) Reprogrammed mouse fibroblasts differentiate into cells of the cardiovascular and hematopoietic lineages. *Stem Cells* **26,** 1537–1546
44. Narazaki, G., Uosaki, H., Teranishi, M., Okita, K., Kim, B., Matsuoka, S., Yamanaka, S., and Yamashita, J. K. (2008) Directed and systematic differentiation of cardiovascular cells from mouse induced pluripotent stem cells. *Circulation* **118,** 498–506
45. Nakagawa, M., Koyanagi, M., Tanabe, K., Takahashi, K., Ichisaka, T., Aoi, T., Okita, K., Mochiduki, Y., Takizawa, N., and Yamanaka, S. (2008) Generation of induced pluripotent stem cells without Myc from mouse and human fibroblasts. *Nat. Biotechnol.* **26,** 101–106
46. Stadtfeld, M., Nagaya, M., Utikal, J., Weir, G., and Hochedlinger, K. (2008) Induced pluripotent stem cells generated without viral integration. *Science* **322,** 945–949
47. Okita, K., Nakagawa, M., Hyenjong, H., Ichisaka, T., and Yamanaka, S. (2008) Generation of mouse induced pluripotent stem cells without viral vectors. *Science* **322,** 949–953
48. Huangfu, D., Maehr, R., Guo, W., Eijkelenboom, A., Snitow, M., Chen, A. E., and Melton, D. A. (2008) Induction of pluripotent stem cells by defined factors is greatly improved by small-molecule compounds. *Nat. Biotechnol.* **26,** 795–797
49. Carey, B. W., Markoulaki, S., Hanna, J., Saha, K., Gao, Q., Mitalipova, M., and Jaenisch, R. (2009) Reprogramming of murine and human somatic cells using a single polycistronic vector. *Proc. Natl. Acad. Sci. U. S. A.* **106,** 157–162
50. Zhou, H., Wu, S., Joo, J. Y., Zhu, S., Han, D. W., Lin, T., Trauger, S., Bien, G., Yao, S., Zhu, Y., Siuzdak, G., Scholer, H. R., Duan, L., and Ding, S. (2009) Generation of induced pluripotent stem cells using recombinant proteins. *Cell Stem Cell* **4,** 381–384
51. Woltjen, K., Michael, I. P., Mohseni, P., Desai, R., Mileikovsky, M., Hamalainen, R., Cowling, R., Wang, W., Liu, P., Gertsenstein, M., Kaji, K., Sung, H. K., and Nagy, A. (2009) piggyBac transposition reprograms fibroblasts to induced pluripotent stem cells. *Nature* **458,** 766–770
52. Yu, J., Hu, K., Smuga-Otto, K., Tian, S., Stewart, R., Slukvin, I. I., and Thomson, J. A. (2009) Human induced pluripotent stem cells free of vector and transgene sequences. *Science* **324,** 797–801
53. Yang, L., Soonpaa, M. H., Adler, E. D., Roepke, T. K., Kattman, S. J., Kennedy, M., Henckaerts, E., Bonham, K., Abbott, G. W., Linden, R. M., Field, L. J., and Keller, G. M. (2008) Human cardiovascular progenitor cells develop from a KDR+ embryonic-stem-cell-derived population. *Nature* **453,** 524–528

Received for publication June 26, 2009.
Accepted for publication September 24, 2009.

The NEW ENGLAND JOURNAL of MEDICINE

ESTABLISHED IN 1812 OCTOBER 7, 2010 VOL. 363 NO. 15

Patient-Specific Induced Pluripotent Stem-Cell Models for Long-QT Syndrome

Alessandra Moretti, Ph.D., Milena Bellin, Ph.D., Andrea Welling, Ph.D., Christian Billy Jung, M.Sc., Jason T. Lam, Ph.D., Lorenz Bott-Flügel, M.D., Tatjana Dorn, Ph.D., Alexander Goedel, M.D., Christian Höhnke, M.D., Franz Hofmann, M.D., Melchior Seyfarth, M.D., Daniel Sinnecker, M.D., Albert Schömig, M.D., and Karl-Ludwig Laugwitz, M.D.

ABSTRACT

BACKGROUND

Long-QT syndromes are heritable diseases associated with prolongation of the QT interval on an electrocardiogram and a high risk of sudden cardiac death due to ventricular tachyarrhythmia. In long-QT syndrome type 1, mutations occur in the *KCNQ1* gene, which encodes the repolarizing potassium channel mediating the delayed rectifier I_{Ks} current.

METHODS

We screened a family affected by long-QT syndrome type 1 and identified an autosomal dominant missense mutation (R190Q) in the *KCNQ1* gene. We obtained dermal fibroblasts from two family members and two healthy controls and infected them with retroviral vectors encoding the human transcription factors OCT3/4, SOX2, KLF4, and c-MYC to generate pluripotent stem cells. With the use of a specific protocol, these cells were then directed to differentiate into cardiac myocytes.

RESULTS

Induced pluripotent stem cells maintained the disease genotype of long-QT syndrome type 1 and generated functional myocytes. Individual cells showed a "ventricular," "atrial," or "nodal" phenotype, as evidenced by the expression of cell-type–specific markers and as seen in recordings of the action potentials in single cells. The duration of the action potential was markedly prolonged in "ventricular" and "atrial" cells derived from patients with long-QT syndrome type 1, as compared with cells from control subjects. Further characterization of the role of the R190Q–KCNQ1 mutation in the pathogenesis of long-QT syndrome type 1 revealed a dominant negative trafficking defect associated with a 70 to 80% reduction in I_{Ks} current and altered channel activation and deactivation properties. Moreover, we showed that myocytes derived from patients with long-QT syndrome type 1 had an increased susceptibility to catecholamine-induced tachyarrhythmia and that beta-blockade attenuated this phenotype.

CONCLUSIONS

We generated patient-specific pluripotent stem cells from members of a family affected by long-QT syndrome type 1 and induced them to differentiate into functional cardiac myocytes. The patient-derived cells recapitulated the electrophysiological features of the disorder. (Funded by the European Research Council and others.)

From the Cardiology Division, First Department of Medicine (A.M., M.B., C.B.J., J.T.L., L.B.-F., T.D., A.G., M.S., D.S., A.S., K.-L.L.), and the Plastic Surgery Department (C.H.), Klinikum rechts der Isar; the Cardiology Department, German Heart Center Munich (A.M., M.B., C.B.J., J.T.L., L.B.-F., T.D., A.G., M.S., D.S., A.S., K.-L.L.); and the Institute of Pharmacology and Toxicology (A.W., F.H.) — all at the Technical University of Munich, Munich, Germany. Address reprint requests to Dr. Laugwitz at the Cardiology Division, First Department of Medicine and German Heart Center Munich, Klinikum rechts der Isar, Technical University of Munich, Ismaninger Str., 22, D-81675 Munich, Germany, or at klaugwitz@med1.med.tum.de.

Drs. Moretti, Bellin, and Welling contributed equally to this article.

This article (10.1056/NEJMoa0908679) was published on July 21, 2010, at NEJM.org.

N Engl J Med 2010;363:1397-1409.

The long-QT syndrome is a familial, usually autosomal dominant disease characterized by an abnormally prolonged ventricular repolarization phase and a propensity toward polymorphic ventricular tachycardia (often termed torsades de pointes) and sudden cardiac death.[1-3] At least 10 different forms of the long-QT syndrome have been described, but in approximately 45% of genotyped patients, the underlying causes are mutations in the *KCNQ1* (also known as *KVLQT1* or *Kv7.1*) gene, which encodes the pore-forming alpha subunits of the channels generating I_{Ks}, an adrenergic-sensitive, slow outward potassium current.[2,4,5] This form of the long-QT syndrome is designated as long-QT syndrome type 1.

Although it is believed that a reduction in I_{Ks} is the cause of the disease phenotype of long-QT syndrome type 1, this has not been established in the case of KCNQ1 channels in human cardiomyocytes. Heterologous expression systems and genetic animal models have been used to determine the underlying mechanisms of the long-QT syndrome; however, cardiac myocytes have distinct and complex electrophysiological properties, and these properties differ among species.[6,7] Thus, a human cell-based system would be extremely useful for understanding the pathogenesis of the disease and for testing patient-specific therapies.[8]

The generation of pluripotent stem cells from human adult somatic tissues[9-13] offers the opportunity to produce large numbers of patient-specific stem cells. In recent studies, investigators have been successful in deriving pluripotent stem cells from individual patients among whom there is a variety of simple and complex genetic disorders and in differentiating them into the specific cell lineages affected by the diseases.[14-19] The capacity of induced human pluripotent stem cells to generate functional cardiac myocytes has been reported,[20-23] but to our knowledge, the use of this approach to generate myocytes harboring a disease phenotype has not yet been shown. In this study, we generated patient-specific pluripotent stem cells from members of a family affected by long-QT syndrome type 1 and showed the capacity of these cells to give rise to functional cardiomyocytes that recapitulate the electrophysiological characteristics of the disorder.

Figure 1 (facing page). Generation of Pluripotent Stem Cells from Patients with Long-QT Syndrome Type 1.

Panel A shows the pedigree of the proband with the long-QT syndrome (Patient III-2; QT interval corrected for heart rate [QTc], 445 msec) and his father (Patient II-2; QTc, 462 msec), as well as his affected aunt and grandfather (QTc, 481 msec and 453 msec, respectively). Squares indicate male family members, circles female family members, solid symbols family members with long-QT syndrome type 1, and open symbols unaffected family members. Panel B shows the results of sequence analysis of genomic KCNQ1 obtained from fibroblasts derived from one of the two control subjects and Patient II-2, revealing a heterozygous missense mutation in KCNQ1 exon 2, in position 569 of the coding sequence (569G→A; NM_000218), resulting in the substitution of the positively charged arginine for an uncharged glutamine at position 190 of the protein (R190Q; NP_000209). The same results were obtained with DNA from all the induced pluripotent stem-cell lines derived from controls and from patients with the long-QT syndrome. Panel C is a schematic representation of the KCNQ1 and KCNE1 proteins, with the R190Q mutation located in the cytoplasmic loop between transmembrane segments S2 and S3 of the KCNQ1 protein. The six transmembrane domains (S1 to S6) are flanked by amino (NH2)–terminal and carboxyl (COOH)–terminal regions; P denotes the pore region. Functional I_{Ks} channels result from the coassembly of four KCNQ1 alpha subunits and at least two auxiliary KCNE1 beta subunits. Panel D shows primary skin fibroblasts derived from Patient II-2 and a representative induced pluripotent stem-cell colony from the same patient. Panel E shows the presence of alkaline phosphatase activity in a representative colony of pluripotent stem cells derived from Patient II-2. Panel F shows immunofluorescence analyses of pluripotency markers NANOG (red) and TRA1-81 (green) in a representative pluripotent stem-cell clone derived from Patient III-2, with nuclear staining (DNA, blue) of all cells, including mouse embryonic fibroblast feeders. The lower right-hand image is a magnification of the area framed in the adjacent image.

METHODS

CLINICAL HISTORY AND GENETIC PHENOTYPE

During the clinical evaluation of an 8-year-old boy for attention deficit–hyperactivity disorder, an electrocardiogram showed a prolonged QT interval (QT interval corrected for heart rate [QTc], 445 msec). Sequencing of the *KCNQ1* gene revealed a heterozygous single base exchange (569G→A), resulting in an R190Q missense mutation previously known to be associated with long-QT syndrome type 1[24-26]

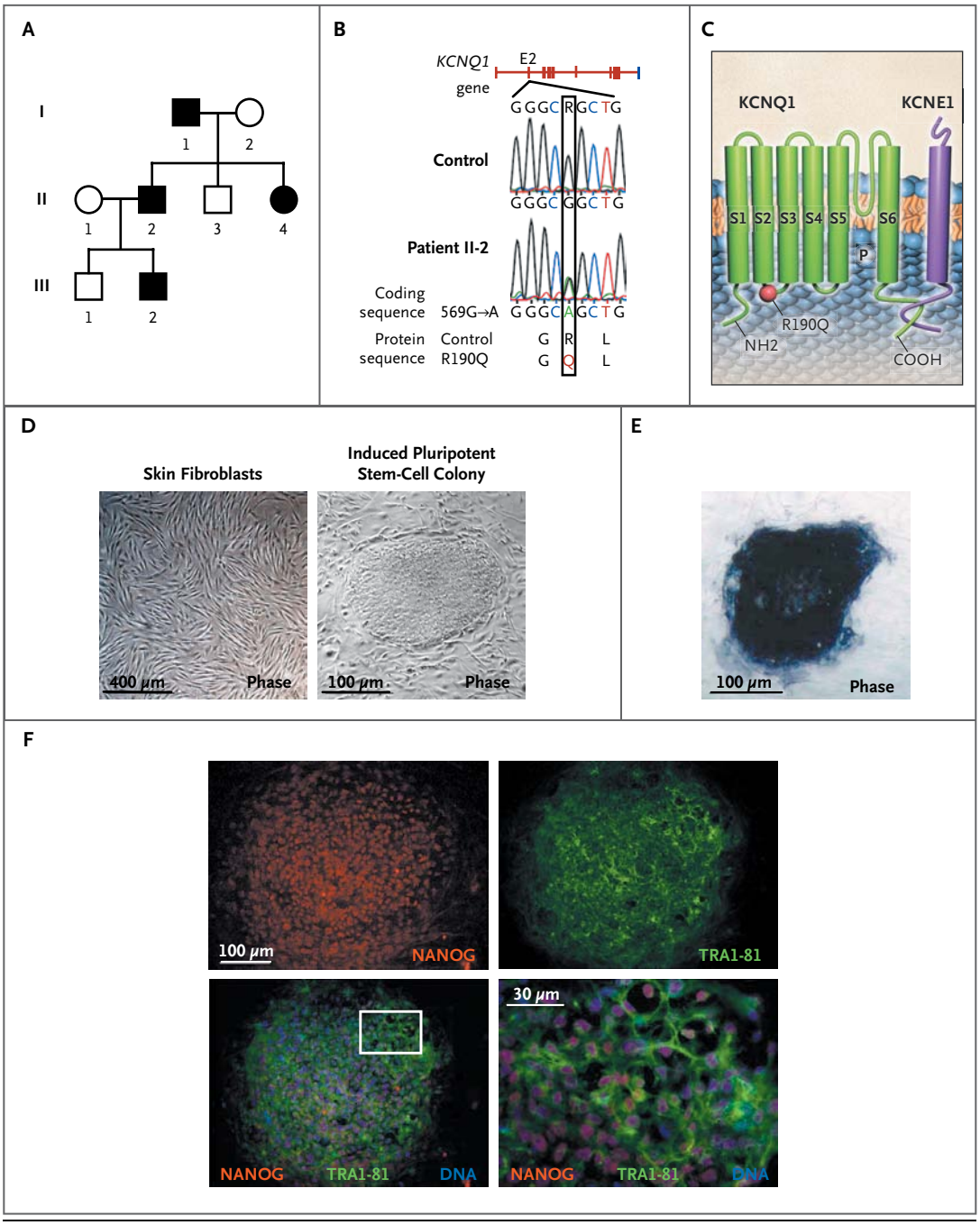

(Fig. 1A and 1B). The mutation is located in the cytoplasmic loop between the transmembrane segments S2 and S3 of the KCNQ1 protein[24] (Fig. 1C).

Subsequent screening of members of the boy's family revealed prolonged QT intervals in the 42-year-old father (QTc, 462 msec), the 39-year-old aunt (QTc, 481 msec), and the 70-year-old grandfather (QTc, 453 msec), and genetic testing showed that these family members had the same heterozygous mutation, confirming autosomal dominant inheritance in this family (Fig. 1A and 1B). The father and son have thus far been as-

ymptomatic. The grandfather and aunt have reported periods of dizziness and palpitations. All the genetically affected family members are being treated with beta-blockers.

GENERATION OF PATIENT-SPECIFIC PLURIPOTENT STEM CELLS

For the generation of pluripotent stem cells, we recruited the father and son in the family affected by long-QT syndrome type 1 along with two healthy control subjects. The protocols for research involving human subjects and for stem-cell research were approved by the institutional review board and the committee charged with oversight of embryonic stem-cell research at the Technical University of Munich. All the study participants provided written informed consent.

Dermal-biopsy specimens were minced and placed on culture dishes. Fibroblasts migrating out of the explants were passaged twice and then infected with a combination of retroviruses encoding the human transcription factors OCT3/4, SOX2, KLF4, and c-MYC.[9] After 6 days, infected cells were seeded on murine embryonic fibroblast feeders and cultured in standard human embryonic stem-cell medium until induced pluripotent stem-cell colonies appeared. Details of the study methods are provided in the Supplementary Appendix, available with the full text of this article at NEJM.org.

IN VITRO CARDIAC DIFFERENTIATION

We differentiated induced pluripotent stem cells as embryoid bodies by detaching the stem-cell colonies from the feeder cells and maintaining them for 3 days in feeder-cell-conditioned human embryonic stem-cell medium in low attachment plates.[27,28] At day 4, the medium was replaced with differentiation medium containing 20% fetal-calf serum. Embryoid bodies were plated on gelatin-coated dishes on day 7. Between days 20 and 30, areas that exhibited spontaneous contraction (indicative of cardiac differentiation) were microdissected, plated on fibronectin-coated plates, and maintained in culture in differentiation medium containing 2% fetal-calf serum. For single-cell analysis, microdissected areas were dissociated with the use of type II collagenase. Single cells were plated on fibronectin-coated slides for immunohistochemical and electrophysiological analysis.

IMMUNOHISTOCHEMICAL ASSESSMENTS

Immunostaining was performed according to standard protocols with the use of antibodies specific for the following: Nanog (Abcam), TRA-1-81 (BD Pharmingen), cardiac troponin T (Lab Vision), α-actinin (Sigma–Aldrich), myosin light chain 2a and myosin light chain 2v (Synaptic Systems), KCNQ1 (Abcam), and protein disulfide isomerase (Abcam). Staining was also performed for F-actin with the use of fluorescence-labeled phalloidin (Invitrogen).

POLYMERASE-CHAIN-REACTION ASSAYS

The polymerase chain reaction (PCR) was used to amplify the mutated region of the *KCNQ1* gene for sequencing. Quantitative real-time PCR was used in allelic-discrimination assays and for the assessment of expression of pluripotency genes, retroviral transgenes, and cell-lineage markers. Reverse-transcriptase (RT)–PCR was used to assay cardiomyocyte phenotype markers in single cells. Detailed methods are provided in the Supplementary Appendix; primers are listed in Table 1 in the Supplementary Appendix.

ELECTROPHYSIOLOGICAL ASSESSMENTS

Whole-cell recordings were obtained with the use of standard patch-clamp techniques.[7,29] Culture differentiation medium was used as the external bath solution. Action potentials and currents were recorded at approximately 35°C. All currents were normalized to cell capacitance.

STATISTICAL ANALYSIS

Data that passed tests for normality and equal variance were analyzed with the use of one-way analysis of variance followed by Tukey's test, when appropriate. The Wilcoxon signed-rank test and the Kruskal–Wallis test followed by Dunn's test were used to analyze the remaining data. Two-sided P values of less than 0.05 were considered to indicate statistical significance.

RESULTS

GENERATION OF PLURIPOTENT STEM CELLS

We generated pluripotent stem cells from primary fibroblasts derived from two patients with long-QT syndrome type 1 and two control subjects after retroviral transduction of the reprogramming factors. Starting at 3 weeks after viral

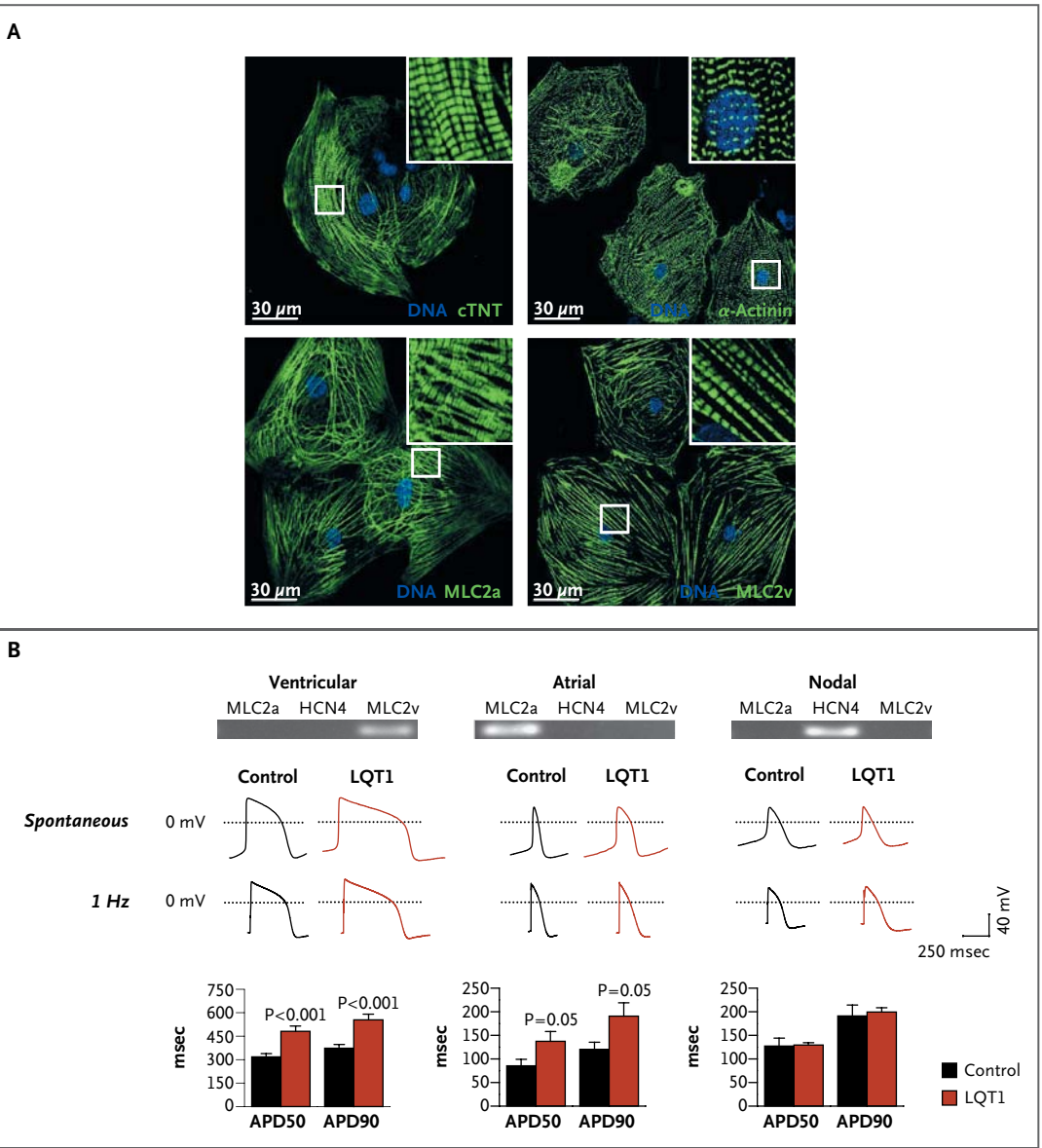

Figure 2. Disease Phenotype of Long-QT Syndrome Type 1 Cardiac Myocytes Generated from Induced Pluripotent Stem Cells.

Panel A shows immunofluorescence analysis for cardiomyocyte markers in single cells dissociated from long-QT syndrome type 1 (LQT1) explants. The insets, which are magnifications of the framed areas, show the organization of cardiac troponin T (cTNT), α-actinin, and atrial and ventricular isoforms of myosin light chain 2 (MLC2a and MLC2v) into mature sarcomeric structures. The top of Panel B shows the results of single-cell RT-PCR from three representative patched cells with respect to the expression of specific myocyte markers: MLC2v, MLC2a, and hyperpolarization-activated, cyclic nucleotide-gated channel 4 (HCN4). The middle of the panel shows examples of typical spontaneous and paced (at 1 Hz) "ventricular," "atrial," and "nodal" action potentials recorded in cardiomyocytes derived from induced pluripotent stem cells from a control subject and a patient with LQT1. The bar graphs at the bottom of the panel represent the averaged action-potential duration at 50% repolarization (APD50) and at 90% repolarization (APD90) for each of the three myocyte subtypes at a 1-Hz stimulation rate. Between 4 and 40 cells from six different induced pluripotent stem-cell clones (three clones from each person) were analyzed per group (see Table 3 in the Supplementary Appendix). P values are for the comparison between LQT1 myocytes and control myocytes, with the use of one-way analysis of variance.

infection, colonies with stem-cell morphologic characteristics appeared and were clonally expanded on murine embryonic fibroblasts (Fig. 1D). Three clones from each subject were chosen for further characterization.

The genomic *KCNQ1* locus was sequenced in all the induced pluripotent stem-cell clones, confirming the integrity of the locus and the absence of retroviral DNA. The expected 569G→A mutation was detected in all stem-cell clones and skin fibroblasts derived from the patients with long-QT syndrome type 1 but not in cells derived from control subjects. The presence of alkaline phosphatase activity (Fig. 1E), immunoreactivity for embryonic stem-cell–associated antigens, including NANOG and TRA-1-81 (Fig. 1F), reactivation of endogenous pluripotency genes (*OCT3/4, SOX2, REX1, NANOG,* and *CRIPTO/TDGF1*) (Fig. 1A in the Supplementary Appendix), and silencing of retroviral transgenes (Fig. 1B in the Supplementary Appendix) indicated that there had been successful reprogramming of putative induced pluripotent stem-cell clones. On spontaneous embryoid-body differentiation, all induced pluripotent stem-cell clones showed up-regulation of lineage markers representative of the three embryonic germ layers, endoderm (*PDX1*, *SOX7*, and *AFP*), mesoderm (*CD31*, *DESMIN*, *ACTA2*, *SCL*, *MYL2*, and *CDH5*), and ectoderm (*KTR14*, *NCAM1*, *TH*, and *GABRR2*) (Fig. 2 in the Supplementary Appendix), confirming their pluripotent nature.[28]

ASSESSMENT OF THE LONG-QT SYNDROME TYPE 1 PHENOTYPE

Using a specific differentiation protocol, we directed induced pluripotent stem cells from both affected family members and controls into the cardiac lineage (see Methods, Results, and Fig. 3 in the Supplementary Appendix). Spontaneously contracting foci started to appear after approximately 12 days of differentiation (see video 1, available at NEJM.org) and were explanted and then dissociated into single cells that maintained the expression of distinct myocyte markers (Fig. 2A) and spontaneous contraction (video 2). No major differences in the efficiency of differentiation into myocyte lineages were observed among the three clones from each of the four subjects (Fig. 3E in the Supplementary Appendix).

To assess whether the myocytes derived from induced pluripotent stem cells from patients with long-QT syndrome type 1 recapitulated the disease phenotype, we recorded the action potentials in single cells. Both spontaneously beating cells that had been dissociated from long-QT syndrome type 1 explants and those that had been dissociated from control explants responded to pacing and generated three distinct types of action potentials. These were designated as "ventricular," "atrial," and "nodal," on the basis of their similarity to the action potentials of ventricular, atrial, and nodal cardiomyocytes from human fetal hearts[30] (Fig. 2B; for detailed classification, see Results, Discussion, and Fig. 4 in the Supplementary Appendix). The classification based on action-potential properties correlated with gene-expression analysis of specific myocyte-lineage markers, as shown with the use of single-cell RT-PCR on patched cells (Fig. 2B, and Fig. 4 and 5 in the Supplementary Appendix).

Whereas the characteristics of the action potential of "nodal" myocytes were similar between cells derived from patients with long-QT syndrome type 1 and cells derived from control subjects, the action potentials of "ventricular" and "atrial" myocytes derived from patients with long-QT syndrome type 1 were significantly longer and had a slower repolarization velocity than did those derived from controls (Fig. 2B, and Tables 2 and 3 in the Supplementary Appendix). With electrical pacing set at 1 Hz, the mean (±SE) duration of the action potential measured at 90% repolarization was 554.2±35.6 msec and 190.8±28.1 msec in "ventricular" and "atrial" myocytes, respectively, in cells derived from patients with long-QT syndrome type 1, as compared with 373.2±22.6 msec and 119.9±15.5 msec in the corresponding cells from control subjects (Fig. 2B). Increasing the stimulation frequency decreased the duration of the "ventricular" myocyte action potential in both groups, with little change in other features of the action potential. However, adaptation of the action-potential duration to higher pacing frequencies was significantly less pronounced in the myocytes from the patients with long-QT syndrome type 1 than in those from the control subjects (Fig. 6 in the Supplementary Appendix). The results were similar in all the clones from the two patients and in all the clones from the two healthy controls (Fig. 7 in the Supplementary Appendix), suggesting that there was phenotypic homogeneity among

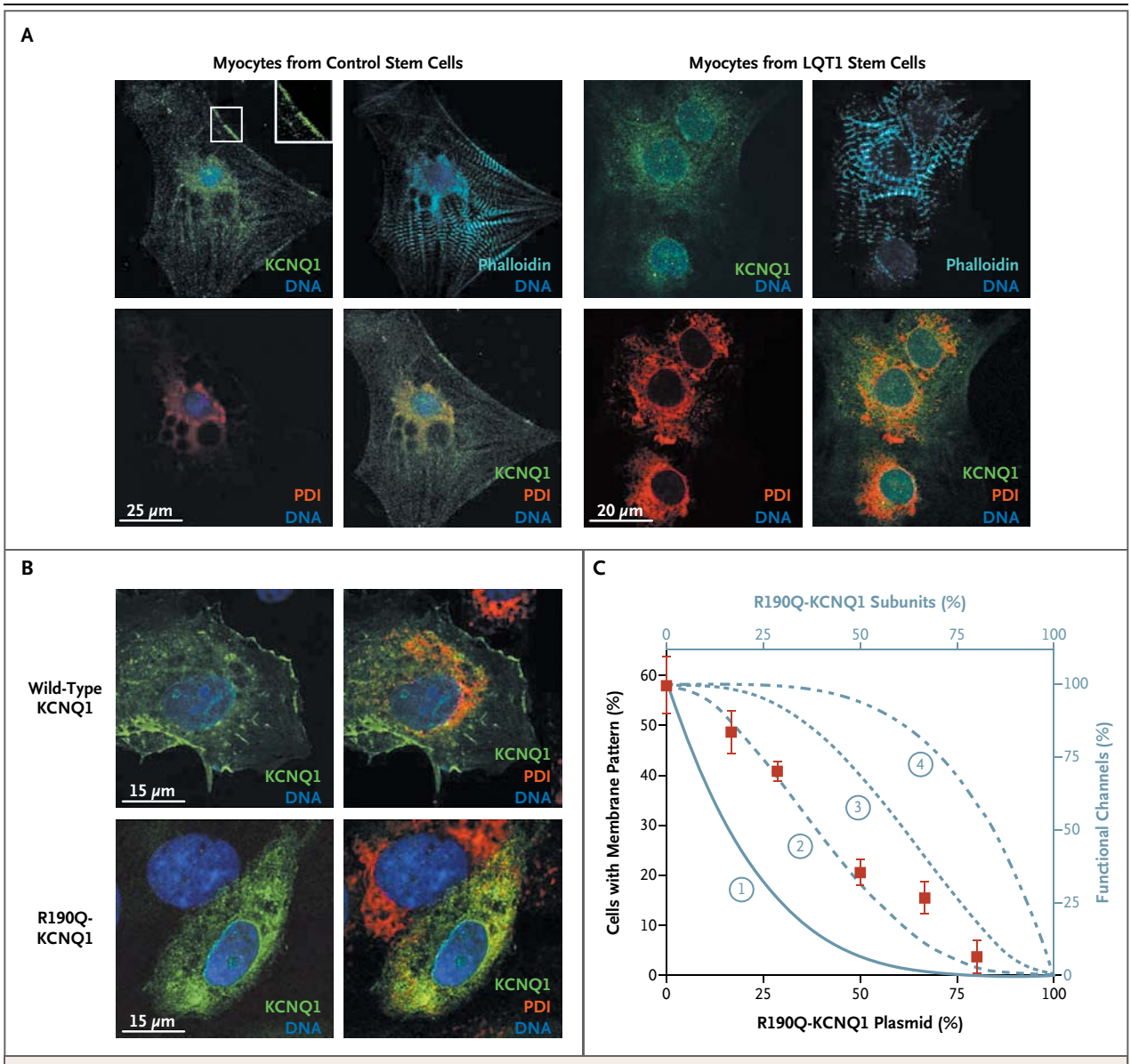

Figure 3. Characterization of the Role of the R190Q-KCNQ1 Mutation in the Pathogenesis of Long-QT Syndrome Type 1.

Panel A shows immunofluorescence analysis of the cellular distribution of KCNQ1 in representative myocytes derived from induced pluripotent stem cells from a control subject and a patient with long-QT syndrome type 1. KCNQ1 (green) can be seen in the endoplasmic reticulum, stained by protein disulfide isomerase (PDI, red), and on the plasma membrane (inset in upper left-hand image) of control myocytes but remains mostly in the endoplasmic reticulum of long-QT syndrome type 1 myocytes. Phalloidin staining (cyan) was used to identify differentiated striated myocytes. Panel B shows immunofluorescence analysis of the cellular distribution of KCNQ1 in H9c2 cells transfected with wild-type or R190Q-KCNQ1 expression vector. Wild-type KCNQ1 (green, upper images) is enriched in the plasma membrane of the cell, whereas R190Q-KCNQ1 (green, lower images) shows aberrant membrane translocation. Panel C shows the effect of cotransfecting increasing amounts of an expression vector encoding R190Q-KCNQ1, fused to a cyan fluorescent protein, together with a constant amount of a construct expressing wild-type KCNQ1, fused to yellow fluorescent protein, on the percentage of cells displaying yellow fluorescence in a plasma membrane or vesicular staining pattern (experimental data shown in red, with I bars indicating standard errors). The expected percentage of functional channels is plotted against the percentage of available R190Q-KCNQ1 subunits, assuming that the presence of 1, 2, 3, or 4 R190Q-KCNQ1 subunits (indicated by the encircled numbers) in a channel tetramer is sufficient to render the channel nonfunctional.

induced pluripotent stem-cell lines from the same person and no evident difference in the disease phenotype of the cells from the two patients with long-QT syndrome type 1. Therefore, we limited our further analysis to three clones from one patient with long-QT syndrome type 1 and three clones from one control subject.

ROLE OF R190Q-KCNQ1 IN THE PATHOGENESIS OF LONG-QT SYNDROME TYPE 1

The analysis of gene expression with the use of quantitative RT-PCR and immunoblotting revealed that *KCNQ1* messenger RNA and protein levels were similar between myocytes derived from subjects with long-QT syndrome type 1 and those derived from controls. In addition, there was similar allelic expression of wild-type and mutated 569G→A transcripts in explants derived from two different clones from the patient with long-QT syndrome type 1 (Fig. 8 in the Supplementary Appendix). To further investigate the functional consequences of the R190Q-KCNQ1 mutation in the induced pluripotent stem-cell model, we examined the cellular distribution of the KCNQ1 protein. Immunocytochemical tests for KCNQ1 in myocytes derived from patients with long-QT syndrome type 1 revealed a reticular, intracellular expression pattern, in which KCNQ1 partially colocalized with the endoplasmic-reticulum marker protein disulfide isomerase. In contrast, in cells from control subjects, the channel subunit was enriched in the cell surface compartment (Fig. 3A). Arginine 190 of KCNQ1 is known to be part of a basic endoplasmic-reticulum retention signal.[31,32] This suggests that the subcellular distribution of KCNQ1 observed in myocytes derived from patients with long-QT syndrome type 1 may be due to a trafficking defect.

To confirm this hypothesis, we expressed R190Q-KCNQ1 subunits and wild-type KCNQ1 subunits in the cardiomyoblast H9c2 cell line and analyzed their subcellular localization. As was seen in the immunodetection pattern of KCNQ1 in induced pluripotent stem-cell–derived myocytes, wild-type KCNQ1 protein achieved cell-membrane targeting, whereas R190Q-KCNQ1 failed to do so (Fig. 3B). Expression vectors encoding wild-type KCNQ1, fused to a yellow fluorescent protein, and R190Q-KCNQ1, fused to a cyan fluorescent protein, were then cotransfected into H9c2 cells in various ratios. The percentage of cells presenting a yellow fluorescent protein signal in a cell membrane pattern decreased as the proportion of mutant channel subunits increased, suggesting a model in which a tetrameric channel containing more than one R190Q subunit loses the ability to translocate to the cell

Figure 4 (facing page). Electrophysiological Analysis of I_K Current in Myocytes Derived from Induced Pluripotent Stem Cells from Control Subjects and from Patients with Long-QT Syndrome Type 1.

Panel A shows the isolation of the slow and rapid components of I_K (I_{Ks} and I_{Kr}) in "ventricular" myocytes from induced pluripotent stem cells. The graphs on the left show sample traces of whole-cell current from control and long-QT syndrome type 1 (LQT1) cells and the voltage protocol used for the recordings. The holding potential was at −40 mV, and test potentials were at +10, +30, and +50 mV, lasting 5 seconds. Tail current was recorded after the test potential was back to −40 mV. After a recording without drugs (a and a′), the cells were perfused with 10 μM chromanol 293B (b) or with 1 μM E4031 (b′), and I_{Ks} and I_{Kr} were defined as the chromanol-sensitive (c) and E4031-sensitive (c′) currents, respectively. The graphs on the right show quantification of I_{Ks} and I_{Kr}. Current amplitudes measured at the end of depolarization (I_{Ks} or I_{Kr}) and at the peak of the tail (I_{Ks} tail or I_{Kr} tail) were plotted against membrane voltages. The control myocytes included 9 cells from three induced pluripotent stem-cell clones derived from one of the control subjects, and the LQT1 myocytes included 12 cells from three clones derived from Patient II-2. There was a significant reduction in I_{Ks} current density in LQT1 cells as compared with control cells at the specified membrane voltages. Asterisks denote $P<0.05$, with the use of one-way analysis of variance. Current density is measured as picoamperes per picofarad (pA/pF). Panel B shows the voltage dependence of I_{Ks} activation. Peak values of chromanol-sensitive I_{Ks} tail currents were normalized to the maximum amplitude value recorded from each particular cell and plotted against the test potentials. The holding potential was at −40 mV, and test potentials were at 0 to +50 mV, in steps of 10 mV, each lasting 5 seconds. The control "ventricular" myocytes included 7 cells from three clones derived from one of the control subjects, and LQT1 "ventricular" myocytes included 8 cells from three clones derived from Patient II-2. Panel C shows the voltage dependence of I_{Ks} deactivation kinetics. I_{Ks} was activated by a 5-second test pulse to +50 mV from a holding potential of −40 mV. The cells were then clamped back to different potentials ranging from −40 to −10 mV, and the deactivation time course of the tail current was fitted by a single exponential function. Measurements were performed in the presence of 1 μM E4031 in order to block I_{Kr}. The graph shows the time constant (τ) of deactivation plotted against the membrane potential. The control "ventricular" myocytes included 7 cells from two clones derived from one of the control subjects, and LQT1 "ventricular" myocytes included 8 cells from two clones derived from Patient II-2. $P<0.05$, with the use of a one-way analysis of variance.

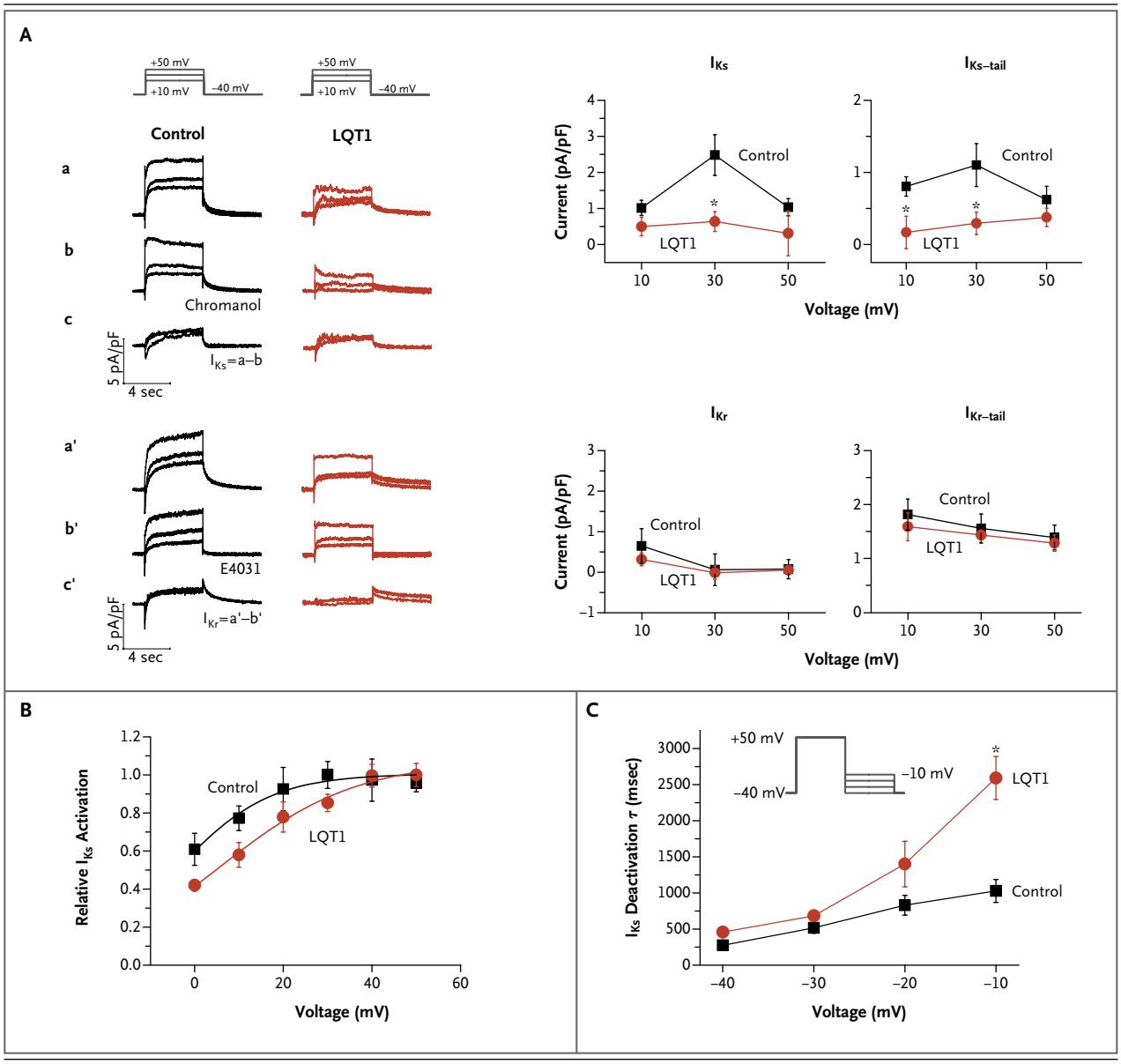

surface compartment (Fig. 3C; for details on the model, see the Methods section in the Supplementary Appendix). Analysis of fluorescence resonance energy transfer showed that the R190Q mutation did not alter the capacity of the mutant subunit to coassemble with wild-type subunits (Fig. 9 in the Supplementary Appendix).[33]

ELECTROPHYSIOLOGICAL ANALYSIS OF K^+ CURRENTS

To provide further mechanistic insight into the function of the mutated KCNQ1 protein, we performed single-cell electrophysiological analysis of various repolarizing K^+ currents in "ventricular" myocytes. With the use of a distinct voltage protocol that preferentially elicits the outward delayed rectifier current, I_K, cardiac myocytes derived from induced pluripotent stem cells from patients with long-QT syndrome type 1, as compared with those from control subjects, showed a substantial reduction in K^+ current (Fig. 4A).

Further characterization with the use of channel blockers specific for the slow and rapid components of I_K — chromanol 293B (which blocks I_{Ks}) and E4031 (which blocks I_{Kr})[34] — showed that I_{Ks} current densities in myocytes from patients with long-QT syndrome type 1, as compared with those from control subjects, were decreased, whereas I_{Kr} conductance was unaffected. At +30

mV, I_{Ks} and tail I_{Ks} were diminished by approximately 75%, suggesting that in heterozygous "ventricular" myocytes from patients with long-QT syndrome type 1, the mutant form of KCNQ1 interferes with the function of the wild-type subunit (Fig. 4A). Furthermore, both activation and deactivation properties of the tail I_{Ks} current in cells from patients with long-QT syndrome type 1, as compared with cells from controls, appeared to be altered, with activation being slightly shifted toward more positive voltages (Fig. 4B) and deactivation being decelerated (Fig. 4C). We next analyzed the transient outward (I_{to}) and inward currents that function in the hyperpolarization state. As with the results for I_{Kr}, I_{to} and diastolic current densities did not differ between "ventricular" myocytes from patients with long-QT syndrome type 1 and those from control subjects (Fig. 10 in the Supplementary Appendix), showing that there was a specific genotype–phenotype correlation.

PROTECTIVE ACTION OF BETA-BLOCKADE

Since fatal arrhythmias are precipitated by increased sympathetic tone in patients with long-QT syndrome type 1,[3,35] we tested whether adrenergic stimulation can affect the phenotype of long-QT syndrome type 1 cardiomyocytes derived from pluripotent stem cells. First, we analyzed the effect of catecholamines on the duration of the action potential in paced "ventricular" myocytes. At 2 Hz, isoproterenol induced approximately a 20% reduction in the interval between 30% and 90% repolarization of the action potential in control myocytes, whereas in cells from patients with long-QT syndrome type 1 this interval was almost unaffected (Fig. 5A). Accordingly, I_{Ks} was markedly enhanced by adrenergic stimulation in "ventricular" myocytes from control subjects, and the increase was significantly smaller in cells from patients with long-QT syndrome type 1, suggesting that defective responsiveness to adrenergic challenge is due to an abnormal I_{Ks} current (Fig. 5B).[36]

We further investigated the effect of isoproterenol on spontaneously beating myocytes. In cells from control subjects, isoproterenol had a positive chronotropic effect accompanied by a shortening of the duration of the action potential, resulting in a 30% reduction in the ratio of the action-potential duration at 90% repolarization to the action-potential interval. In contrast, in myocytes from patients with long-QT syndrome type 1, this ratio was increased by 15%, thereby exacerbating the long-QT syndrome type 1 phenotype and increasing the risk of arrhythmic events (Fig. 5C). In fact, under conditions of adrenergic stress, six of nine "ventricular" myocytes from patients with long-QT syndrome type 1 developed early afterdepolarizations (4.1±1.5 early

Figure 5 (facing page). Adrenergic Modulation and Protective Effect of Beta-Blockade in Control and Long-QT Syndrome Type 1 "Ventricular" Myocytes.

Panel A shows an overlay of single action potentials from a representative cell from a control subject and from a patient with long-QT syndrome type 1 (LQT1) at a 2-Hz stimulation rate before (basal) and after application of 100 nM isoproterenol. The bar graph represents the percent change induced by isoproterenol on the interval from the action-potential duration (APD) at 30% repolarization (APD30) to APD90 (APD30–APD90), on APD90, and on APD. Data are means ±SE for 10 cells in each group (from three clones derived from one of the control subjects and three clones derived from Patient II-2). Panel B shows the effect of adrenaline on I_{Ks} tail current. On the left are representative overlapped I_{Ks} tail-current traces from a control and an LQT1 myocyte before and after treatment with 1 μM adrenaline recorded at +30 mV depolarization with the use of the voltage protocol depicted at the top of the panel. Measurements were performed in presence of 1 μM E4031 in order to block I_{Kr}. The bar graph represents the factor increase in I_{Ks} tail current induced by 1 μM adrenaline at the specified depolarization voltages in control and LQT1 myocytes. Data are means ±SE for 8 cells in each group (from two clones derived from one of the control subjects and from two clones derived from Patient II-2). Panel C shows representative recordings of single-cell spontaneous action potentials from a control and an LQT1 "ventricular" myocyte before (baseline) and during exposure to a combination of 100 nM isoproterenol and 200 nM propranolol or to 100 nM isoproterenol alone. Cells were pretreated for 2 minutes with 200 nM propranolol before application of the combination of 100 nM isoproterenol and 200 nM propranolol (traces not shown). The bar graph represents the percent change in the ratio of APD90 to the action-potential interval (APD90/AP interval) induced by the combination of 100 nM isoproterenol and 200 nM propranolol or by 100 nM isoproterenol alone. Action potentials affected by early afterdepolarizations (EAD) were excluded from the analysis. Data are means ±SE for 8 control cells (from three clones derived from one of the control subjects) and 9 LQT1 cells (from three clones derived from Patient II-2). P values in the three panels are for the comparison between LQT1 myocytes and control myocytes, with the use of the Wilcoxon signed-rank test.

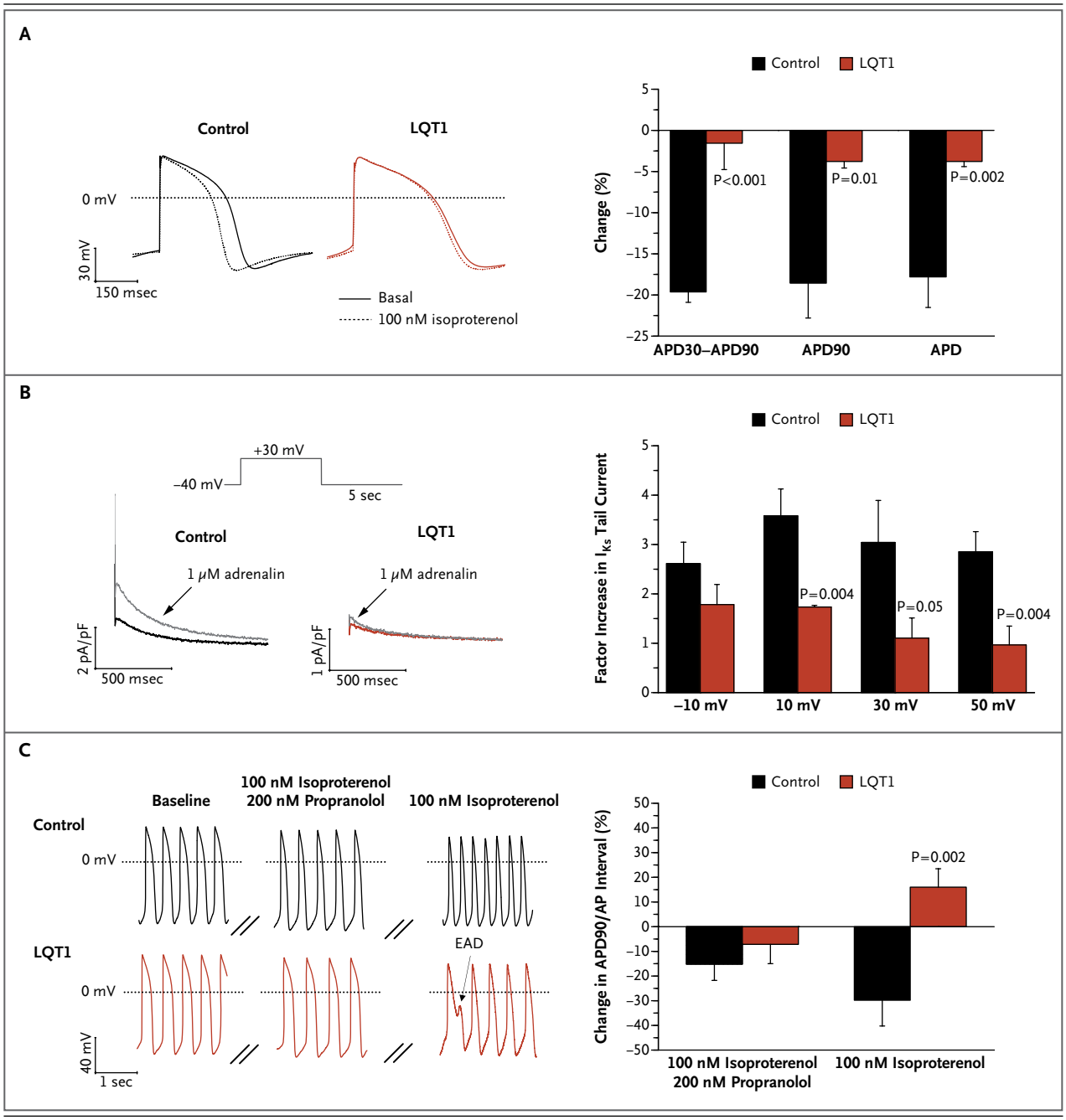

afterdepolarizations per 20 sec, with 9.2±2.1% of the beats affected by early afterdepolarizations), whereas none of the eight cells from control subjects did. Pretreatment with propranolol, a nonselective beta-blocker, substantially blunted the effect of isoproterenol in myocytes from both control subjects and patients with long-QT syndrome type 1 (0.6±0.3 early afterdepolarizations per 20 sec, with 1.7±0.8% of the beats affected), thus protecting the diseased cells from catecholamine-induced tachyarrhythmia due to impaired rate adaptation of the action potential (Fig. 5C).

DISCUSSION

Since the initial reports on induced human pluripotent stem-cell technology were published, several patient-specific induced pluripotent stem-

cell lines for neurodegenerative and metabolic disorders have been developed.[14,16,18,19,37] Establishing reliable models of human disease in such cells has remained challenging, owing to difficulties in directing cell differentiation and in identifying disease-related mechanisms. In this study, we reprogrammed fibroblasts derived from members of a family with autosomal-dominant long-QT syndrome type 1 and used these induced pluripotent stem cells to generate patient-specific cardiomyocytes. These myocytes showed expression of specific markers and electrophysiological characteristics that suggested that the reprogramming process did not affect the ability of the cells to function normally. Furthermore, we observed disease-specific abnormalities in the duration of the action potential, the action-potential rate adaptation, and I_{Ks} currents, owing to an R190Q-KCNQ1 trafficking defect, as well as vulnerability to catecholaminergic stress.

To date, insights into the pathogenesis of the long-QT syndrome have come primarily from heterologous expression systems and genetic animal models. Depending on the cell type used, both haploinsufficiency and dominant negative effects have been postulated as the mechanism of disease associated with the R190Q mutation.[24-26] In our induced pluripotent stem-cell model of long-QT syndrome type 1, a reduction in I_{Ks} current density by approximately 75%, combined with subcellular localization, showed that the R190Q mutant suppresses channel trafficking to the plasma membrane in a dominant negative manner. Owing to differences among species in the channels that generate the main cardiac repolarizing currents, none of the available mouse models of the long-QT syndrome fully emulate the human disease phenotype. Recently, transgenic rabbit models of long-QT syndrome type 1 and long-QT syndrome type 2 have been engineered by means of overexpression of dominant negative pore mutants of the human genes *KCNQ1* and *KCNH2*.[38] In these animals, both transgenes caused a down-regulation of the complementary I_{Kr} and I_{Ks} currents. In contrast, no alterations in repolarizing currents other than in I_{Ks} were observed in patient-specific myocytes derived from persons with the R190Q-KCNQ1 mutation associated with long-QT syndrome type 1. This discrepancy, which may be mutant-dependent or model-dependent, shows the importance of alternative systems in which human genetic disorders can be studied in the physiologic and disease-causing contexts on a patient-specific level.

Our data provide clear evidence that the pathogenesis of the R190Q mutation can be modeled in myocyte lineages generated from pluripotent stem cells derived from patients with long-QT syndrome type 1. Moreover, our findings suggest that there may be alternative approaches to the development of candidate drugs, such as compounds to promote the delivery of the mutant to the plasma membrane or I_{Ks} activators. The observed protective effects of beta-blockade show that it is possible to investigate the therapeutic action of medications for treating human cardiac disease in vitro with the use of patient-specific cells. This approach is particularly attractive because of the pluripotent nature of these cells and the potentially unlimited number of induced cardiomyocytes available for high-throughput drug development.

Even though the incidence of the long-QT syndrome is only 1 case per 2500 live births, this syndrome provides a platform for showing the suitability of induced pluripotent stem-cell technology as a means of exploring disease mechanisms in human genetic cardiac disorders. Larger sets of long-QT syndrome cell lines harboring different channel mutations will be needed to further validate the disease phenotype and compare pathogenetic mechanisms in diverse forms of the disease. Clinically, the severity of manifestations of the long-QT syndrome varies among family members, and incomplete penetrance exists.[39] However, we did not observe any phenotypic differences in the prolongation of the action potential between the myocytes from our two patients, a finding that is probably due to the similarity of the clinical phenotype in these cases.

In summary, we derived pluripotent stem cells from patients with long-QT syndrome type 1 and directed them to differentiate into cardiac myocytes. As compared with myocytes derived in a similar fashion from healthy controls, cells from patients with long-QT syndrome type 1 exhibited prolongation of the action potential, altered I_{Ks} activation and deactivation properties, and an abnormal response to catecholamine stimulation, with a protective effect of beta-blockade, thus showing that induced pluripotent stem-cell models can recapitulate aspects of genetic cardiac diseases.

Supported by grants from the European Research Council (Marie Curie Excellence Team Grant, MEXT-23208), the German Research Foundation (Research Unit 923 and La 1238 3-1/4-1), and the German Ministry for Education and Research (01 GN 0826).

Disclosure forms provided by the authors are available with the full text of this article at NEJM.org

We thank Takashi Kitamura and Shinya Yamanaka for providing viral vectors through Addgene; Jacques Barhanin for KCNE1 and wild-type and mutant (R190Q) KCNQ1 complementary DNAs; Stefan Engelhardt and Andrea Ahles for the fluorescent β1-receptor fusion construct; Diana Grewe, Christina Scherb, and Sabine Teuber for their technical assistance in cell culture and immunohistochemical assessments; and especially the members of the family affected by long-QT syndrome type 1 and the healthy volunteers who provided us with skin-biopsy specimens for the reprogramming.

REFERENCES

1. Priori SG, Bloise R, Crotti L. The long QT syndrome. Europace 2001;3:16-27.
2. Moss AJ, Shimizu W, Wilde AA, et al. Clinical aspects of type-1 long-QT syndrome by location, coding type, and biophysical function of mutations involving the KCNQ1 gene. Circulation 2007;115:2481-9.
3. Roden DM. Long-QT syndrome. N Engl J Med 2008;358:169-76.
4. Li GR, Feng J, Yue L, Carrier M, Nattel S. Evidence for two components of delayed rectifier K+ current in human ventricular myocytes. Circ Res 1996;78:689-96.
5. Marx SO, Kurokawa J, Reiken S, et al. Requirement of a macromolecular signaling complex for beta adrenergic receptor modulation of the KCNQ1-KCNE1 potassium channel. Science 2002;295:496-9.
6. Hofmann F, Lacinová L, Klugbauer N. Voltage-dependent calcium channels: from structure to function. Rev Physiol Biochem Pharmacol 1999;139:33-87.
7. Ludwig A, Zong X, Jeglitsch M, Hofmann F, Biel M. A family of hyperpolarization-activated mammalian cation channels. Nature 1998;393:587-91.
8. Laugwitz KL, Moretti A, Caron L, Nakano A, Chien KR. Islet1 cardiovascular progenitors: a single source for heart lineages? Development 2008;135:193-205.
9. Takahashi K, Tanabe K, Ohnuki M, et al. Induction of pluripotent stem cells from adult human fibroblasts by defined factors. Cell 2007;131:861-72.
10. Yu J, Vodyanik MA, Smuga-Otto K, et al. Induced pluripotent stem cell lines derived from human somatic cells. Science 2007;318:1917-20.
11. Park IH, Zhao R, West JA, et al. Reprogramming of human somatic cells to pluripotency with defined factors. Nature 2008;451:141-6.
12. Lowry WE, Richter L, Yachechko R, et al. Generation of human induced pluripotent stem cells from dermal fibroblasts. Proc Natl Acad Sci U S A 2008;105:2883-8.
13. Jaenisch R, Young R. Stem cells, the molecular circuitry of pluripotency and nuclear reprogramming. Cell 2008;132:567-82.
14. Dimos JT, Rodolfa KT, Niakan KK, et al. Induced pluripotent stem cells generated from patients with ALS can be differentiated into motor neurons. Science 2008;321:1218-21.
15. Park IH, Arora N, Huo H, et al. Disease-specific induced pluripotent stem cells. Cell 2008;134:877-86.
16. Ebert AD, Yu J, Rose FF Jr, et al. Induced pluripotent stem cells from a spinal muscular atrophy patient. Nature 2009;457:277-80.
17. Raya A, Rodríguez-Pizà I, Guenechea G, et al. Disease-corrected haematopoietic progenitors from Fanconi anaemia induced pluripotent stem cells. Nature 2009;460:53-9.
18. Soldner F, Hockemeyer D, Beard C, et al. Parkinson's disease patient-derived induced pluripotent stem cells free of viral reprogramming factors. Cell 2009;136:964-77.
19. Maehr R, Chen S, Snitow M, et al. Generation of pluripotent stem cells from patients with type 1 diabetes. Proc Natl Acad Sci U S A 2009;106:15768-73.
20. Zhang J, Wilson GF, Soerens AG, et al. Functional cardiomyocytes derived from human induced pluripotent stem cells. Circ Res 2009;104(4):e30-e41.
21. Yokoo N, Baba S, Kaichi S, et al. The effects of cardioactive drugs on cardiomyocytes derived from human induced pluripotent stem cells. Biochem Biophys Res Commun 2009;387:482-8.
22. Gai H, Leung EL, Costantino PD, et al. Generation and characterization of functional cardiomyocytes using induced pluripotent stem cells derived from human fibroblasts. Cell Biol Int 2009;33:1184-93.
23. Freund C, Davis RP, Gkatzis K, Ward-van Oostwaard D, Mummery CL. The first reported generation of human induced pluripotent stem cells (iPS cells) and iPS cell-derived cardiomyocytes in the Netherlands. Neth Heart J 2010;18:51-4.
24. Chouabe C, Neyroud N, Richard P, et al. Novel mutations in KvLQT1 that affect Iks activation through interactions with Isk. Cardiovasc Res 2000;45:971-80.
25. Donger C, Denjoy I, Berthet M, et al. KVLQT1 C-terminal missense mutation causes a forme fruste long-QT syndrome. Circulation 1997;96:2778-81.
26. Wang Z, Tristani-Firouzi M, Xu Q, Lin M, Keating MT, Sanguinetti MC. Functional effects of mutations in KvLQT1 that cause long QT syndrome. J Cardiovasc Electrophysiol 1999;10:817-26.
27. Moretti A, Caron L, Nakano A, et al. Multipotent embryonic isl1+ progenitor cells lead to cardiac, smooth muscle, and endothelial cell diversification. Cell 2006;127:1151-65.
28. Moretti A, Bellin M, Jung CB, et al. Mouse and human induced pluripotent stem cells as a source for multipotent Isl1+ cardiovascular progenitors. FASEB J 2010;24:700-11.
29. Laugwitz KL, Moretti A, Lam J, et al. Postnatal isl1+ cardioblasts enter fully differentiated cardiomyocyte lineages. Nature 2005;433:647-53. [Erratum, Nature 2007;446:934.]
30. Mummery C, Ward-van Oostwaard D, Doevendans P, et al. Differentiation of human embryonic stem cells to cardiomyocytes: role of coculture with visceral endoderm-like cells. Circulation 2003;107:2733-40.
31. Pan N, Sun J, Lv C, Li H, Ding J. A hydrophobicity-dependent motif responsible for surface expression of cardiac potassium channel. Cell Signal 2009;21:349-55.
32. Wilson AJ, Quinn KV, Graves FM, Bitner-Glindzicz M, Tinker A. Abnormal KCNQ1 trafficking influences disease pathogenesis in hereditary long QT syndromes (LQT1). Cardiovasc Res 2005;67:476-86.
33. Voigt P, Dorner MB, Schaefer M. Characterization of p87PIKAP, a novel regulatory subunit of phosphoinositide 3-kinase gamma that is highly expressed in heart and interacts with PDE3B. J Biol Chem 2006;281:9977-86.
34. Lerche C, Bruhova I, Lerche H, et al. Chromanol 293B binding in KCNQ1 (Kv7.1) channels involves electrostatic interactions with a potassium ion in the selectivity filter. Mol Pharmacol 2007;71:1503-11. [Erratum, Mol Pharmacol 2007;72:796.]
35. Vyas H, Hejlik J, Ackerman MJ. Epinephrine QT stress testing in the evaluation of congenital long-QT syndrome: diagnostic accuracy of the paradoxical QT response. Circulation 2006;113:1385-92.
36. Imredy JP, Penniman JR, Dech SJ, Irving WD, Salata JJ. Modeling of the adrenergic response of the human IKs current (hKCNQ1/hKCNE1) stably expressed in HEK-293 cells. Am J Physiol Heart Circ Physiol 2008;295:H1867-81.
37. Lee G, Papapetrou EP, Kim H, et al. Modelling pathogenesis and treatment of familial dysautonomia using patient-specific iPSCs. Nature 2009;461:402-6.
38. Brunner M, Peng X, Liu GX, et al. Mechanisms of cardiac arrhythmias and sudden death in transgenic rabbits with long QT syndrome. J Clin Invest 2008;118:2246-59.
39. Priori SG, Schwartz PJ, Napolitano C, et al. Risk stratification in the long-QT syndrome. N Engl J Med 2003;348:1866-74.

Dantrolene rescues arrhythmogenic RYR2 defect in a patient-specific stem cell model of catecholaminergic polymorphic ventricular tachycardia

*Christian B. Jung[1†], Alessandra Moretti[1,2†], Michael Mederos y Schnitzler[3†], Laura Iop[1], Ursula Storch[3], Milena Bellin[1], Tatjana Dorn[1], Sandra Ruppenthal[4], Sarah Pfeiffer[3], Alexander Goedel[1,2], Ralf J. Dirschinger[1,2], Melchior Seyfarth[5], Jason T. Lam[1], Daniel Sinnecker[1,2], Thomas Gudermann[3]***, Peter Lipp[4]**, Karl-Ludwig Laugwitz[1,2]**

Keywords: CPVT; dantrolene; disease modelling; induced pluripotent stem cells; ryanodine receptor 2

DOI 10.1002/emmm.201100194

Received August 30, 2011
Revised December 01, 2011
Accepted December 05, 2011

Coordinated release of calcium (Ca^{2+}) from the sarcoplasmic reticulum (SR) through cardiac ryanodine receptor (RYR2) channels is essential for cardiomyocyte function. In catecholaminergic polymorphic ventricular tachycardia (CPVT), an inherited disease characterized by stress-induced ventricular arrhythmias in young patients with structurally normal hearts, autosomal dominant mutations in *RYR2* or recessive mutations in calsequestrin lead to aberrant diastolic Ca^{2+} release from the SR causing arrhythmogenic delayed after depolarizations (DADs). Here, we report the generation of induced pluripotent stem cells (iPSCs) from a CPVT patient carrying a novel RYR2 S406L mutation. In patient iPSC-derived cardiomyocytes, catecholaminergic stress led to elevated diastolic Ca^{2+} concentrations, a reduced SR Ca^{2+} content and an increased susceptibility to DADs and arrhythmia as compared to control myocytes. This was due to increased frequency and duration of elementary Ca^{2+} release events (Ca^{2+} sparks). Dantrolene, a drug effective on malignant hyperthermia, restored normal Ca^{2+} spark properties and rescued the arrhythmogenic phenotype. This suggests defective inter-domain interactions within the RYR2 channel as the pathomechanism of the S406L mutation. Our work provides a new *in vitro* model to study the pathogenesis of human cardiac arrhythmias and develop novel therapies for CPVT.

(1) Klinikum rechts der Isar, Technische Universität München, I. Medizinische Klinik, Kardiologie, München, Germany
(2) Deutsches Herzzentrum, Technische Universität München, Erwachsenenkardiologie, München, Germany
(3) Walther-Straub-Institut für Pharmakologie and Toxikologie, Ludwig-Maximilians Universität München, Goethetraße, München, Germany
(4) Institut für Molekulare Zellbiologie, Medizinische Fakultät, Universitätsklinikum Homburg/Saar, Universität des Saarlandes, Homburg/Saar, Germany
(5) Helios Klinikum Wuppertal-Universität Witten-Herdecke, III. Medizinische Klinik, Kardiologie, Wuppertal, Germany
***Corresponding author:** Tel: +49 89 41402947; Fax: +49 89 41404901; E-mail: klaugwitz@med1.med.tum.de
****Corresponding author:** Tel: +49 6841 1626103; Fax: +49 6841 1626104; E-mail: peter.lipp@uniklinikum-saarland.de
*****Corresponding author:** Tel: +49 89 218075702; Fax: +49 89 218075701; E-mail: thomas.gudermann@lrz.uni-muenchen.de

†These authors contributed equally to this work.

INTRODUCTION

Catecholaminergic polymorphic ventricular tachycardia (CPVT) is an inherited life-threatening arrhythmia leading to syncope and sudden cardiac death at a young age. CPVT patients, who usually do not show any detectable cardiac disease, manifest ventricular premature beats and bidirectional or polymorphic ventricular tachycardia in response to emotional or physical stress (Scheinman & Lam, 2006). Although the very high mortality rate (30–35% by the age of 35 years) calls for effective preventive and therapeutic measures, current clinical management of CPVT is based on the symptomatic treatment with β-blockers to reduce the frequency of arrhythmias and the implantation of automated defibrillators (ICDs) to terminate fatal arrhythmias (Kaufman, 2009). Two genetic forms of the disease have been described: one accounting for at least 50% of all cases and associated with autosomal dominant mutations in the cardiac ryanodine receptor, RYR2 (CPVT1; Priori et al, 2001) and a very rare one linked to recessive mutations in calsequestrin (CPVT2; Postma et al, 2002). Both proteins belong to the multimolecular calcium (Ca^{2+}) release channel complex of the sarcoplasmic reticulum (SR) which supports myocyte Ca^{2+} cycling and contractile activity (Berridge, 2003; Bers, 2004; Gyorke & Terentyev, 2008; Kaye et al, 2008; Lanner et al, 2010). Accumulating evidence from animal models suggests that CPVT mutations result in Ca^{2+} diastolic leak from the SR causing arrhythmogenic delayed after depolarizations (DADs) in cardiac myocytes (Liu et al, 2009). However, the molecular mechanisms underlying the pathogenesis of these mutations are still controversial.

Dantrolene, a hydantoin derivative that acts as muscle relaxant, is currently the only specific and most effective treatment for malignant hyperthermia, a rare life-threatening familial disorder caused by mutations in the skeletal ryanodine receptor (RYR1) (Kobayashi et al, 2009). It is also used in the management of other disorders, such as neuroleptic malignant syndrome and muscle spasticity (Krause et al, 2004). The therapeutic action of dantrolene seems to be due to its binding to an amino-terminal sequence of RYR1, which restores interdomain interactions critical for the closed state of the channel (Paul-Pletzer et al, 2002). Recently, dantrolene has been shown to target a corresponding sequence in RYR2 (Paul-Pletzer et al, 2005) and to improve intracellular Ca^{2+} handling in failing cardiomyocytes from a canine model of heart failure (Kobayashi et al, 2009) and arrhythmias in a mouse model of CPVT1 (Kobayashi et al, 2010; Uchinoumi et al, 2010). Although experimental animals have been extremely valuable for investigating cardiac function and pathogenesis as well as for drug assessment and development, they cannot completely model human cardiomyocytes. Induced pluripotent stem cells (iPSCs) offer the possibility to obtain human myocytes *in vitro* from patients with cardiac abnormalities (Carvajal-Vergara et al, 2010; Moretti et al, 2010b; Takahashi et al, 2007; Yazawa et al, 2011). Here, we report the generation of the first human patient-specific iPSC-based system of CPVT1 and tested whether dantrolene can rescue the disease phenotype and thus represent a potential novel drug compound for the causal treatment of CPVT.

RESULTS

Derivation of iPSC lines and their differentiation into the cardiac lineage

Dermal fibroblasts were obtained from a 24-year-old woman with a diagnosis of familial CPVT, who underwent cardiac arrest at the age of 23 years and received an ICD after cardiac resuscitation. Genetic screening showed that she carried a novel autosomal dominant S406L missense mutation in the *RYR2* gene, caused by a C → T nucleotide substitution in exon 14 at position 1217 of the coding region (Fig 1A and B). The mutation is located in the N-terminal domain (amino acids 1–600) of the RYR2 Ca^{2+} release channel, which represents, together with the central domain (amino acids 2000–2500) and the carboxy-terminal transmembrane domain, one of the three hotspots for CPVT-associated RYR2 mutations (George et al, 2007; Thomas et al, 2010; Fig 1C). Fibroblast transduction with retroviral vectors encoding for SOX2, OCT4, KLF4 and c-MYC generated several CPVT patient-specific iPSC clones, three of which were further characterized and used for cardiomyocyte differentiation. Similarly, control iPSCs were created using fibroblasts from a 32-year-old healthy female (Moretti et al, 2010b). The S406L heterozygous mutation was identified exclusively in CPVT-iPSCs. All iPSC lines showed human embryonic stem cell morphology, expression of the pluripotency markers NANOG and TRA1-81, alkaline phosphatase activity, reactivation of endogenous pluripotency genes (OCT4, SOX2, NANOG, REX1 and TDGF1), silencing of the four retroviral transgenes and normal karyotype (Fig 1D–F; Fig S1A and B of Supporting information). Pluripotency of each iPSC line was assessed by upregulation of genes specific of all three germ layers in *in vitro*-differentiating embryoid bodies (EBs) (Fig S1C of Supporting information).

To direct iPSCs into the cardiac lineage, we used the EB differentiation system as previously described (Moretti et al, 2010a,b). Spontaneously beating areas, which started to appear within 10–12 days, were manually explanted and allowed to further mature for additional 2–4 months. Quantitative real-time PCR (qRT-PCR) in cardiac explants revealed that, after 2 months maturation, expression of most genes involved in myocytic Ca^{2+} handling and excitation–contraction (EC) coupling reaches similar levels to those of fetal human heart and is comparable among different control and CPVT-iPSC clones (Fig 2A). Consistent with already reported transcriptional profile data on human iPSC-/ESC-derived cardiac explants (Gupta et al, 2010), calsequestrin (CASQ2) expression is almost undetectable in all iPSC-derived cardiac explants at this maturation stage, while RYR2 is already expressed. However, protein analysis by western blotting at 3–4 months maturation demonstrated similar expression levels of pivotal Ca^{2+} handling proteins, such as RYR2, CASQ2, triadin (TRDN), junctin (JCTN) and phospholamban (PLN), among control-, CPVT-iPSC-derived cardiomyocytes and adult human heart tissue, suggesting further development of Ca^{2+} cycling molecular components (Fig 2B). Moreover, we evaluated the expression and subcellular localization of RYR2 by confocal immunofluorescence analysis on single control and diseased iPSC-derived cardiomyocytes

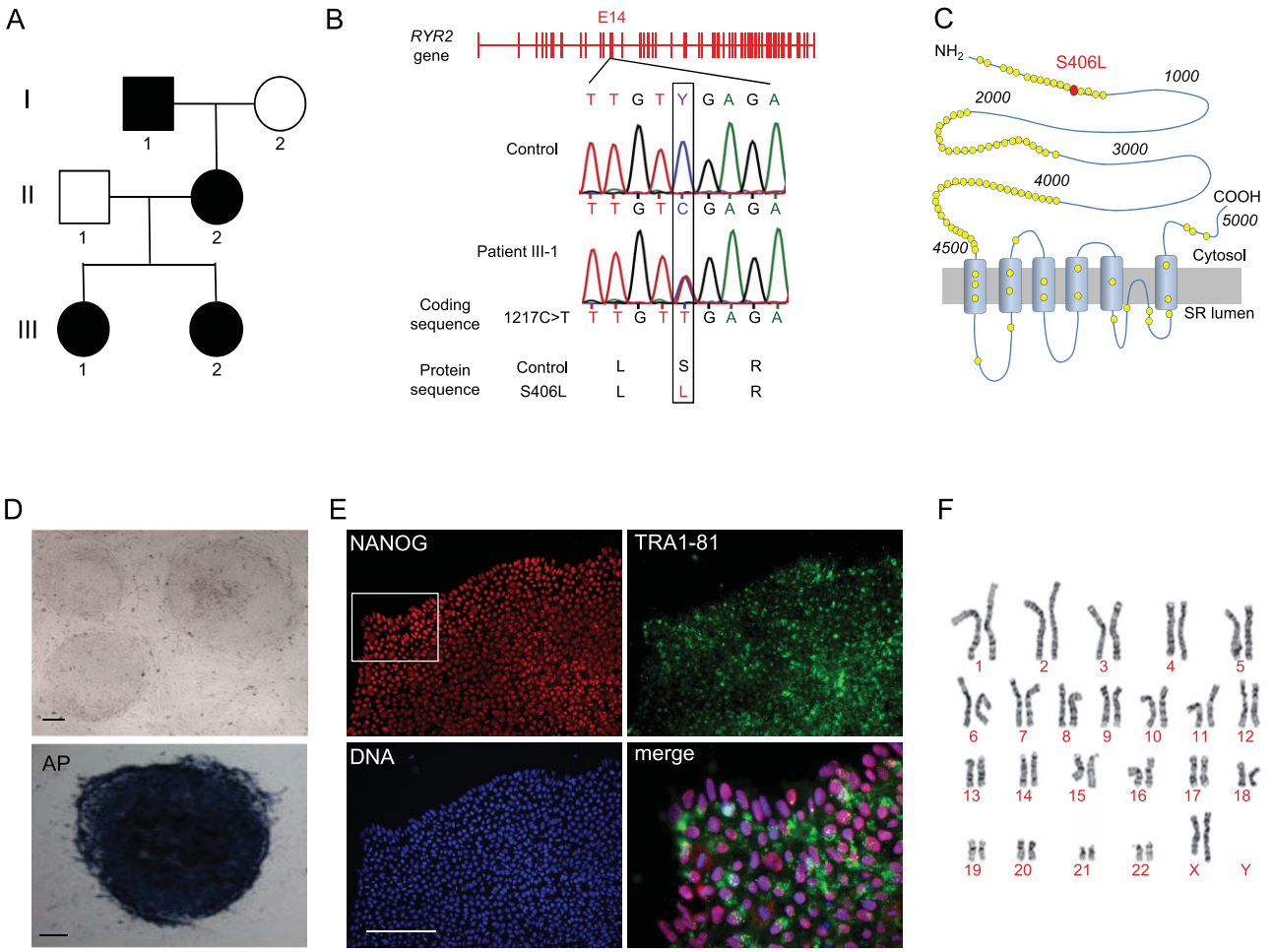

Figure 1. Generation of CPVT-iPSCs.

A. Pedigree of the CPVT-affected patient (III-1) showing autosomal dominant inheritance in the family.

B. Sequence analysis of *RYR2* gene in fibroblasts from control and CPVT patient, revealing a novel heterozygous missense mutation in exon 14 (position 1217C > T of the coding sequence). Same results were obtained from all analysed control and CPVT-iPSC clones.

C. Schematic representation of RYR2 channel and localization of the S406L mutation (red circle) at the N-terminal domain. Yellow circles indicate reported putative pathogenic mutations.

D. Representative images of CPVT-iPSC colonies in bright field (top, clone a) and after staining for alkaline phosphatase (AP) activity (bottom, clone c). Scale bars, 100 μm.

E. Representative images of a CPVT-iPSC colony (clone b) after immunostaining for the pluripotency markers NANOG (red) and TRA1-81 (green). Merged image is the magnified area marked by the white box. Scale bars, 100 μm.

F. Karyogram of CPVT-iPSC clone a.

(Fig 2C). In both cells, RYR2 was similarly distributed in the cytosol and perinuclear region, and partially co-localized with the myofilaments (Fig 2C). Importantly, RYR2 spatial cluster density was also comparable in control and CPVT myocytes (Fig 2D), suggesting that the S406L mutation does not interfere with trafficking of the homotetrameric channel.

Stress-induced Ca^{2+} cycling abnormalities in CPVT-iPSC-derived cardiomyocytes

To assess whether CPVT-iPSC-derived cardiomyocytes recapitulate the disease phenotype, we analysed Ca^{2+} handling properties in single cells at 3–4 months maturation. We first examined whether CPVT myocytes display altered control of Ca^{2+} release during excitation–contraction (EC) by measuring electrically evoked Ca^{2+} transients at different pacing rates in absence and in presence of isoproterenol to mimic catecholaminergic stress (Fig 3 and Fig S2 of Supporting information). Increasing stimulation frequencies from 0.5 to 1.5 Hz correlated with a higher percentage of cells with abnormal Ca^{2+} handling in both control and CPVT myocytes (Fig 3A). However, this effect was significantly more pronounced in the diseased cells and was comparable among different CPVT-iPSC lines (Fig 3A and Fig S3 of Supporting information). We could observe three types of stress-induced Ca^{2+} cycling abnormalities, which

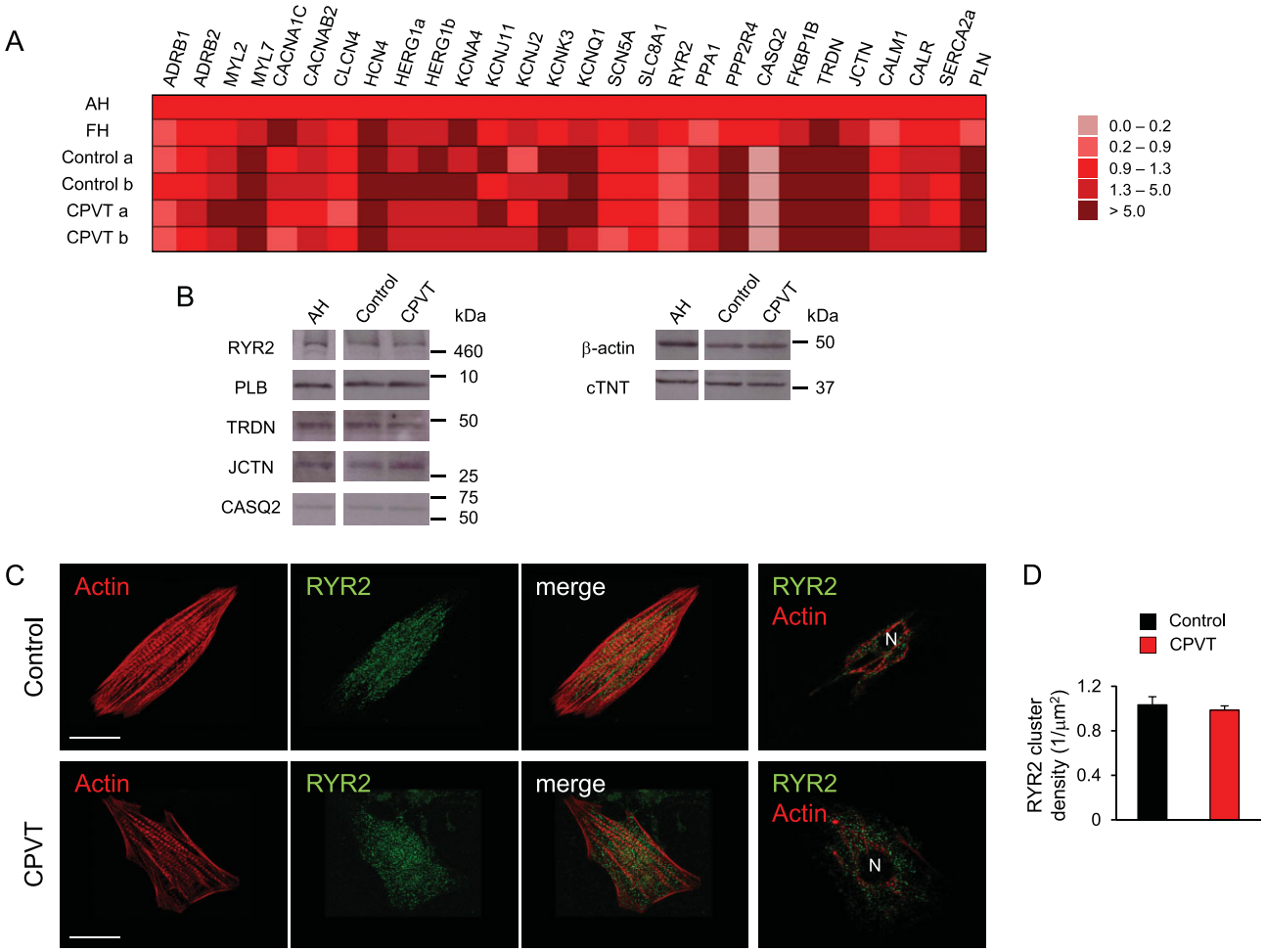

Figure 2. Expression analysis of genes involved in myocytic Ca^{2+} handling and excitation–contraction coupling in iPSC-derived cardiomyocytes.

A. Comparison of transcriptional profile of 2-month-old iPSC-derived cardiac explants, human adult (AH) and fetal (FH) heart tissue. qRT-PCR analysis was performed on 28 key genes involved in cardiomyocyte EC-coupling. All values are normalized for *TNNT2* and relative to AH tissue.

B. Western blot of whole cell extracts from 3 to 4-month-old iPSC-derived cardiac explants and human adult heart tissue (AH). Cardiac troponin T (cTNT) and β-actin were used as loading controls.

C. Confocal immunofluorescence images of RYR2 (green) and actin (red) in human cardiomyocytes generated from control (top) and CPVT-iPSCs (bottom). Actin is marked by phalloidin. From left to right, the third panels display the merged image of the first two panels and the last panels depict RYR2 and actin expression patterns in a optical section at the nuclear plane. N indicates the cell nucleus. Scale bars, 15 μm.

D. RYR2 cluster density in cardiomyocytes derived from control (black) and CPVT-iPSCs (red) ($n = 17$ in each group).

associated with different severities of arrhythmogenicity: Ca^{2+} alternans, in which Ca^{2+} transients alternate between large and small on successive beats (AR1); Ca^{2+} transient fusion, characterized by absence of triggered Ca^{2+} transients at every second stimulation (AR2); and very irregular Ca^{2+} oscillations (AR3). Thus, frequency-induced stress appears to be one major arrhythmic trigger in CPVT-iPSC-derived myocytes. Deeper analysis of Ca^{2+} cycling properties in rhythmic cells revealed that, under basal conditions, control and CPVT myocytes presented comparable resting Ca^{2+} levels, similar systolic and diastolic Ca^{2+} concentration during electrical stimulation at different rates and equal SR Ca^{2+} content, determined by caffeine application (Fig 3B–E and Fig S4 of Supporting information). However, in presence of isoproterenol diastolic Ca^{2+} was significantly elevated in CPVT compared to control cells, while systolic Ca^{2+} levels remained similar (Fig 3C and D). Moreover, in contrast to control myocytes, SR Ca^{2+} load was not increased by isoproterenol treatment in CPVT cells (Fig 3E). These data suggest that in situations of catecholamine-induced elevated luminal Ca^{2+} the S406L-mutation in the RYR2 channels results in diastolic Ca^{2+} leak from the SR. This effect may be attributable to an increased S406L-RYR2 Ca^{2+} sensitivity, which lowers the release threshold to produce spontaneous activity during the diastolic period (Eisner et al, 2009; Priori & Chen, 2011). To investigate whether CPVT-iPSC-derived myocytes indeed possess an enhanced spontaneous Ca^{2+} release during adrenergic stimulation, we measured Ca^{2+} sparks in single cells during rest (Fig 4 and Movies S1-S4 of Supporting information).

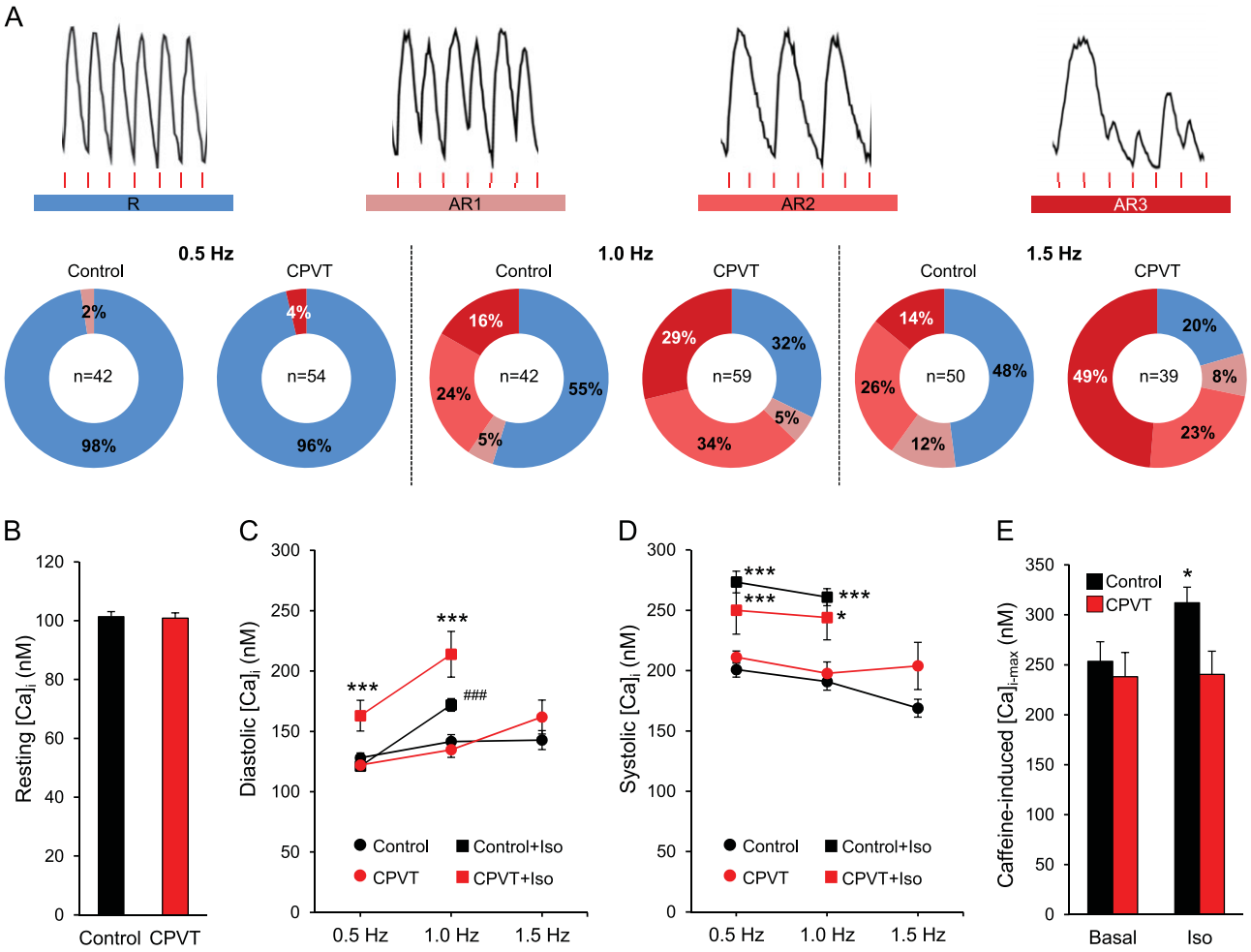

Figure 3. Intracellular Ca^{2+} signalling in control and CPVT-iPSC-derived cardiomyocytes.

A. Images of Fura-2 Ca^{2+} recordings depicting normal (R) and aberrant (AR1, AR2 and AR3) Ca^{2+} cycling in electrically stimulated iPSC-derived myocytes (top, from CPVT cells) and their percentage occurrence during pacing at either 0.5, 1.0 or 1.5 Hz (bottom). Red lines indicate electric stimulation and *n* the number of cells analysed.

B. Bar graphs comparing the average resting intracellular Ca^{2+} ($[Ca^{2+}]_i$) before electrical stimulation started in control (black, $n = 191$) and CPVT (red, $n = 211$) myocytes from three different iPCS lines per group. Data are means ± SEM from four independent differentiation experiments.

C,D. Average of diastolic and systolic $[Ca^{2+}]_i$ in control (black) and CPVT (red) rhythmic myocytes during sequential pacing at 0.5, 1.0 and 1.5 Hz in absence (circles) and in presence (squares) of 10 μM isoproterenol. Between 4 and 42 cells were analysed per group; no rhythmic cells were observed with isoproterenol at 1.5 Hz. Data are means ± SEM. $^{***}p < 0.001$ *versus* CPVT and Control + Iso, $^{\#\#\#}p = 0.001$ versus Control in **C**; $^{*}p = 0.04$, $^{***}p < 0.001$ versus same group without isoproterenol in **D**; two-tailed *t*-test.

E. Average (±SEM) of maximum caffeine-induced $[Ca^{2+}]_i$ as measurement of SR Ca^{2+} content, in control (black) and CPVT (red) myocytes in absence (basal, $n = 33$ *vs.* $n = 8$ cells) and in presence of isoproterenol ($n = 24$ *vs.* $n = 17$ cells); $^{*}p = 0.03$ *versus* control basal and CPVT + Iso, two-tailed *t*-test.

Ca^{2+} sparks are the elementary release events in cardiac EC coupling and derive from the local activity of RYR2 channel clusters (Cheng et al, 1993). Under basal conditions, Ca^{2+} spark frequency did not differ between control and CPVT myocytes, although Ca^{2+} spark amplitude, full width at 50% peak amplitude and decay time were significantly higher in diseased cells (Fig 4A–C). Moreover, only in CPVT myocytes, abnormal Ca^{2+} sparks with a prolonged plateau phase were observed (Fig 4B, *ii*). Under catecholaminergic stress, Ca^{2+} spark frequency considerably increased in CPVT compared to control cells, and associated with a greater decay time constant and even longer abnormal sparks (Fig 4B and C and Movies S3 and S4 of Supporting information). These results indicate that elevated diastolic Ca^{2+} and reduced SR Ca^{2+} load during catecholaminergic challenge in CPVT-iPSC-derived myocytes are caused by hyperactivity of individual Ca^{2+} release units.

Since in CPVT patients tachycardia is restricted to the ventricles under stress condition, it might be expected that CPVT is a disease of ventricular cardiomyocytes. Our cardiac differentiation protocol leads to the generation of all three

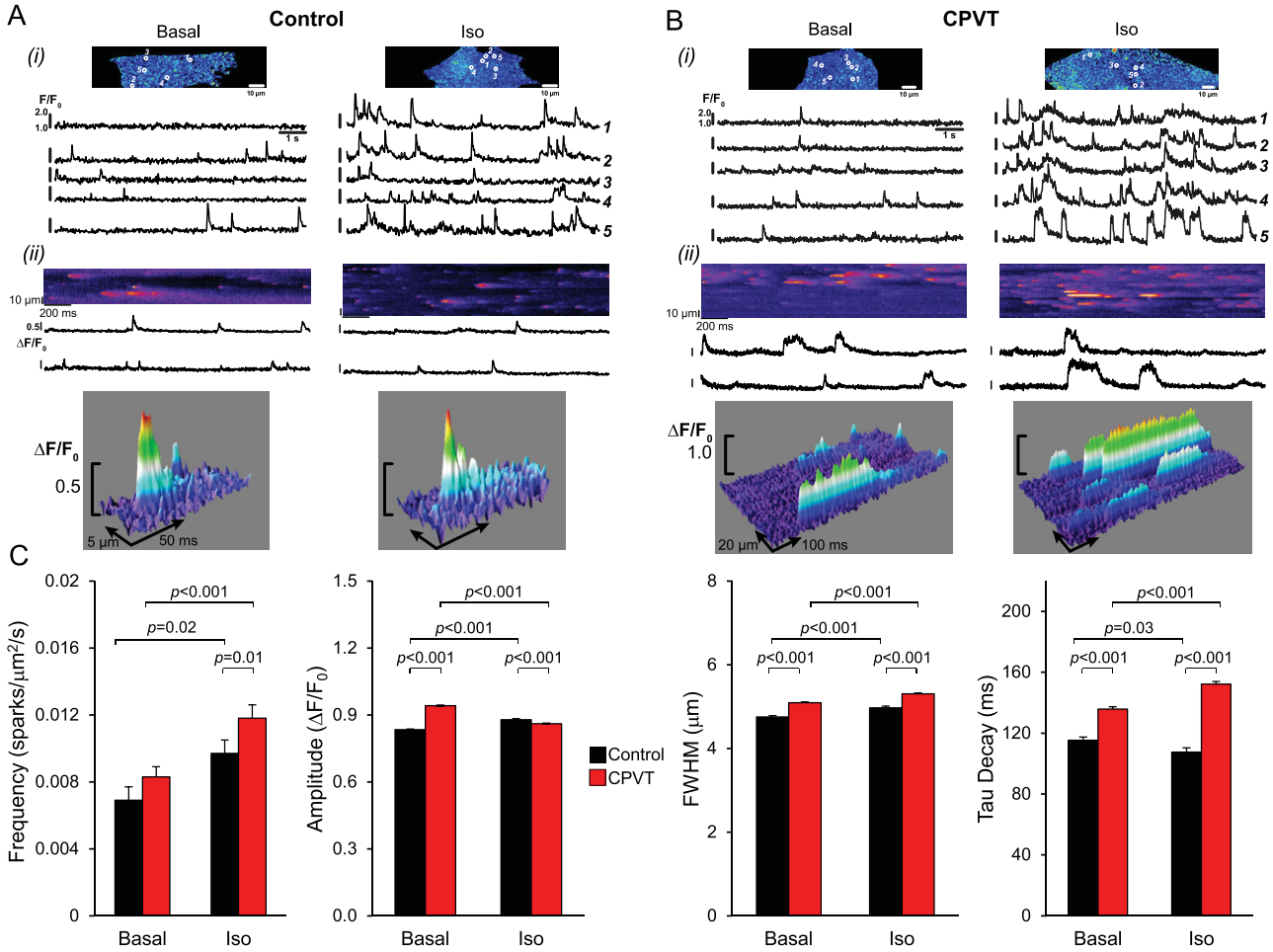

Figure 4. Ca^{2+} spark properties in control and CPVT-iPSC-derived myocytes.

A,B. Panel (i) shows representative pseudo-coloured images of fluo-4-AM loaded control (**A**) and CPVT (**B**) myocytes in the absence (left) or in the presence (right) of 1 μM isoproterenol. Below, typical Ca^{2+} traces, recorded at 105 images/s, corresponding to each of the five individual regions of interest marked in the top images. Panel (ii) displays original line-scan images of Ca^{2+} sparks at a higher temporal resolution (1000 lines/s, top), a portion of the corresponding Ca^{2+} traces (middle), and 3D surface plots of representative Ca^{2+} sparks (bottom), highlighting the extended time course of CPVT-sparks.

C. Summary of Ca^{2+} spark characteristics from control (black) and CPVT (red) myocytes in absence (basal) or presence of 1 μM isoproterenol. FWHM, full width at half maximum. Between 38 and 142 cells from three iPSC lines were analysed per group. Data are means ± SEM from four independent experiments; *p*-values from two-tailed *t*-test.

subtypes of cardiomyocytes, namely ventricular-like, atrial-like and nodal-like cells, which can be distinguished by the expression of specific myocytic lineage markers and by the shape of the action potential (Moretti et al, 2010b). Immunohistochemical analysis for ventricular and atrial myosin light chain 2 (MLC2v and MLC2a) proteins and electrophysiological measurements of action potentials in single iPSC-derived myocytes demonstrated that the ventricular subtype is largely predominant, accounting for 70–80% of all myocytes similarly in both control and CPVT groups (Fig 5A). To assess whether Ca^{2+} spark properties were specifically altered only in ventricular cells, we stained the cells with an antibody against MLC2v retrospectively and analysed spark data from ventricular ($MLC2v^{+}$ cells) and non-ventricular ($MLC2v^{-}$ cells) myocytes separately. The observed differences in Ca^{2+} spark properties between control and CPVT cells persisted in the ventricular and non-ventricular subpopulations (Fig 5B), indicating that the mutated S406L-RYR2 channels are dysfunctional in all myocytes.

Rescue of S406L-RYR2 malfunction by dantrolene in CPVT-iPSC-derived cardiomyocytes

Two mechanisms have been proposed to explain how CPVT-RYR2 mutations alter the sensitivity of the channel to luminal and/or cytosolic Ca^{2+} activation, leading to enhanced stress-induced diastolic Ca^{2+} release: (a) weakening of the interdomain interactions within the RYR2 channels, which destabilizes the closed state ('domain unzipping'; George et al, 2007; Ikemoto & Yamamoto, 2000) and (b) disruption of critical interaction between the RYR2 channels and their modulating proteins

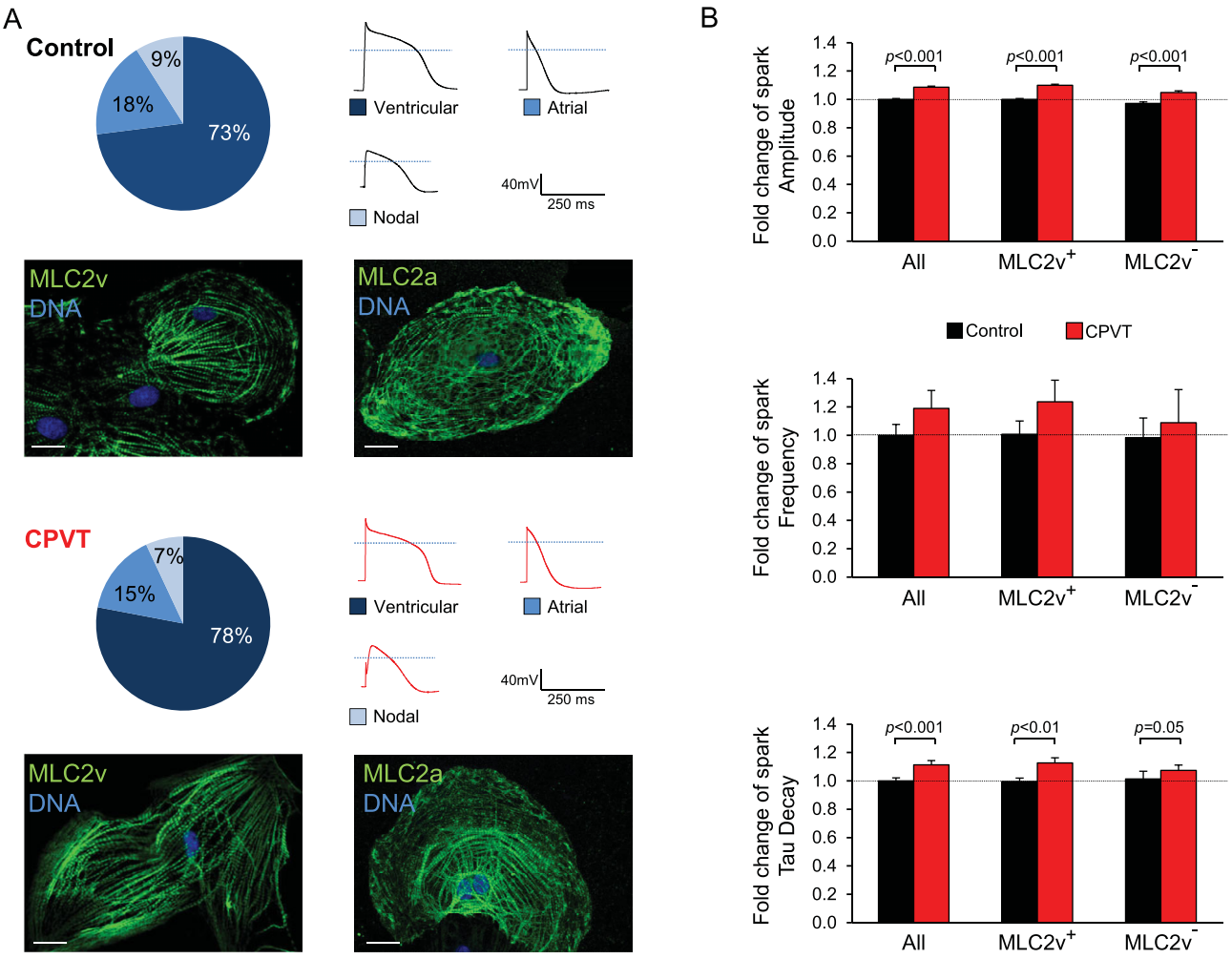

Figure 5. Myocytic subtypes of iPSC-derived myocytes and their Ca^{2+} spark properties.

A. Percentage of ventricular-, atrial- and nodal-like myocytes after 3–4 month cardiac iPSC differentiation based on single cell electrophysiological measurements of action potentials ($n = 47–50$ cells) and expression of specific myocytic lineage markers (MLC2v, for ventricular cells, and MLC2a, for atrial cells) by immunohistochemistry ($n = 100$ cells). Scale bars, 10 μm. Dotted lines in the action potential traces indicate 0 mV.

B. Summary of Ca^{2+} spark characteristics from control (black) and CPVT (red) cells under basal conditions when all myocytes or specifically ventricular ($MLC2v^{+}$) and non-ventricular ($MLC2v^{-}$) subtypes are analysed. Fold changes are relative to all myocytes control. Staining for MLC2v was performed after Ca^{2+} spark imaging. Between 21 and 113 cells from three iPSC lines were analysed per group. Data are means ± SEM from three independent experiments; *p*-values from two-tailed *t*-test.

(Priori & Chen, 2011; Wehrens et al, 2003). The N-terminal and central regions, although separated by ~2000 residues in the linear sequence, interact with each other to form a ''domain switch'' that stabilizes the closed state of RYR channels (Liu et al, 2010; Yamamoto et al, 2000). Disturbance of this interaction leads to a prolongation of Ca^{2+} sparks (Uchinoumi et al, 2010), as observed in the CPVT myocytes. Docking of the recent crystal structure of RYR1 amino-terminal residues 1–559 into 3D reconstructions from cryo-electron microscopy of RYR1 has suggested that indeed multiple domain-domain interfaces are involved in disruption of Ca^{2+} regulation by various disease-causing mutations in RYR1 and RYR2 (Tung et al, 2010). Similar modelling for the N-terminal region of RYR2 has revealed that the S406L mutation is indeed located at the interface between two domains (Fig S5 of Supporting information). Thus, 'domain unzipping' is likely to be the pathomechanism of this mutation. To further verify this hypothesis, we investigated whether dantrolene, which is believed to stabilize the 'domain switch' by binding to a N-terminal sequence of skeletal and cardiac RYRs (Kobayashi et al, 2005, 2009, 2010; Paul-Pletzer et al, 2002, 2005; Wang et al, 2011), could suppress the impact of the S406L mutation in CPVT-iPSC-derived myocytes. Treatment with dantrolene restored normal Ca^{2+} spark properties in CPVT myocytes under basal conditions and corrected S406L-RYR2 hyperactivity induced by adrenergic stimulation, with minimal effects in control cells (Fig 6A). It has been demonstrated that

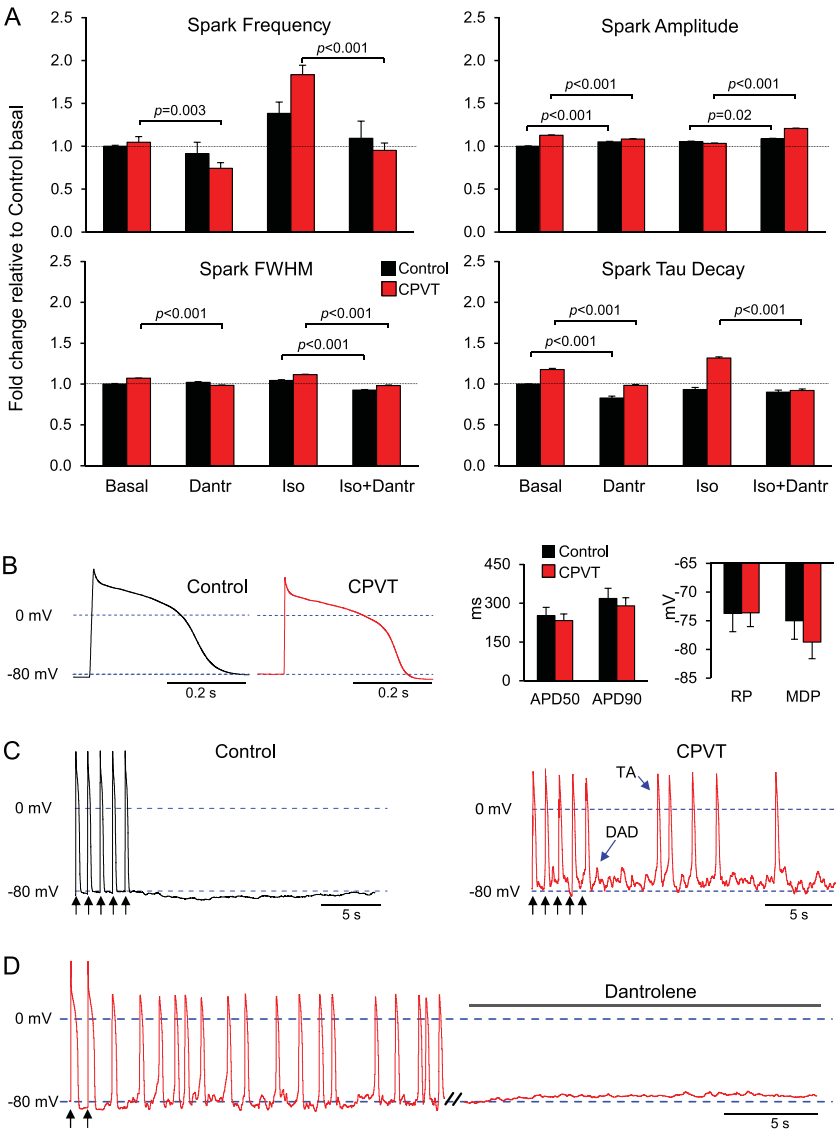

Figure 6. Dantrolene corrects the disease phenotype in CPVT-iPSC-derived myocytes.

A. Fold change of Ca^{2+} spark characteristics relative to control cells under basal conditions in control (black) and CPVT (red) myocytes after treatment with 10 μM dantrolene alone, 1 μM isoproterenol alone or both drugs combined. Between 32 and 142 cells from three iPSC lines were analysed per group. Data are means ± SEM from four independent experiments; *p*-values from one-way ANOVA followed by Tukey's test.

B. Representative traces of electrically evoked action potentials from control (black) and CPVT (red) ventricular myocytes (left) and bar graphs of the averaged action potential duration at 50% (APD50) and 90% (APD90) repolarization, the maximum diastolic potential and the resting potential (right) during stimulation at 1 Hz.

C. Typical action potential recordings from a control (black) and a CPVT (red) ventricular myocyte. Black arrows indicate the last five paced action potentials at 1 Hz stimulation; blue arrows mark an example of DAD and triggered activity.

D. Representative action potential recording from a CPVT ventricular cell showing that superfusion with 10 μM dantrolene completely abolished DADs and TA. Black arrows indicate the last two paced action potentials at 1 Hz stimulation.

elevated spontaneous Ca^{2+} release during diastole can be arrhythmogenic by activation of the Na^{+}/Ca^{2+} exchanger, which generates a transient depolarizing current leading to DADs and triggered activity (TA; Schlotthauer & Bers, 2000). Therefore, we finally examined the incidence of spontaneous DADs/TA in iPSC-derived myocytes by measuring membrane potentials in single ventricular and atrial cells following electrical stimulation (Fig 6B–D and Fig S6 of Supporting information). All investigated cells presented no spontaneous activity before pacing and we did not observe any differences in resting membrane potential nor in the duration of electrically induced action potentials between equivalent subtype of myocytes in control and CPVT groups (Fig 6B and Fig S6C of Supporting information). When stimulated at 1 Hz, 56% of the control ventricular-like myocytes (5:9 cells) and 11% of the control atrial-like cells (1:9 cells) showed no spontaneous after-potentials and maintained stable resting voltage after electric pacing ended (Fig 6C, left, and Fig S6A of Supporting information). However, we observed DADs and TA in 88 and 89% of the ventricular-like and atrial-like CPVT cells, respectively (14:16 ventricular cells, Fig 6C, right; 8:9 atrial cells, Fig S6B of Supporting information). Moreover, when compared to control cells, diseased myocytes exhibited a much higher incidence of spontaneous action potentials after termination of pacing (1.4 ± 0.3/s versus 0.5 ± 0.3/s for ventricular and 1.1 ± 0.3/s versus 0.2 ± 0.1/s for the atrial cells). Interestingly, DADs and triggered arrhythmias were completely abolished by dantrolene treatment in all investigated CPVT cells (Fig 6D and Fig S6B of Supporting information), suggesting that a defective inter-domain interaction within the RYR2 is the underlying arrhythmogenic mechanism of the S406L mutation. Moreover, the rescue of the CPVT-disease phenotype in a patient-specific iPSC-based system by dantrolene provides the first evidence that, as in the case of malignant hyperthermia, correction of defective inter-domain interaction within mutated human RYR2 may represent an effective novel causal therapy for CPVT1.

DISCUSSION

We have developed the first human stem cell-based model for CPVT1, bearing a novel S406L missense mutation in *RYR2*, and demonstrated its suitability to recapitulate molecular and physiological aspects of the disease phenotype. Until now, only heterologous expression systems and genetic mouse models have been used to study the cellular and molecular aspects of CPVT-linked RYR2 mutations. Based on these studies, two mechanisms for RYR2-mediated CPVT have been proposed. The first mechanism suggests that RYR2 mutants reduce the binding affinity of the channel for its auxiliary stabilizing protein FKBP12.6 and this is further aggravated in situation of catecholamine-induced hyperphosphorylation of RYR2 with consequential dissociation of FKBP12.6 and Ca^{2+} leakage from the SR (Lehnart et al, 2008; Marx et al, 2000; Wehrens et al, 2003). Although it may be possible that selected mutations alter FKBP12.6 binding to RYR2, this hypothesis has been recently challenged and increasing body of evidence clearly demonstrates that alterations in FKBP12.6-RYR2 interaction are unlikely to be the common cause of CPVT1 (George et al, 2003; Guo et al, 2010; Jiang et al, 2005; Liu et al, 2006; Xiao et al, 2007). Alternatively, it has been proposed that RYR2 mutations in the N-terminal and central regions of the protein weaken interactions between these two domains that are critical in stabilizing the closed state of the channel, resulting in an increased open probability and enhanced spontaneous Ca^{2+} release during stress-induced SR Ca^{2+} overload (Ikemoto & Yamamoto, 2000; Tateishi et al, 2009). In support of this 'domain unzipping' mechanism, dantrolene has been shown to suppress abnormal Ca^{2+} leak from mutated RYR1 and RYR2 by binding to a N-terminal sequence and stabilizing domain–domain contacts within the N-terminal and central regulatory regions (Kobayashi et al, 2005, 2009; Paul-Pletzer et al, 2002, 2005). Interestingly, dantrolene binding to RYR2 seems to be dependent on a particular conformational state of the channel that takes place only in disease conditions (Kobayashi et al, 2009; Paul-Pletzer et al, 2005). Therefore, the results that this drug rescues the disease phenotype in our patient-specific iPSC-based CPVT model would indicate that 'domain unzipping' is likely to be the pathomechanism of the novel N-terminal S406L-RYR2 mutation. Evidence for unzipping of the interaction between N-terminal and central domains raises the question of whether 'domain unzipping' is present in other regions of RYR2 in which CPVT mutations are located. Thus, it would be of great interest to investigate dantrolene effects in other patient-specific iPSC-CPVT models bearing different RYR2 mutations situated throughout the molecule. Our study on a human model of CPVT provides valuable insights into the pathophysiology of the disease and suggests dantrolene as a potential novel drug for the causal treatment of cardiac arrhythmias in CPVT1 patients carrying N-terminal mutations. Yet, clinical trials demonstrated that current treatments with β-blockers and ICDs are not fully protective in all CPVT patients and showed that these regimens are less attractive in CPVT compared to other forms of inherited ventricular tachycardia, such as long QT or Brugada syndrome (Kaufman, 2009). Although the precise mechanistic basis of CPVT most likely depends on the hotspot in which mutations are residing and hence might call for the development of location-specific drugs to address the functional heterogeneity, our work highlights the potential of human iPSCs in the emerging field of personalized medicine (Zhu et al, 2011) by demonstrating the ability to screen the effects of potential disease aggravators and novel customized treatment options.

MATERIALS AND METHODS

Human iPSC generation and cardiomyocyte differentiation

After approval by the institutional review board, we recruited a 24-year-old caucasian female CPVT patient and a 32-year-old female caucasian control without history of cardiac disease scheduled for plastic surgery to undergo dermal biopsy after obtaining written informed consent. Reprogramming of primary skin fibroblasts and differentiation into cardiomyocytes were performed as described previously (Moretti et al, 2010a,b). Briefly, fibroblasts were infected with retroviruses encoding OCT4, SOX2, KLF4 and c-MYC and cultured on murine embryonic feeder cells until iPSC colonies could be picked. EB differentiation was achieved by aggregating the cells on low-attachment plates and EBs were plated on gelatin-coated dishes at day 7. Spontaneously contracting areas were manually dissected and cultured further until day 90–130 of differentiation. Cells for physiological experiments were collagenase-dissociated into single cells, plated on fibronectin-coated glass coverslips, and analysed within 3–6 days.

Genomic sequencing and karyotype analysis

The presence of the RYR2-S406L mutation in the patient and its absence in the control and in blood samples of 100 coronary artery disease patients without CPVT was verified by polymerase chain reaction-based sequencing of genomic DNA isolated from skin fibroblasts, from iPSCs and from blood using a Genomic DNA Purification Kit (Gentra Systems). Karyotyping of the iPSC lines was performed at the Institute of Human Genetics of the Technical University Munich using standard methodology.

Quantitative real-time PCR

Total mRNA was isolated from fibroblasts, iPSC clones, EBs, and myocytic explants using the Stratagene Absolutely RNA kit. One microgram of total RNA was used to synthesize cDNA from fibroblasts, iPSC clones and EBs, using the High-Capacity cDNA Reverse Transcription kit (Applied Biosystems). RNA from cardiomyocyte explants and from human adult and fetal heart (Clontech) was linearly amplified using the RNA Amplification RampUP Kit (Genisphere) and subsequently 1 μg of amplified RNA was used to synthetize cDNA. Gene expression was quantified by qRT-PCR using 1 μl of the RT reaction and the Power SYBR Green PCR Master Mix (Applied Biosystems). Gene expression levels were normalized to *GAPDH* or to *TNNT2*, as indicated in the dedicated figure legends. Primer sequences are provided in Table S1 of Supporting information.

Phenotypic characterization of iPSC lines and their differentiated progeny

Differential gene expression was assessed by qRT-PCR reaction as described previously (Moretti et al, 2010a,b). For histochemistry, cells

The paper explained

PROBLEM:

Catecholaminergic polymorphic ventricular tachycardia (CPVT) is an inherited cardiac disease that, under physical and emotional stress, leads to life-threatening arrhythmia followed by syncopes and sudden cardiac death at a young age in patients with structurally normal heart. Despite the very high mortality rate, no causative treatment exists and the development of new drugs is hampered by the difficulty of obtaining patient cardiac myocytes and maintaining them in culture without loss of their physiological properties.

RESULTS:

Taking dermal fibroblasts from a 24-year-old woman with a diagnosis of familial CPVT, we generated iPSC lines that were subsequently differentiated into cardiomyocytes. These cardiomyocytes recapitulated, under catecholaminergic stress, all major hallmarks of the disease, such as elevated diastolic Ca^{2+} concentrations, a reduced SR Ca^{2+} content, and an increased susceptibility to arrhythmias. Additionally, we found the drug dantrolene to be protective and efficient in suppressing stress-induced arrhythmic events in CPVT cardiac myocytes.

IMPACT:

In this study, we generated the first human model of CPVT. Our findings indicate that cardiomyocytes derived from CPVT patient-specific iPSCs can be used as an *in vitro* model system to study disease mechanisms, screen drug compounds for individual risk stratification and develop patient-specific therapies.

were fixed with 3.7% v/v formaldehyde. Nuclei were visualized with Hoechst-33528 (1 μg/ml), F-actin with Phalloidin-Alexa-Fluor-594-conjugate (Invitrogen, 1:40), and alkaline phosphatase activity with NBT/BCIP substrate (Roche). Immunostaining was performed with standard protocols using the following primary antibodies: human NANOG (rabbit polyclonal, Abcam, 1:500), TRA1-81-Alexa-Fluor-488-conjugated (mouse monoclonal, BD Pharmingen, 1:20), RYR2 (mouse monoclonal, Thermo Scientific, 4 μg/ml), MLC2a (mouse monoclonal, Synaptic Systems, 5 μg/ml) and MLC2v (mouse monoclonal, Synaptic Systems, 5 μg/ml). Bright-field and fluorescence microscopy were performed using imaging systems (DMI6000-AF6000), filters and software from Leica microsystems. Confocal imaging (Leica SP5-II LSCM) was used to analyse expression of sarcomeric proteins and to assess RYR2 subcellular distribution. RYR2 cluster density was calculated based on particle counting after thresholding with ImageJ PlugIns (Wayne Rasant, NIH, Bethesda, USA). Western blotting on whole cell lysate from iPSC-derived cardiac explants and human adult heart (Imgenex) was performed with standard protocols using 20 μg proteins and the following primary antibodies: RYR2 (mouse monoclonal, Thermo Scientific, 0.4 μg/ml), PLB (mouse monoclonal, Thermo Scientific, 2 μg/ml), TRDN (goat polyclonal, Santa Cruz, 1 μg/ml), JCTN (goat polyclonal, Santa Cruz, 1 μg/ml), CASQ2 (rabbit polyclonal, Abcam, 0.08 μg/ml), β-actin (rabbit polyclonal, Abcam, 1:1000) and cTNT (mouse monoclonal, NeoMarkers, 0.2 μg/ml).

Physiological characterization of iPSC-derived cardiomyocytes

Intracellular free Ca^{2+} was measured at 20–22°C in cells loaded with fura-2-AM (5 μM for 20 min; Fluka, Buchs, Switzerland) in HEPES-buffered saline (in mM: NaCl (140), KCl (5.4), $MgCl_2$ (1), $CaCl_2$ (2), glucose (10), HEPES (10), pH 7.4) containing 0.1% w/v bovine serum albumin on a monochromator-equipped (Polychrome-V, TILL-Photonics, Gräfelfing, Germany) inverted microscope (Olympus-IX 71 with an UPlanSApo 20×/0.85 oil immersion objective). Fluorescence was excited at 340 and 380 nm, emission recorded at 22–24 Hz with a 14-bit EMCCD camera (iXON3 885, Andor, Belfast, UK), and Ca^{2+} concentrations calculated as described previously (Grynkiewicz et al, 1985). For field stimulation, 5 ms depolarizing voltage pulses at 90 V (Stimulator Type 201, Hugo Sachs Elektronik, March-Hugstetten, Germany) were applied using platinum electrodes (RC-37FS, Warner Instruments, Hamden, USA). Drugs were applied by solution exchange via continuous perfusion. Caffeine (100 mM) was applied 25 s after the stimulation period.

Spontaneous Ca^{2+} sparks were imaged at 20–22°C in cells loaded with fluo-4-AM (0.6 μM for 30 min, Invitrogen) in extracellular solution (in mM: NaCl (135), KCl (5.4), $MgCl_2$ (2), $CaCl_2$ (1.8), HEPES (10), glucose (10), pH 7.35) on an inverted confocal microscope (Leica SP5-II LSCM) through a 63x oil immersion objective (HCX PL APO, 1.4, Leica), exciting with the 488 nm line of an Arg/Kr laser (Lasos, Jena, Germany) and collecting emission at 495–600 nm, acquiring 512 × 120 pixel frames at 105 Hz using the resonant scanner, keeping laser, spectral and gain settings constant throughout all experiments. Time series (each 1000 images) were recorded at a 1-min interval. Drug effects were assessed 10–15 min after manual solution exchange, which was verified not to alter Ca^{2+} spark properties by a mock solution exchange. Images stored in a database (OMERO, www.openmicroscopy.org) were analysed off-line using a custom-designed algorithm performing automatic cell- and spark-detection and subsequent fitting of the single spark fluorescence distributions with a 2D Gauss over time approach.

Myocyte action potentials were recorded at 35 ± 0.5°C in the current clamp mode of the perforated patch-clamp technique using 300 μg/ml water-soluble amphotericin B (Sigma–Aldrich, Deisenhofen, Germany) in the pipette solution (in mM: KCl (30), K-aspartate (110), $MgCl_2$ (1), HEPES (10), EGTA (0.1), pH 7.2), sampling at 10 kHz with an EPC10 patch-clamp amplifier (HEKA, Lambrecht, Germany). Cells were superfused with bath solution (in mM: NaCl (135), KCl (5), $MgCl_2$ (1), $CaCl_2$ (2), glucose (10), HEPES (10), pH 7.4), additionally containing 10 μM dantrolene where indicated. The liquid junction potential was +13.8 mV and offset corrections were made by the Patchmaster software. Pipette series resistance ranged from 5.5 to 19 MΩ. Perforation started shortly after seal formation and reached steady state within 3–5 min.

All experiments and analysis were performed by investigators blinded to the genotype of the cells.

Statistical analysis

Data that passed tests for normality and equal variance were analysed with the use of Student's *t*-test or one-way analysis of variance followed by Tukey's test, when appropriate. Two-sided *p*-values of <0.05 were considered statistically significant. All data are shown as means $\pm$ SEM.

For more detailed Materials and Methods see the Supporting information.

Author contributions

KLL, DS, TG and PL conceived the experiments; CBJ, AM, and MB generated and characterized control and CPVT iPSCs; Generation and characterization of human cardiomyocytes was performed by CBJ, LI, MB, TD, AG and JTL; CBJ performed histochemistry/immunostaining with LI and SR and western blotting with TD; MMS, US and SP conducted Ca^{2+} imaging and electrophysiological measurements and PL Ca^{2+} spark experiments; RJD and MS recruited the CPVT patient family; DS performed docking structure modelling; KLL, DS and AM wrote the manuscript.

Acknowledgements

We thank T. Kitamura and S. Yamanaka for providing viral vectors through Addgene, and especially the member of the CPVT family and the healthy volunteers who provided us with skin biopsies for the reprogramming. We would like to acknowledge Diana Grewe and Christina Scherb for their technical assistance in cell culture and Gabi Lederer (Cytogenetic Department, TUM) for karyotyping. This work was supported by grants from the European Research Council (Marie Curie Excellence Team Grant MEXT-23208; ERC 261053–CHD-iPS), the German Research Foundation (Research Unit 923, Mo 2217/1-1 and La 1238 3-1/4-1) and the German Ministry for Education and Research (01 GN 0826). CBJ was supported by a scholarship (AFR-PHD-09-169) granted by the National Research Fund, Luxembourg.

Supporting information is available at EMBO Molecular Medicine online.

The authors declare that they have no conflict of interest.

References

Berridge MJ (2003) Cardiac calcium signalling. Biochem Soc Trans 31: 930-933

Bers DM (2004) Macromolecular complexes regulating cardiac ryanodine receptor function. J Mol Cell Cardiol 37: 417-429

Carvajal-Vergara X, Sevilla A, D'Souza SL, Ang YS, Schaniel C, Lee DF, Yang L, Kaplan AD, Adler ED, Rozov R, *et al* (2010) Patient-specific induced pluripotent stem-cell-derived models of LEOPARD syndrome. Nature 465: 808-812

Cheng H, Lederer WJ, Cannell MB (1993) Calcium sparks: elementary events underlying excitation–contraction coupling in heart muscle. Science 262: 740-744

Eisner DA, Kashimura T, Venetucci LA, Trafford AW (2009) From the ryanodine receptor to cardiac arrhythmias. Circ J 73: 1561-1567

George CH, Higgs GV, Lai FA (2003) Ryanodine receptor mutations associated with stress-induced ventricular tachycardia mediate increased calcium release in stimulated cardiomyocytes. Circ Res 93: 531-540

George CH, Jundi H, Thomas NL, Fry DL, Lai FA (2007) Ryanodine receptors and ventricular arrhythmias: emerging trends in mutations, mechanisms and therapies. J Mol Cell Cardiol 42: 34-50

Grynkiewicz G, Poenie M, Tsien RY (1985) A new generation of Ca^{2+} indicators with greatly improved fluorescence properties. J Biol Chem 260: 3440-3450

Guo T, Cornea RL, Huke S, Camors E, Yang Y, Picht E, Fruen BR, Bers DM (2010) Kinetics of FKBP12.6 binding to ryanodine receptors in permeabilized cardiac myocytes and effects on Ca sparks. Circ Res 106: 1743-1752

Gupta MK, Illich DJ, Gaarz A, Matzkies M, Nguemo F, Pfannkuche K, Liang H, Classen S, Reppel M, Schultze JL, *et al* (2010) Global transcriptional profiles of beating clusters derived from human induced pluripotent stem cells and embryonic stem cells are highly similar. BMC Dev Biol 10: 98

Gyorke S, Terentyev D (2008) Modulation of ryanodine receptor by luminal calcium and accessory proteins in health and cardiac disease. Cardiovasc Res 77: 245-255

Ikemoto N, Yamamoto T (2000) Postulated role of inter-domain interaction within the ryanodine receptor in Ca(2+) channel regulation. Trends Cardiovasc Med 10: 310-316

Jiang D, Wang R, Xiao B, Kong H, Hunt DJ, Choi P, Zhang L, Chen SR (2005) Enhanced store overload-induced Ca2+ release and channel sensitivity to luminal Ca2+ activation are common defects of RyR2 mutations linked to ventricular tachycardia and sudden death. Circ Res 97: 1173-1181

Kaufman ES (2009) Mechanisms and clinical management of inherited channelopathies: long QT syndrome, Brugada syndrome, catecholaminergic polymorphic ventricular tachycardia, and short QT syndrome. Heart Rhythm 6: S51-S55

Kaye DM, Hoshijima M, Chien KR (2008) Reversing advanced heart failure by targeting Ca2+ cycling. Annu Rev Med 59: 13-28

Kobayashi S, Bannister ML, Gangopadhyay JP, Hamada T, Parness J, Ikemoto N (2005) Dantrolene stabilizes domain interactions within the ryanodine receptor. J Biol Chem 280: 6580-6587

Kobayashi S, Yano M, Suetomi T, Ono M, Tateishi H, Mochizuki M, Xu X, Uchinoumi H, Okuda S, Yamamoto T, *et al* (2009) Dantrolene, a therapeutic agent for malignant hyperthermia, markedly improves the function of failing cardiomyocytes by stabilizing interdomain interactions within the ryanodine receptor. J Am Coll Cardiol 53: 1993-2005

Kobayashi S, Yano M, Uchinoumi H, Suetomi T, Susa T, Ono M, Xu X, Tateishi H, Oda T, Okuda S, *et al* (2010) Dantrolene, a therapeutic agent for malignant hyperthermia, inhibits catecholaminergic polymorphic ventricular tachycardia in a RyR2(R2474S/+) knock-in mouse model. Circ J 74: 2579-2584

Krause T, Gerbershagen MU, Fiege M, Weisshorn R, Wappler F (2004) Dantrolene—a review of its pharmacology, therapeutic use and new developments. Anaesthesia 59: 364-373

Lanner JT, Georgiou DK, Joshi AD, Hamilton SL (2010) Ryanodine receptors: structure, expression, molecular details, and function in calcium release. Cold Spring Harb Perspect Biol 2: a003996

Lehnart SE, Mongillo M, Bellinger A, Lindegger N, Chen BX, Hsueh W, Reiken S, Wronska A, Drew LJ, Ward CW, *et al* (2008) Leaky Ca2+ release channel/ryanodine receptor 2 causes seizures and sudden cardiac death in mice. J Clin Invest 118: 2230-2245

Liu N, Colombi B, Memmi M, Zissimopoulos S, Rizzi N, Negri S, Imbriani M, Napolitano C, Lai FA, Priori SG (2006) Arrhythmogenesis in catecholaminergic polymorphic ventricular tachycardia: insights from a RyR2 R4496C knock-in mouse model. Circ Res 99: 292-298

Liu N, Rizzi N, Boveri L, Priori SG (2009) Ryanodine receptor and calsequestrin in arrhythmogenesis: what we have learnt from genetic diseases and transgenic mice. J Mol Cell Cardiol 46: 149-159

Liu Z, Wang R, Tian X, Zhong X, Gangopadhyay J, Cole R, Ikemoto N, Chen SR, Wagenknecht T (2010) Dynamic, inter-subunit interactions between the N-terminal and central mutation regions of cardiac ryanodine receptor. J Cell Sci 123: 1775-1784

Marx SO, Reiken S, Hisamatsu Y, Jayaraman T, Burkhoff D, Rosemblit N, Marks AR (2000) PKA phosphorylation dissociates FKBP12.6 from the calcium release channel (ryanodine receptor): defective regulation in failing hearts. Cell 101: 365-376

Moretti A, Bellin M, Jung CB, Thies TM, Takashima Y, Bernshausen A, Schiemann M, Fischer S, Moosmang S, Smith AG, *et al* (2010a) Mouse and human induced pluripotent stem cells as a source for multipotent Isl1+ cardiovascular progenitors. FASEB J 24: 700-711

Moretti A, Bellin M, Welling A, Jung CB, Lam JT, Bott-Flugel L, Dorn T, Goedel A, Hohnke C, Hofmann F, *et al* (2010b) Patient-specific induced pluripotent stem-cell models for long-QT syndrome. N Engl J Med 363: 1397-1409

Paul-Pletzer K, Yamamoto T, Bhat MB, Ma J, Ikemoto N, Jimenez LS, Morimoto H, Williams PG, Parness J (2002) Identification of a dantrolene-binding sequence on the skeletal muscle ryanodine receptor. J Biol Chem 277: 34918-34923

Paul-Pletzer K, Yamamoto T, Ikemoto N, Jimenez LS, Morimoto H, Williams PG, Ma J, Parness J (2005) Probing a putative dantrolene-binding site on the cardiac ryanodine receptor. Biochem J 387: 905-909

Postma AV, Denjoy I, Hoorntje TM, Lupoglazoff JM, Da Costa A, Sebillon P, Mannens MM, Wilde AA, Guicheney P (2002) Absence of calsequestrin 2 causes severe forms of catecholaminergic polymorphic ventricular tachycardia. Circ Res 91: e21-e26

Priori SG, Chen SR (2011) Inherited dysfunction of sarcoplasmic reticulum Ca2+ handling and arrhythmogenesis. Circ Res 108: 871-883

Priori SG, Napolitano C, Tiso N, Memmi M, Vignati G, Bloise R, Sorrentino V, Danieli GA (2001) Mutations in the cardiac ryanodine receptor gene (hRyR2) underlie catecholaminergic polymorphic ventricular tachycardia. Circulation 103: 196-200

Scheinman MM, Lam J (2006) Exercise-induced ventricular arrhythmias in patients with no structural cardiac disease. Annu Rev Med 57: 473-484

Schlotthauer K, Bers DM (2000) Sarcoplasmic reticulum Ca(2+) release causes myocyte depolarization. Underlying mechanism and threshold for triggered action potentials. Circ Res 87: 774-780

Takahashi K, Tanabe K, Ohnuki M, Narita M, Ichisaka T, Tomoda K, Yamanaka S (2007) Induction of pluripotent stem cells from adult human fibroblasts by defined factors. Cell 131: 861-872

Tateishi H, Yano M, Mochizuki M, Suetomi T, Ono M, Xu X, Uchinoumi H, Okuda S, Oda T, Kobayashi S, *et al* (2009) Defective domain–domain interactions within the ryanodine receptor as a critical cause of diastolic Ca2+ leak in failing hearts. Cardiovasc Res 81: 536-545

Thomas NL, Maxwell C, Mukherjee S, Williams AJ (2010) Ryanodine receptor mutations in arrhythmia: the continuing mystery of channel dysfunction. FEBS Lett 584: 2153-2160

Tung CC, Lobo PA, Kimlicka L, Van Petegem F (2010) The amino-terminal disease hotspot of ryanodine receptors forms a cytoplasmic vestibule. Nature 468: 585-588

Uchinoumi H, Yano M, Suetomi T, Ono M, Xu X, Tateishi H, Oda T, Okuda S, Doi M, Kobayashi S, *et al* (2010) Catecholaminergic polymorphic ventricular tachycardia is caused by mutation-linked defective conformational regulation of the ryanodine receptor. Circ Res 106: 1413-1424

Wang R, Zhong X, Meng X, Koop A, Tian X, Jones PP, Fruen BR, Wagenknecht T, Liu Z, Chen SR (2011) Localization of the dantrolene-binding sequence near the FK506-binding protein-binding site in the three-dimensional structure of the ryanodine receptor. J Biol Chem 286: 12202-12212

Wehrens XH, Lehnart SE, Huang F, Vest JA, Reiken SR, Mohler PJ, Sun J, Guatimosim S, Song LS, Rosemblit N, *et al* (2003) FKBP12.6 deficiency and defective calcium release channel (ryanodine receptor) function linked to exercise-induced sudden cardiac death. Cell 113: 829-840

Xiao J, Tian X, Jones PP, Bolstad J, Kong H, Wang R, Zhang L, Duff HJ, Gillis AM, Fleischer S, *et al* (2007) Removal of FKBP12.6 does not alter the conductance and activation of the cardiac ryanodine receptor or the susceptibility to stress-induced ventricular arrhythmias. J Biol Chem 282: 34828-34838

Yamamoto T, El-Hayek R, Ikemoto N (2000) Postulated role of interdomain interaction within the ryanodine receptor in Ca(2+) channel regulation. J Biol Chem 275: 11618-11625

Yazawa M, Hsueh B, Jia X, Pasca AM, Bernstein JA, Hallmayer J, Dolmetsch RE (2011) Using induced pluripotent stem cells to investigate cardiac phenotypes in Timothy syndrome. Nature 471: 230-234

Zhu H, Lensch MW, Cahan P, Daley GQ (2011) Investigating monogenic and complex diseases with pluripotent stem cells. Nat Rev Genet 12: 266-275

